November 2016

Evaluating the Role of Glutathione in Detoxification of Metal-Based Nanoparticles in Plants

Chuanxin Ma
University of Massachusetts, Amherst

EVALUATING THE ROLE OF GLUTATHIONE IN DETOXIFICATION OF METAL-BASED NANOPARTICLES IN PLANTS

A Dissertation Presented

by

CHUANXIN MA

Submitted to the Graduate School of the University of Massachusetts Amherst in partial fulfillment of the requirements for the degree of

DOCTOR OF PHILOSOPHY

September 2016

Plant & Soil Sciences

EVALUATING THE ROLE OF GLUTATHIONE IN DETOXIFICATION OF METAL-BASED NANOPARTICLES IN PLANTS

A Dissertation Presented

by

CHUANXIN MA

Approved as to the style and content by:

_____
Om Parkash Dhankher, Co-chair

_____
Baoshan Xing, Co-chair

_____
Dong Wang, member

_____
Geunhwa Jung
Director, Plant & Soil Sciences Graduate Program

ACKNOWLEDGMENTS

First of all, I would like to express my sincere gratitude to my advisors Dr. Om Parkash Dhankher and Dr. Baoshan Xing, for their invaluable directions and supports throughout my Ph.D. study. Their wisdom and immense knowledge have helped shape me into a young scientist. Many thanks go to my committee member, Dr. Dong Wang from Department of Biochemistry and Molecular Biology, for his constructive suggestions to my soybean work and providing *Bradyrhizobium* strain. In addition, I would like to thank Dr. Jason C. White (The Connecticut Agricultural Experiment Station) for metal analysis; Dr. Minocha Rakesh (Forest Service, United States Department of Agriculture) for thiol compound analysis; Dr. Yuanzhi Tang (Georgia Institute of Technology) for metal speciation analysis; Dr. Sarah Weis (University of Massachusetts Amherst) for total nitrogen analysis; Dr. Michelle DaCosta (University of Massachusetts Amherst) for photosynthetic rate measurement.

I am deeply grateful to my colleagues Hesham Mohamed Abdullah, Ryan J. Shepard, Kenny Ablordeppey, Hamid Mashayekhi, Huiyuan Guo, Emily J. Cole, Peng Du, Yingqing Deng, and Heping Shang, in Dr. Parkash's and Dr. Xing's labs, for their generous helps and supports. I would like to thank my seniors Dr. Parul Rana Tomar, Dr. Sudesh Chikkara, Dr. Kareen A. Mosa, Dr. Kundan Kumar and Dr. Lei Song for their constant support and valuable suggestions in the first year of my Ph.D. study.

Thank you to Dr. Hong Liu (Fujian Agriculture and Forestry University), Dr. Guangcai Chen (Research Institute of Subtropical Forestry, Chinese Academy of

Forestry), Dr. Yufeng Wang (Heilongjiang Bayi Agricultural University), Dr. Cuiping Wang (Nankai University), Dr. Yukui Rui (China Agriculture University), Dr. Qing Zhao (Institute of Applied Ecology, Chinese Academy of Sciences) and Dr. Jian Zhao (Ocean University of China) for their kind helps and suggestions in my research.

In addition, I would also like to thank undergraduate students Cameron Richard, Aditi Mankodi, Benjamin Chilcoat, Alex Merlino and many more, for their assistance with the experiments.

I would like to take this opportunity to acknowledge my department, Stockbridge School of Agriculture, for the financial support and scientific advice. Without this, it would be impossible for me to take this program.

I owe special thanks and gratitude to my parents. Thank you for their constant love and unconditional support to me. I also thank all my friends in China, who keep encouraging and supporting me with their best wishes.

ABSTRACT

EVALUATING THE ROLE OF GLUTATHIONE IN DETOXIFICATION OF METAL-BASED NANOPARTICLES IN PLANTS

SEPTEMBER 2016

CHUANXIN MA, B. S., TIANJIN UNIVERSITY OF TECHNOLOGY, CHINA

M. S., TIANJIN UNIVERSITY OF TECHNOLOGY, CHINA

Ph.D., UNIVERSITY OF MASSACHUSETTS AMHERST

Directed by: Professor Om Parkash Dhankher and Professor Baoshan Xing

The potential risks from metal-based nanoparticles (NPs) in the environment have increased with the rapidly rising demand for and use of nano-enabled consumer products. Plant's central roles in ecosystem function and food chain integrity ensure intimate contact with water and soil systems, both of which are considered sinks for NPs accumulation. Thus, this dissertation describes three main objectives to comprehensively understand the interactions between plants and NPs and to characterize the role of glutathione (GSH) in detoxification of metal-based NPs in plants at physiological, biochemical, and molecular levels.

(1) The effects of cerium oxide (CeO_2) and indium oxide (In_2O_3) NPs exposure on *Arabidopsis thaliana* were investigated. In this study, we used the model plant "*A. thaliana*" to test the toxicity of two commonly used NPs, CeO_2 and In_2O_3, in semisolid medium and hydroponic system. The results indicated that CeO_2 NPs could induce oxidative stress in *A. thaliana*. The lipid peroxidation in terms of MDA contents and ROS production were very high in CeO_2 and In_2O_3 treated plants. Activities of ROS

scavengers and stress related enzymes in CeO_2 and In_2O_3 NPs treated *A. thaliana* were also higher than control plants. Relative expression of genes involved in stress response such as the sulfur assimilation and GSH metabolic pathway demonstrated that *A. thaliana* activated the defense mechanism to counteract nanotoxicity.

(2) To explore whether the enhanced level of GSH could protect plants from silver (Ag) NPs toxicity, we used the engineered *Crambe abyssinica* (a member of rassicaseae) plants expressing the *E. coli* γ-glutamylecysteine synthase (γ-ECS) gene. Our results showed that transgenic lines, when exposed to Ag NPs and $AgNO_3$ (Ag^+ ions), were significantly more tolerant in terms of fresh biomass, total chlorophyll contents, transpiration rates. MDA contents were much lower than the wild type (WT) plants. In addition, transgenic γ-ECS lines could accumulate 2-6 folds Ag in shoot and slightly lower or no difference in root relative to WT plant. These results indicate that GSH and related peptides protect plants from Ag nanotoxicity.

(3) The third aim was to investigate the physiological effects of Ag NPs on soybean and to characterize the role of GSH in detoxification of Ag NPs and enhancement of nitrogen assimilation. Our results showed that the presences of Ag NPs could severely compromise the nitrogen fixation via symbiotic relationship in soybean. The total number of nodules and *Rhizobium* sp. growth in HM medium were inhibited upon exposure to Ag NPs. Elemental analysis indicated that Ag NPs mainly accumulated in the root system, and more than 50% Ag was in form of Ag-GSH, and the rest part remained in Ag NPs. The additions of GSH could notably counteract Ag nanotoxicity and enhance total N levels in soybean. Thus, plant might utilize GSH as a nitrogen source and might need

very less help from the symbiotic relationship with *Rhizobium* sp. to assimilate the N. The related work is currently underway to further investigate the role of GSH in metal detoxification and N enhancement.

TABLE OF CONTENTS

LIST OF TABLES

Table **Page**

LIST OF FIGURES

Figure **Page**

CHAPTER 1

LITERATURE REVIEW

1.1 Introduction

Nanotechnology has been thoroughly integrated into modern existence with impacted industries including manufacturing, biomedical applications, electronics, telecommunications, agriculture, and renewable energy. At present, nanoparticles of silver (Ag NPs), titanium oxide (TiO_2 NPs), zinc oxide (ZnO NPs) and cerium oxide (CeO_2 NPs) are the mostly widely used materials, being incorporated into products such as cosmetics, pharmaceuticals, electronic devices, herbicides, and food additive.[1] Approximately 3000 tons of TiO_2 NPs were produced yearly [2] and more than 50% were used in personal care products such as sunscreens.[3] ZnO NPs have uses similar to TiO_2 NPs, including application in sunscreens and paints.[4] Cerium is the most widely used rare earth elements (REEs); CeO_2 NPs possess useful and unique magnetic, catalytic and optic properties, and are mainly used in polishing technologies, fuel cells, cosmetic additives and industrial products.[5] As examples, nanomaterials have been applied in medicine and biology, including as fluorescent biological labels, for drug and gene delivery and as probes of DNA structure.[6, 7] Ag NPs were suggested as playing a role in the treatment of HIV [8] and ZnO NPs have been evaluated for tumor cell destruction and also to serve as a targeted delivery agent for drug treatment.[9]

With the widespread use of consumer products that contain nanomaterials, concerns over the safety of nanotechnology have been increasing.[10, 11] Although nanomaterials bring many benefits, the unique properties of these substances enable them

to more effectively penetrate in the cells and cause nanotoxicity to microorganisms, plants, and animals. Zhao *et al.* indicated that copper oxide nanoparticles (CuO NPs) could cause membrane damage to *Escherichia coli* as demonstrated by K^+ leakage.[12] Zebrafish (*Danio rerio*) is a widely used organism to study toxicological effects of different kinds of nanoparticles. One recent study showed that as exposure days increased, the number of viable embryos was decreased significantly under TiO_2 NPs exposure.[13] Yang *et al.* considered other environmental factors such as sunlight and dissolved organic matter, and observed that nanotoxicity of TiO_2 NPs in the presence of humic acid (HA) was greatly enhanced without simulated sunlight compared to TiO_2 NPs treatment only.[14] The cytotoxicity of cobalt (Co) and CuO NPs to human lung epithelial A549 cells were reported recently.[15, 16] Both of these studies concluded that reactive oxygen species (ROS) were induced upon NPs penetration of A549 cells, causing subsequent irreversible DNA damage as demonstrated by the comet assay.

Plants, being the dominant species, are critical to ecosystem function and food supply integrity. Based on the findings of recent laboratory studies, abiotic and oxidative stresses caused by nanoparticle exposure in plants were described at both physiological and biochemical levels.[17, 18, 19, 20] A common finding from plant nanotoxicity studies is that excess amounts of ROS are produced upon NP (CuO NPs, Ag NPs, CeO_2 NPs) exposure to terrestrial plant species such as wheat (*Triticum aestivum L.),* rice (*Oryza sativa L.),* onion (*Allium cepa L.),* corn (*Zea mays*).[18, 21, 22, 23] ROS could induce damage of critical biological molecules such as lipids, proteins and DNA.[24] For example, ZnO and CeO_2 NPs caused increased chromosomal aberration indices and lipid peroxidation in *A. cepa* [25] and *Arabidopsis thaliana* [20], respectively. In order to understand gene

regulation in plants to NPs exposure, microarrays were used to analyze gene regulation in *A. thaliana* treated with ZnO and TiO_2 NPs. Although both NPs disrupted gene regulation involved in response to abiotic stresses, genotoxicity was highly NP-specific, with ZnO NPs inducing a much greater molecular response than TiO_2.[26]

Overall, it is clear that metal-based NPs can cause toxicity to biota in the environment. Regardless of the pathway of metal-based NPs released or discharged in the environment, their potential risks need to be fully characterized so as to avoid negative impact on environmental and human health.

1.2 Distribution of Metal-based NPs in Higher Plants

1.2.1 Bioaccumulation of Metal-based NPs in plants

For understanding metal-based NPs interactions with terrestrial plants, it is critical to thoroughly characterize the particles distribution and fate within the individual tissues. However, due to differences in plant species, growth conditions such as soil matrix, temperature, humidity, light, and exposure periods, it is difficult to draw conclusions regarding the NPs uptake in plants. Thus, bioaccumulation factor (BAF), defined as [concentration of metal in plant shoot or root] / [exposure concentration in soil or water/hydroponic solution], was calculated to compare and analyze the differences of NPs uptake in higher plants. Investigations where separate root and shoot tissues were harvested from either in soil or hydroponic solution amended with NPs were selected to calculate tissue-specific BAFs. The BAF in shoots and roots exposed to different strengths of Hoagland's solution amended with Ag NPs and CeO_2 NPs are higher than

accumulation in plants grown in soil. In addition, uptake of metal-based NPs in plants is influenced by nanoparticle size, which was demonstrated in cucumber (*Cucumis sativus*) exposed to CeO_2 NPs (7 and 25 nm) [27], as well as for annual ryegrass (*Lolium multifolrum*) exposed to Ag NPs (6 and 25 nm).[28] Interestingly, ZnO NPs seem to behave differently with regard to exposure medium. The BAF in both roots and shoots of perennial ryegrass (*Lolium perenne*) [29] and velvet mesquite (*Prosopis juliflora-velutina*) [30] are lower than that of edible crops (soybean, corn, wheat and green peas) grown in soil. [31, 32, 33, 34] However, comparison across species is confounded by the fact that species-specific mechanisms for metal-based NPs uptake and translocation may occur. Annual ryegrass [28] and perennial ryegrass [29] are related species that were used to conduct phytotoxicity of Ag NPs and ZnO NPs, respectively. The BAF of Ag NPs in annual ryegrass roots is 13-23, depending on nanoparticle size, which is much higher than the BAF of ZnO NPs in perennial ryegrass roots. Both soybean [32] and corn [23, 33] bio-accumulated more ZnO NPs in both shoot and root parts than CeO_2 NPs in the soil amended with these particles. In addition, the BAF in both shoot and root of Ag NPs treated soybean is significantly lower than the ones exposed to CeO_2 NPs and ZnO NPs.[32, 35] These studies showed that NPs enter the plant roots and accumulated in various tissues. However, to fully understand metal-based NPs behavior in plants, more studies are necessary to consider factors such as soil texture, medium strength, and exposure time that affect the NPs uptake and accumulation in plants. Since there is a lack of sufficient data to compare or summarize the uptake patterns of these NPs in plants, we will discuss their impacts from the perspective of nanotoxicity in the sections below.

1.2.2 Nanoparticle Distribution in Plants

The impact of NPs exposure on plants depends on the effective transport, translocation and accumulation of NPs in plant tissues and organelles. Transmission electronic microscopy (TEM) is one of the most common and direct techniques to locate NPs in plant cells. When metal-based NPs are present either in medium or soil matrix, NPs may move through the symplastic or apopolastic region to penetrate the epidermis of roots, pass through cortex, and finally translocate and distributed to stems and leaves via the xylem and phloem. CeO_2 NPs aggregates were confirmed in roots of corn grown in solution containing 200 mg/L CeO_2 NPs and were mainly distributed through apoplastic route.[36] A similar translocation pattern was evident for lanthanum oxide NPs (La_2O_3 NPs) in cucumber exposed to NPs amended distilled water.[37] Fluorescent-labeled mesoporous silica nanoparticles (FLMSNPs) were used to observe how NPs transport in different plant species under hydroponic conditions. Evidence of FLMSNPs accumulation in the casparian strip and flow of fluorescent aggregates towards xylem vessels were observed in wheat roots after 5 days of NPs exposure. Similarly, FLMSNPs were present in the epidermis and endodermis of exposed lupin (*Lupinus L.*) roots.[38] Additionally, transport data of superparamagnetic iron oxide NPs (SPIONs) in soybean and ZnO NPs in corn was reported to occur within xylem vessels.[33, 39] However, other studies demonstrated that NPs transport might involve both xylem and phloem. Au NPs were found in both plasmodesma of the phloem complex and in xylem vessels within exposed woody poplar (*Populus deltoids* × *nigra*), indicating that both sieve tube elements (elongated cells in the phloem vessels) and xylem structures participated in NPs transport.[40] In agriculture, NPs have been used as an additive in pesticide or herbicide formulations due to their

antimicrobial properties [41, 42] that are applied directly to plant leaves via foliar spray. Absorbed NPs from the foliar application could be redistributed to roots or other plant tissues via phloem vessels. Nanoparticles of both CeO_2 and calcium oxide (CaO) were shown to translocate to roots via phloem tissues after foliar application to cucumber seedlings and groundnut (*Arachis hypogaea*), respectively.[43, 44] By contrast, no CeO_2 NPs were evident inside the hydroponically grown cucumber root cells upon exposure to 20 mg/L CeO_2 NPs for 7 days, indicating NPs could not effectively penetrate the root epidermis and likely only aggregated on the root surface.[27]

Few studies have shown the localization and distribution of trace metal oxide nanoparticles, such as CuO NPs and TiO_2 NPs inside plant cells.[45, 46] Both leaves and roots of *Elsholtzia splendens* (a member of mint family Lamiaceae) exposed to CuO NPs had the particles located in the intercellular space or protoplast, as shown by TEM-EDS.[45] TiO_2 NPs were mainly translocated into the vacuole and chloroplasts of plant cells in the roots and shoots of exposed wheat.[46] Similarly, CuO NPs were shown to cross the epidermal cell walls of root of maize seedlings and were localized in the cytoplasm.[47] Faisal *et al.* used TEM to suggest that nickel oxide nanoparticles (NiO NPs) could either accumulate in the intercellular spaces of tomato roots or pass through parenchymal cell wall to eventually locate in the vacuole. However, confirmation of the presumed visualized NPs was not obtained.[48] Although, the translocation and distribution of NPs of trace metal oxides is shown in the above-mentioned studies, the information regarding the translocation and distribution of REEs is not clear.[49, 50]

Micro X-ray fluorescence (μXRF) is another method to trace the distribution of metal elements by providing tri-colored elemental image maps of plant tissues. Upon NPs accumulation in plants, the X-ray absorption spectroscopy (XAS) can clearly show metal-based NPs distribution and biotransformation. The μXRF and XAS analysis of elemental Zn from ZnO NPs exposed velvet mesquite was shown mainly in the root cortex, as well as in vascular tissue and mesophyll of leaves analyzed.[30] Similarly, elemental Ce was found in the transport system of rice roots when treated with 500 mg/L CeO_2 NPs for 10 days by μXRF.[51] NPs size can also influence the location of particles accumulation in plants. Ti from 14 nm TiO_2 NPs tended to accumulate in the root parenchyma of both rice and rapeseed (*Brassica napus*), whereas, 25 nm NPs had Ti largely in the root vascular cylinder as analyzed by μXRF.[52] Other studies have shown that the crystal phase of TiO_2 NPs influenced *in planta* accumulation of TiO_2 in cucumber. For example, anatase-TiO_2 NPs was found predominantly in the xylem and cortex, while rutile-TiO_2 NPs were accumulated in phloem of exposed cucumber as shown by both μXRF and XAS.[53]

Not surprisingly, several groups have shown that the accumulation and translocation of metal-based NPs in plants is also species specific. Differential bioavailability of Au NPs to tobacco and wheat grown in Au NPs amended nutrient solution were reported through μXRF images. No Au was found to penetrate wheat root surfaces upon exposure to three different sizes of Au NPs coated with either citrate or tannate, but elemental Au was observed in tobacco leaves after treatment with 30 nm citrated coated Au NPs.[54] Definitive evidence of TiO_2 NPs and CeO_2 NPs presence in the edible tissues of exposed cucumber and soybean were reported by both μXRF and XAS.[55, 56] These studies clearly showed the accumulation of metal-based NPs within food

crops, including the edible tissues, can readily occur. Once NPs are in the food chain, transfer and accumulation within humans becomes a possibility. Consequently, the potential risks and implications of NPs to the food chain should become a topic of intense investigation.

Although many studies have demonstrated the *in planta* NPs translocation, the mechanisms remain unclear. The plant cell wall has a unique structure, mainly composed of cellulose (40.6-51.2% of the cell wall material) and lignin (10-25% of the cell wall material), both of which can obviously influence the structure and permeability of the cell.[57] The cell wall has ability to physically exclude certain large molecules.[58] The typical pore size of the cell wall is 5-10 nm, which is large enough to allow small protein diffusion [59], but NPs in the environment may be excluded, especially if agglomeration as a function of pH, ionic strength and organic matter has occurred. However, some fraction of NPs will still likely be less than the 5-10 nm range and able to readily penetrate the cell wall. NPs exposure may cause ROS production or have other effects that may alter the cell wall structure. If large amounts of NPs are detected within plant cells by TEM and XAS, cell wall structure should be analyzed for such damage or alteration.[60] Nano zerovalent iron (nZVI) induced OH^- radicals that triggered cell wall loosening in Arabidopsis roots, further reducing cell wall thickness of the seedling.[61] The authors indicated that this NPs induced ROS impact could be one of the most important reasons as a result of NPs accumulation inside of plants. Additional investigations are needed to characterize the role of pore size change of cell walls in the accumulation and translocation of NPs in higher plants.

1.2.3 Biotransformation of metal-based NPs inside plants

Previous studies have demonstrated that metal-based NPs can release ions into the substrate (medium or soil matrix).[29, 62] As such, in experiments evaluating metal-based NPs and plants interactions, ion controls must be included in the design so as to appropriately assess the role of elemental particle size and dissolution in damages at both physiological and genotoxic levels in higher plants. In order to address this issue, XAS can be applied to evaluate potential *in planta* biotransformation of NPs. For example, X-ray absorption near edge structure (XANES) analysis of alfalfa (*Medicago sativa*) exposed to tetrachloroaurate, Au (III), was shown to be converted to Au (0) in the range of 2-20 nm in both roots and shoots; a finding further confirmed by TEM and X-ray EDS.[63] Several studies have used XAS to determine metal speciation in the exposed plant so as to illustrate the form or transition state played the dominant role in oxidative stresses induction. Soybean accumulated both 462 mg/kg Ce and 150 mg/kg Zn when exposed to 4000 mg/L of CeO_2 and ZnO NPs, respectively. Interestingly, Ce (IV) was found in the plant tissues, similar to the form present in the original CeO_2 NPs; however, no ZnO NPs were found, suggesting significant transformation. As such, this study demonstrates that nanotoxicity can be induced by either the NPs itself or from metal ions released from NPs.[64] ZnO NPs can release relatively high amounts of Zn ions at pH 7.5 (19%) [65], which may explain the lack of *in planta* detection of ZnO NPs in this study. Others have reported that CeO_2 NPs accumulate in the roots of edible plants, including cucumber, alfalfa, tomato, corn and kidney bean (*Phaseolus vulgaris*).[66, 67] Further, both Ce and Zn could accumulate in the pods of soybean in soil grown plants in the presences of CeO_2 NPs and Zn-citrate, respectively. However, without ionic metal control, it was

not possible to assess the source and nature of the accumulated metals.[55] Consistent results were reported for several REE NPs, including CeO_2, Yb_2O_3 and La_2O_3 NPs; all were partially biotransformed to phosphate precipitates in cucumber, although the majority of the contaminant was still present as RRE NPs.[68, 37, 50] Similarly, Zn-phosphate formed from Zn ions released from the NPs accumulated in wheat shoots; there was no ZnO NPs signal detected by XAS.[18] By analyzing Zn speciation in the soil matrix, it was noted that ZnO NPs can transform into Zn ions rapidly; after 1 hr, there was no Zn detected in the NPs form.[69] However, both CuO NPs and Cu-sulfide were detected in wheat shoots grown in 500 mg/kg CuO NPs amended sand.[70] Similarly, Shi *et al.* reported that CuO NPs in Elsholtzia (*Elsholtzia splendens*) could be transformed to Cu-Alginate, Cu-Oxalate and Cu-Cysteine.[45] Whether Cu NPs or ions can be taken up first, with subsequent transformation to these compounds is not clear. Hence, more research is needed to provide clear evidence for the mechanisms and temporal/kinetic aspects of NPs transformation in plants.

Although XANES could be helpful to better understand NPs behavior inside plants, the most essential issue is to understand the mechanisms of biotransformation of metal-based NPs, including in both the growth media and the plants. Based on a summary of what is currently known, CeO_2 NPs can be accumulated by many plant species but transformation appears to be limited. However, for plants exposed to ZnO NPs, the metal ions appear to be most abundant inside the exposed plants, which subsequently causes abiotic stress. The question remains open is on the precise means by which ZnO NPs transforms to the ions. We suggest two hypotheses: one is that ZnO NPs release metal ions in the substrates, which are then available for plant uptake, and ZnO

NPs do not enter the plant directly. Once in the plants, the ions may or may not be subsequently reduced to NP form. The second possibility is that ZnO NPs enter the plant directly by unknown means, with dissolution to ions happening subsequently via species-specific processes inside plant. Either mechanism would explain the general lack of *in planta* detection of NPs.

1.3 Phytotoxicity of NPs at physiological and morphological levels in plants

1.3.1 Effects at Physiological levels

Nanotoxicity of metal-based NPs to plants at the physiological level has been demonstrated by root length inhibition, biomass decrease, altered transpiration rate and plant developmental delays.[17, 71, 72, 73, 74] Figure 1.1 describes potential oxidative damage in different organelles within plant cells through interactions with metal-based NPs. Once NPs enter plant tissues, the particles could disrupt the synthesis of chlorophyll in leaves. Chlorophyll content was significantly reduced in wheat exposed to 500 mg/kg CuO and ZnO NPs as compared to controls.[18] Similar results were reported for ZnO NPs (0 to 500 ppm) treated green peas, and Ag NPs (100 and 1000 ppm) treated tomatoes.[34, 75] Ag NPs exposure only inhibited chlorophyll b content in rice [22]. The chlorophyll content in soybean exposed to either 400 or 800 mg/kg CeO_2 and ZnO NPs was not significantly different from control plants.[76] In addition to negative effects on chlorophyll biosynthesis, other NPs such as Au, TiO_2, and ZnO were shown to enhance the chlorophyll content in mustard (*Brassica juncea)*, cucumber and cluster bean (*Cyamopsis tetragonoloba L.*), respectively. [56, 77, 78]

Lipid peroxidation is another important parameter that is indicative of cell membrane integrity. ROS generation is known to be a primary factor that results in cell membrane damage through lipid peroxidation, leading to ion leakage and potential cell death. Both CuO and ZnO NPs at 500 mg/kg induced lipid peroxidation in sand grown wheat [18], although the ion leakage was not assessed in this study. Another study on corn exposed to CeO_2 NPs indicated that lipid peroxidation directly led to ion leakage.[23] Conversely, Rico *et al.* reported no elevation of lipid peroxidation in rice treated with CeO_2 NPs (0-500 mg/L), but ion leakage was observed at the higher exposure concentrations.[79]

Another impact of interest from metal-based NPs exposure involves nutrient transport and assimilation in plants. Several reports suggest this possibility, and if widespread, *in planta* nutrient cycling disruption could be more deleterious to plants than ROS-related effects. CeO_2 NPs were shown to significantly diminish N_2 fixation in the nodules of soybean, which subsequently lead to reduced plant growth from N deficiency.[32] ZnO NPs had no such impacts on N_2 fixation in the same study. Specific nutrients, such as phosphorus (P), could bind to the surface of CeO_2 NPs, which can significantly lower elemental bioavailability and cause nutrient deprivation in plants.[80] Conversely, TiO_2 NPs at 500 mg/L was shown to significantly enhance P and K availability in cucumber fruit.[56] Another study related to Au NPs in Arabidopsis showed evidence of down regulation of genes involved in metal transporters (such as Zn, Na, Ca, Cu, Fe and Mn) and aquaporins (integral membrane pore proteins). This down regulation of cation transporters may be a defense mechanism that inhibits Au uptake and further alleviate phytotoxicity.[81] Although there is indirect evidence that NPs could disrupt ion-

selective channels, analysis of the regulation of genes involved in nutrient transport as a function of exposure may shed light on both the positive and negative impacts of NPs on plant growth.

1.3.2 Effects at Morphological level

Morphological changes in plants, especially in roots, have been observed with NPs exposure. In the roots of *L. multiflorum* exposed to 40 mg/L Ag NPs, highly vacuolated cortical cells and a damaged root cap were observed by light microscopy.[28] REE NPs such as Yb_2O_3 were also shown to cause severe cellular morphological changes in the meristem and root cap of exposed cucumber.[68] Interestingly, a tunneling-like effect was reported in root tip cells of maize treated with 1000 μg/mL ZnO NPs, which could cause cellular disintegration.[19] Since the literature on morphological changes in plant roots is not extensive, it is unclear whether the impacts on plants are dependent on metal-based NPs or plant species or both. Also, a better understanding of whether these morphological changes such as the formation of highly vacuolated cortical cells are the means of defense against abiotic/oxidative stress caused by NPs exposure is needed, as this organelle is known as a primary storage site for toxic substances.

1.4 Metal-Based NPs Induce DNA Damage in Higher Plants

Although a number of studies have demonstrated that metal-based NPs can cause oxidative stress through ROS production, far less is known about the potential for DNA damage upon particle exposure. Atha *et al.* investigated the genotoxic effects of CuO NPs exposure on three terrestrial plants.[82] In this study, the levels of three oxidatively

modified bases: 7,8-dihydro-8-oxoguanine (8-OH-Gua), 2,6-diamino-4-hydroxy-5-formamidopyrimidine (FapyGua) and 4,6-diamino-5-formamidopyrimidine (FapyAde), which can cause G-T, A-C and A-T transversion, respectively, were measured by GC/MS in radish (*Raphanus sativus*) and perennial ryegrass after exposure to different concentrations of CuO NPs (10-1000 mg/L). The amount of all three compounds, expressed as lesions/10^6 DNA bases, were significantly increased as CuO NP exposure increased. The Comet assay is another common procedure to determine DNA damage in plants. TiO_2 NPs induced DNA damage in *A. cepa* when exposed to 4 mM TiO_2 NPs for 3 hours. After 24 hours, % tail DNA in 2 mM TiO_2 NPs treated *A. cepa* was almost three times higher than control group.[83] DNA damage was also noted in tomato and *A. cepa* exposed to NiO NPs and Ag NPs, respectively.[21, 48]

An analysis of the mitotic index (MI), chromosomal aberrations (CA) and micronuclei induction (MN) also provide evidence for the genotoxicity of NPs in plants. A dose-dependent relationship between MI and exposure concentration of Ag NPs and ZnO NPs was observed in the root tips of broad bean (*Vicia faba*) and *A. cepa*, respectively.[25, 84] A similar dose-dependent response of MI/CA was found in TiO_2 NPs treated *Vicia narboensis L.*, maize [85], and *A. cepa* exposed to Ag NPs.[21] The random amplified polymorphic DNA assay (RAPD) is another method that has been used to assess DNA damage and stability in plants treated with different metal-based NPs. Lopez-Moreno *et al.* exposed soybean to ZnO NPs and CeO_2 NPs, nanoceria was found to cause DNA instability/alteration at both 2000 and 4000 mg/L.[64] Although DNA damage induced by metal-based NPs in plants has been documented, the mechanism of that damage, it's severity relative to plant health, and whether plants can recover from

that DNA damage need further investigations. In addition, to further understand molecular and biochemical responses of plant to metal-based NPs, it is necessary to study the global response of plants at transcriptome, proteome and metablome levels in plants.[86]

1.5 Production of excessive ROS in response to metal-based NPs toxicity

Under the non-stressed environmental conditions, reactive oxygen species (ROS) can be byproducts of normal metabolic pathways localized in organelles such as chloroplasts, mitochondrion and peroxisomes.[87] These ROS are balanced or removed by specific housekeeping antioxidant enzymes such as superoxide dismutase (SOD), catalase (CAT) or ascorbic peroxidase (APX), whose activity helps to avoid oxidative damages in plants.[88] However, abiotic stresses (e.g., salt, high or low temperature and heavy metals) can generate excessive amounts of ROS, which can cause severe oxidative damage to plant biomolecules through electron transfer.[89] There are four important types of ROS, including singlet oxygen ($^1O_2$), superoxide ($O_2^{\bullet-}$), hydrogen peroxide (H_2O_2) and hydroxyl radical ($HO^{\bullet}$).[90] In order to lower the toxicity of ROS to plants, specific defensive antioxidant enzymes such as SOD, can convert highly toxic ROS ($O_2^{\bullet-}$) to less toxic species (H_2O_2). However, H_2O_2 can initiate the Fenton reaction, which is catalyzed by metal ions (Fe^{2+}, Cu^{2+}), and generate $HO^{\bullet}$, highly reactive ROS (hROS), which cannot be detoxified by any known enzymatic system. In plants, this hROS has the ability to induce adverse and irreversible damage on biomolecules such as lipids, DNA, and proteins.[90, 91] So far, there are no reports on $HO^{\bullet}$ determination in plants as a function of metal-based NPs exposure.

The levels of H_2O_2 can be readily measured to determine ROS production as a function of metal-based NPs exposure in plant tissues. H_2O_2 levels in a two rice cultivars exposed to same concentration of CeO_2 NPs showed varied response. H_2O_2 level in rice cultivar 'Neptune' was almost three times higher than the control group upon exposure to 500 mg/L CeO_2 NPs [51], whereas cultivar 'Cheniere' showed no significant difference upon exposure to the same concentration of CeO_2 NPs.[79] However, low dose exposure (62.5 mg/L) in both rice cultivars showed that H_2O_2 was scavenged.[51, 79] Lee *et al.* provided evidence to demonstrate that CeO_2 NPs at lower exposure concentration (50 mg/L) could eliminate ROS through a Fenton-type reaction.[92] Zhao *et al.* measured H_2O_2 level in corn grown in CeO_2 NPs amended soil, and reported effective antioxidant defense through CAT and APX activities, both of which converted ROS to H_2O. The authors also reported that the H_2O_2 was predominantly located in epidermal, parenchyma and bundle sheath cells within the leaf tissue.[23]

Other metal-based NPs such as Ag NPs and ZnO NPs have been shown to generate excessive amounts of ROS, which subsequently caused a series of adverse effects on plants, such as cell death, DNA damage, pollen membranes integrity and chlorophyll content.[21, 34, 93] Panda *et al.* not only reported higher H_2O_2 levels in *A. cepa* upon exposure to Ag NPs but also that the level of $O_2^{\bullet-}$ was significantly elevated.[21] To our knowledge, this is the only report on $O_2^{\bullet-}$ level in plant tissues when treated with NPs. The relationship between $O_2^{\bullet-}$ and H_2O_2 production and NPs-induced phytotoxicity is still unclear. As mentioned earlier, in order to defend against oxidative stresses, plants are capable of converting more toxic ROS ($O_2^{\bullet-}$) into less toxic species. Hence, it is necessary to determine the relationship among different types of ROS induced by metal-bases NPs,

and to gain additional information to further understand the roles of protective antioxidant enzymes on ROS scavenging. As mentioned above, no known antioxidant systems can successfully transform HO• produced in response to NPs exposure. Therefore, further studies should be focused on differentiating between the types of ROS formed in response to exposure to various NPs, which will help us in understanding the mechanisms of antioxidant enzymes for protecting plants from oxidative stress.

1.6 Role of glutathione and its related peptides in detoxification of metal-based NPs in plants

GSH as a well characterized antioxidant and a critical component of defenses for oxidative stresses caused as a result of heavy metals exposure.[94, 95, 96] The GSH biosynthesis pathway starts with sulfur assimilation through the activity of sulfate adenylyltransferase (ATPS), adenosine-5'-phosphosulfate reductase (APSR) and sulfite reductase (SiR), to generate sulfite which is a precursor of cysteine.[97, 98, 99] GSH biosynthesize is catalyzed by cysteine synthase (CS), γ-glutamylcysteine synthase (γECS) and glutathione synthase (GS) to produce cysteine, γEC and GSH, respectively.[96, 99] GSH can scavenge ROS and be oxidized to a disulfide form (GSSG), which can then be recycled by glutathione reductase (GR). Phytochelatins (PCs), synthesized by phytochelatin synthase using GSH as substrate, play important roles in the detoxification of heavy metals by chelating metal ions, with subsequent storage in vacuoles and the cell wall.[100, 101, 102]

The heavy metal detoxification pathway through GSH biosynthesis has been well characterized. By overexpressing γECS gene in shoots of *A. thaliana*, Li *et al.* showed

that significantly higher levels of GSH and PCs were produced upon arsenic (As) and mercury (Hg) exposure, leading directly to increased metal tolerance as evident in the phenotype of transgenic plant.[103] Similarly, Pauolse *et al.* and Zulfiqar *et al.* reported that transcripts involved in sulfur assimilation and glutathione biosynthesis were upregulated in *Abyssinian mustard* (*Crambe abyssinica* Hochst. Ex Fries) that was treated with As and Cr.[104, 105]

Whether the similar phenomenon is activated upon NPs phytotoxicity is still unclear, although some studies have begun to assess GSH levels in plants exposed to metal-based NPs. Plant gene regulation involved in sulfur assimilation and GSH biosynthesis upon metal-based NPs exposure were first reported in *A. thaliana* exposed to CeO_2 and In_2O_3 NPs.[20] This study showed that both CeO_2 and In_2O_3 NPs could induce upregulation of genes related to both sulfur assimilation and GSH biosynthesis pathways. GSH or GSSG quantification may be used as an alternative method to demonstrate the role of the GSH biosynthesis pathway in NPs detoxification. Dimkpa *et al.* measured transcripts encoding metallothionein (MT), which is a cysteine-rich protein, and GSSG in wheat were determined after exposure to Ag NPs, Ag^+ ions and bulk Ag in sand. MT and GSSG levels were highly induced with the Ag NPs and Ag^+ ions treatments.[62] Consistent results showed that the level of GSSG in wheat shoots and roots grown in CuO and ZnO NPs mixed sandy soil were elevated as well.[18] However, increased levels of GSSG could not be used to directly show that high levels of GSH were depleted to convert ROS into H_2O. There was a dose-dependent response between GSH levels and exposure to NiO NPs.[48] GSH level was found to increase in tomatoes treated with 1000 mg/L NiO NPs, although a slight decline of GSH level was observed at 1500 and 2000 mg/L NiO NPs

doses but the concentration was still significantly higher as compared to the control. These studies indicate that GSH is involved either in detoxification of metal ions released from NPs or tackling of ROS generated in response to NPs exposure in plants. To date, except one study [20], there is no reported studies evaluating either gene regulation or antioxidant levels, such as cysteine, GSH and PCs, as part of the sulfur assimilation and GSH metabolic pathway in response to NPs phytotoxicity. Understanding plant's response to nanotoxicity at the molecular level will be critical to accurately assessing overall exposure, risk concerns and developing strategies to mitigate those nanoparticles associated risks. Therefore, in order to understand the interaction between several metal-based NPs and plants at molecular and biochemical levels, and to investigate the role of GSH in detoxification of metal-based NPs in plants, we propose the following specific aims:

Specific Aims

1. Analysis of *Arabidopsis thaliana* for physiological and molecular response to CeO_2 and In_2O_3 NPs exposure.
2. Investigation of the enhanced level of GSH on alleviating Ag NPs toxicity to *Crambe abyssinica*.
3. Characterization of the role of GSH in detoxification of silver nanoparticles and enhancement of nitrogen assimilation to improve yield in soybean (*Glycine max*).

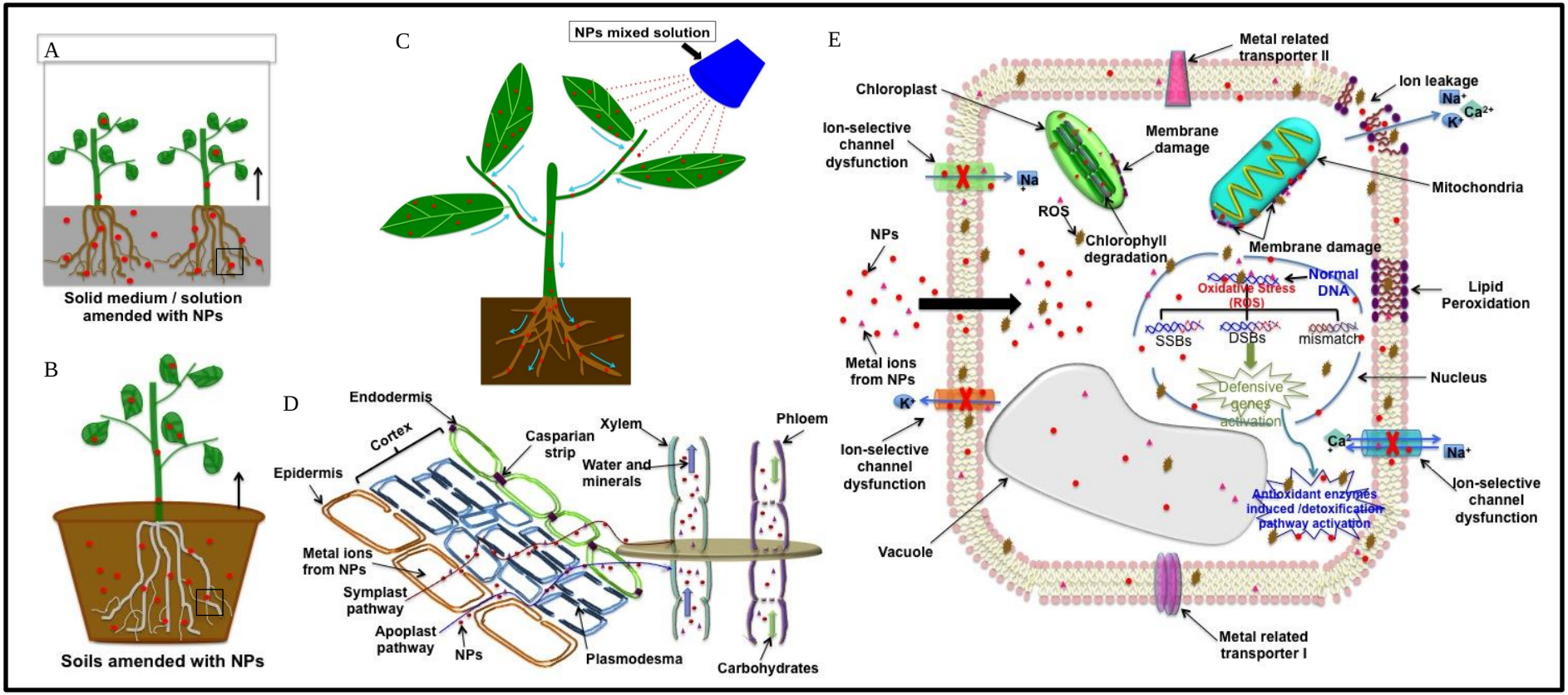

Figure 1. 1 Schematic diagram of possible routes of NPs uptake by roots and cell damages caused by NPs exposure. (**A**) Plants grown in a medium amended with NPs. (**B**) Plants grown in soils amended with NPs. (**C**) NPs exposed on plants via foliar spray. (**D**) Symplast and apoplast could be mostly possible routes for NPs entering plants. (**E**) Potential damages could be caused by NPs at the cellular level. Other damages at molecular and biochemical levels, such as DNA damages and transcription levels of genes involved in NPs detoxification pathways are also present.

CHAPTER 2

PHYSIOLOGICAL AND MOLECULAR RESPONSES OF *ARABIDOPSIS THALIANA* TO CEO_2 AND IN_2O_3 NPS EXPOSURES

2.1 Introduction

The use of nanotechnology in industries such as medicine, energy, cosmetics and agriculture has increased rapidly, and as such, concerns over the risk of nanomaterial exposure to the environment and to human health have been frequently raised.[106,107] According to the model of Keller and Lazareva, the release of engineered nanomaterials (ENMs) in the United States will be from 7-20% of that produced, although the precise amount at a given location will vary with wastewater management/treatment techniques and biosolids disposal.[2] Once released to soil, the fate, bioavailability and toxicity of nanoparticles (NPs) are dependent on particle aggregation, surface properties, soil characteristics, and ion release.[108, 109] Investigations focusing on the effects of NPs on plant species is a prerequisite for understanding the ultimate risk posed by these materials in the environment. So far, most of the studies related to nanotoxicity in the environment have focused mainly on two different aspects: investigation on nanotoxicity to living organisms in environmentally realistic scenarios and characterizing the underlying biochemical/molecular mechanisms of nanotoxicity under the laboratory conditions. A growing number of laboratory studies have been conducted where high (500-5000 mg/kg) doses of NPs are applied to evaluate nanotoxicity to terrestrial plants over short time periods. Investigations focusing on phytotoxicity caused by NPs exposure at more environmentally relevant concentrations over longer periods of time are far more limited.[110] By the simulated application of contaminated sewage and biosolids, Colman

et al. demonstrated that low exposure dose (0.14mg/kg) of Ag NPs resulted in *Microstegium vimeneum* biomass decreases by 32% and significantly declined the microbial richness (101±22 operational taxonomic unit, OTUs).[111] Similarly, upon exposure to 2.5 mg/L Ag NPs, phytoplankton cell density was reduced during the first 4 days of the test.[112]

Plants are critical to both ecosystem function and to the human food supply; however, information on the interactions of REE oxide NPs with these organisms is rather limited. Ma *et al.* (2010) measured the effect of several REE oxide NPs on the root elongation of a number of plants and reported both species- and particle-specific effects.[49] Oxides of Gd, La, and Yb proved to be quite phytotoxic, whereas NP CeO_2 had negative effects on only one of seven species tested. Similarly, Birbaum *et al.* (2010) failed to observe CeO_2 NP translocation in exposed maize.[113] A number of additional reports have addressed the effects of CeO_2 NPs on plant species such as *Medicago sativa*, *Cucumis Sativus*, and *Lycopersicon esculentum*. In general, results showed that CeO_2 NPs may accumulate in some plant species as exposure concentrations increases; however, traditional measures of phytotoxicity were largely unaffected by particle exposure.[114,115,50,116] Interestingly, Lopez-Moreno *et al.* (2010) noted that NP CeO_2 negatively impacted the germination of four crops but also generally increased root and shoot elongation of seedlings of the same species.[116] In another study, Lopez-Moreno *et al.* (2010) described NP-specific changes in the molecular profile of soybean upon exposure to CeO_2 NPs as measured by random amplified polymorphic DNA assays.[114] More recently, Zhao *et al.* (2012) reported that ROS production caused by CeO_2 NPs exposure in *Zea mays* induced catalase and ascorbate peroxidase, both of which are

related to stress defense.[117] Notably, no reports were found in which the phytotoxicity of NP In_2O_3 was investigated. To achieve the necessary comprehensive understanding of plant-NP interactions, including overall response, effects, and accumulation; under REE oxide NPs exposure, parallel biochemical and molecular endpoints must be evaluated.

In the present study, *Arabidopsis thaliana* was used as model plant to investigate the effects of CeO_2 NPs and In_2O_3 NPs exposure. Representative parameters such as biomass, root length, chlorophyll and anthocyanin content, lipid peroxidation, and elemental content (NPs accumulation and nutrient contents) were measured to understand the plant's defense and response to abiotic stress caused by the REE oxide NPs. In order to achieve a comprehensive understanding of detoxification pathways in plants, the underlying molecular mechanism for defense response was also fully investigated. Activities of ROS scavengers, such as SOD, CAT, APX and POD, and stress related enzymes, including GST, GR, PAL, and PPO, were measured in both NPs treated *A. thaliana*. In addition, upon on exposures to CeO_2 and In_2O_3 NPs, quantitative real-time polymerase chain reaction (qRT-PCR) was used to analyze: the transcript levels of the important genes involved in sulfur assimilation, GSH biosynthesis pathway, as well as iron transport in *A. thaliana*. Our goal was to comprehensively evaluate *A. thaliana* antioxidant defense mechanisms, detoxification pathways, and nutrient status in response to metal oxide NP exposure.

2.2 Methods and Materials

2.2.1 Nanoparticle characterization

Nanoparticle CeO_2 (99.97%, 10 nm to 30 nm) and In_2O_3 (99.995%, 20 nm to 70 nm) were purchased from US Research Nanomaterials, Inc. Solutions at 250 and 1000 mg/L of both NPs were twice dispersed by ultrasonic treatment in half-strength Hoagland's solution and deionozed H_2O for 1 h. The solutions were then maintained in the dark at ambient temperature overnight as described in Lin and Xing (2008).[29] The hydrodynamic diameter (DLS) and zeta potential of NP suspension were analyzed using a Nano Zetasizer; the results are presented in Table 2.1.

2.2.2 Experimental design

A. thaliana seeds were sterilized by 70% (v/v) of ethanol for 5 min and then were soaked in 30% (v/v) of Clorox for 30 min. The seeds were then washed five times with autoclaved deionized H_2O.[118] Twenty five sterilized seeds were placed on each petri dish; there were four replicate dishes for each NPs concentration. Seeds were stratified at 4°C for 24 h prior to transfer to a controlled-environment cabinet (cycling 16 h light and 8 h dark at 22°C and 18°C, respectively) and incubated vertically after germination to facilitate shoot and root growth for an additional 25 days. At harvest, shoot biomass and root length measurements were taken from each replicate dish. Harvested plant tissues were stored at -80 °C until further analysis.

In addition, a hydroponic system was established similar to that described in Dixit and Dhankher.[119] Fourteen days old *A. thaliana* seedlings were transferred to magenta

boxes containing half-strength MS liquid medium amended with 250 mg/L and 1000 mg/L CeO_2 NPs and In_2O_3 NPs separately. Plants were grown in an identical environment as described above. After an exposure period of 5 d, *A. thaliana* root and shoot tissues were harvested and were rinsed with 1 millimol/L nitric acid (HNO_3), followed by three washes with deionized (DI) H_2O.[79] Fresh tissues were oven-dried at 65 °C for 48 h prior to analysis of nutrient uptake and for total N measurement.

2.2.3 Chlorophyll measurement

Chlorophyll content was determined modifying the method of Lichtenthaler (1987).[120] Briefly, 50 mg of fresh leaves were cut into pieces (less than 1 cm) and added to 10 mL of 95% ethanol to extract chlorophyll. All samples were incubated in the dark for 3-d and the absorbance of supernatant was measured at 664.2 nm and 648.6 nm by UV-Vis spectrophotometer (Spectronic Genesis 2). Chlorophyll a, chlorophyll b and total chlorophyll were determined by: $Chla=13.36A_{664.2}-5.19A_{648.6}$, $Chlb=27.43A_{648.6}-8.12A_{664.2}$ and Total chlorophyll=Chla + Chlb.

2.2.4 Anthocyanin measurement

Anthocyanin is an antioxidant as well as a stress response pigment produced by plants as a defense against ROS damage.[121] Harvested *A. thaliana* tissues (50 mg) were ground in liquid nitrogen and then mixed with 1 mL of 1% (v/v) HCl in methanol prior to incubation in the dark at 4 °C overnight. After adding 500 μL of chloroform and 500 μL of DI H_2O to the extracts, the samples were vortexed and centrifuged at 12,000 rpm for 2 min. The absorbance of the supernatant was measured at 530 nm and 657 nm by UV-Vis

spectrophotometer (Agilent 8453). The final anthocyanin concentration was determined by using A_{530} - 1/4 A_{657}.[122]

2.2.5 Lipid peroxidation measurement

Lipid peroxidation was measured by the TBARS assay.[123] Malondialdehyde (MDA), which forms during fatty acid degradation and is indicative of lipid peroxidation, was determined as a function of REE oxide NPs treatment. Specifically, 200 mg of plant tissues (shoots, roots) were homogenized in 4 mL of 0.1% of trichloroacetic acid (TCA). The extracts were centrifuged at 10,000 rpm for 15 min and then 1 mL of supernatant was pipetted into mixture solution containing 2 mL of 20% TCA and 2 mL of 0.5% TBA. After heating at 95 °C for 30 min and cooling on ice, absorbance of supernatant was read at 532 nm and 600 nm by UV-Vis spectrophotometer (Agilent 8453). The final MDA concentration, which is produced by reacting with TBA, was calculated based on Lambert-Beer's equation (extinction coefficient of MDA is 155 mM/cm).

2.2.6 Analysis of ROS production

Total ROS were measured in control and NP treated *A. thaliana* seedlings by using the fluorescent dye 2',7'-dichlorofluorescein diacetate (DCFDA).[123] *A. thaliana* seedlings were soaked in a solution of 1 millimol/L DCFDA for 15 min in dark. Plant tissues were imaged using a Spinning Disc Confocal microscope on a Nikon Ti system running Metamorph imaging software (Yokogawa Electric Corp.) with settings of 400 ms exposure time and a Plant GFP Disk. Fluorescence intensity in each image was calculated by ImageJ 1.49r software.

Hydrogen peroxide (H_2O_2) and superoxide anion ($O_2^{\bullet-}$) were measured in control and NP treated *A. thaliana* seedlings using diaminobenzidine tetrahydrochloride (DAB) and nitroblue tetrazolium chloride (NBT), respectively.[123]

For the H_2O_2 staining assay, *A. thaliana* seedlings were soaked in 1mg/mL DAB solution at pH 3.8. The plant tissues were vacuum-infiltrated at 100 to 150 mbar for 1 min, and this step was repeated 3 times. The plant tissues were then incubated for 5 h in a high humidity environment until dark colored precipitates were observed. Before observing the levels of H_2O_2 in the plant tissues under light microscopy, chlorophyll was removed by 95% ethanol washes. Relative color intensity was calculated in histogram function in Adobe Photoshop CS version 8.0.

For the $O_2^{\bullet-}$ staining assay, the plant tissues were immersed into a staining mixture containing 0.1% (w/v) NBT, 10 millimol/L sodium azide, and 50 millimol/L potassium phosphate and then vacuum-infiltrated at 100 to150 mbar for 1 min, which was again repeated 3 times. The plant tissues were incubated in the mixture for 15 min, and then the infiltrated seedlings were exposed to cool fluorescent light for 20 min at room temperature. The samples were treated with 95% ethanol to stop the reaction and to remove the chlorophyll. Blue staining was then observed in each *A. thaliana* seedling by light microscopy.

2.2.7 Analysis of total protein and antioxidant Enzyme Activity

Fresh root and shoot tissues were homogenized in liquid nitrogen to fine powder. A 0.5 g sample of homogenized tissue was then mixed with 5 mL extraction buffer vigorously for 5 min using a vortex mixer. The mixture was centrifuged at 4421×*g* for 20 min, and the

supernatant in each treatment was used for measuring total protein and antioxidant enzyme activities.

Catalase (CAT) was extracted in 25 mM KH_2PO_4 with pH 7.4. Decreased absorbance in the reaction that contained 100 μL of supernatant and 1900 μL of reaction buffer (10 mM H_2O_2) was recorded at 240 nm for 3 min. The H_2O_2 extinction coefficient was 23.148 mM^{-1} cm^{-1}.[23]

Ascorbate peroxidase (APX) was extracted in 100 mM phosphate buffer (pH 7.0) containing 0.1 mM EDTA, 0.1 mM ascorbate and 2% β-mercaptoethanol. The reaction buffer was made of 50 mM phosphate buffer (pH 7.0) and 0.6 mM ascorbic acid. The total 2 mL reaction system contained 100 μL of enzyme extract and 1900 μL of reaction buffer. Decreased absorbance was monitored at 290 nm for 3 min after initiating the reaction with 10% H_2O_2.[124]

Superoxide dismutase (SOD) was extracted in 50 mM phosphate (pH 7.8) containing 0.1% (w/v) ascorbate, 0.1 % (w/v) bovine serum albumin (BSA), and 0.05% (w/v) β-mercaptoethanol. Nitroblue tetrazolium (NBT) was used to indirectly determine SOD activities. Briefly, 100 μL of enzyme extract and 1900 μL of 50 mM phosphate buffer (pH 7.8) containing 9.9 mM L-methionine, 57 μM NBT, 0.0044% (w/v) riboflavin and 0.025% (w/v) Triton X-100 were mixed in cuvette and placed under fluorescent tube light (light intensity: 250 μmol $m^{-2}s^{-1}$) for 20 min. Reduction in the absorbance of NBT was recorded at 560 nm.[124]

Peroxidase (POD) was extracted in 50 mM phosphate (pH 7.0) containing 1% (w/v) polyvinylpyrrolidone. Briefly, 50 μL of enzyme extract was mixed with reaction

buffer containing 1.75 mL of 50 mM sodium phosphate buffer (pH 7.0) and 0.1 mL of 4% guaiacol in cuvette and 0.1 mL of 1% H_2O_2 was used to initiate the reaction. Increased absorbance was recorded at 470 nm for 2 min.[125]

Polyphenol oxidase (PPO) was extracted in the same buffer as stated in POD extraction. The reaction mixture consisted of 200 μL of enzyme extract and 2.8 mL of 10 mM catechol. PPO activity was recorded by measuring its ability of oxidizing catechol at 410 nm.[125, 126]

Phenylalanin ammonialyase (PAL) was extracted in 0.1 M sodium borate buffer (pH 8.8). 100 μL of enzyme extract was used to react with 2.9 mL of reaction buffer containing 100 mM sodium borate buffer (pH 8.8) and 50 mM 1-phenylalanine at 37 °C for 1 hr. The absorbance change was monitored at 298 nm.[125, 126]

Glutathione S-transferase (GST) was extracted in 50 mM phosphate buffer (pH 7.5) containing 1 mM Ethylenediaminetetraacetic acid (EDTA) and 1 mM dithiothreitol (DTT). 1-Chloro-2,4-dinitrobenzene (CDNB) was used to conjugate with thiol group of glutathione (GSH) and form GS-DNB conjugate. The increase of absorbance recorded at 340 nm for 5 min represents GST activity.[124]

Glutathione reductase (GR) was extracted in 100 mM phosphate buffer (pH 7.5) containing 0.5 mM EDTA. A sample of 100 μL of enzyme extract was added into a reaction buffer containing 500 μL of 2 mM oxidized GSH (GSSG), 50 μL of β-Nicotinamide adenine dinucleotide phosphate, reduced (NADPH) and 350 μL of assay buffer (100 mM potassium phosphate buffer with 1 mM EDTA). The decrease in absorbance was recorded at 340 nm for 2 min.[127]

2.2.8 Elemental analysis of *A. thaliana* tissues

Dry shoot or root tissues were ground to fine powder and approximately 50 mg was transferred into a glass tube containing 3 mL concentrated HNO_3. All samples were digested at 105 °C for 40 min in a heating block and then 500 μL H_2O_2 was added for 20 min to complete the digestion. All digests were diluted with deionized (DI) H_2O to 50 mL prior to elemental analysis for Ce and In by inductively coupled plasma mass spectroscopy (ICP-MS) and for macro- and micronutrients by inductively coupled plasma optical emission spectrometry (ICP-OES).[35]

2.2.9 Quantitative analysis of gene expression in *A. thaliana*

Total plant tissue was homogenized in liquid nitrogen and kept under -80 °C for RNA isolation. RNeasy plant mini kits (Qiagen) were used to isolate total RNA from *A. thaliana* according to the manufacturer instructions. The RNA concentration was quantified by NanoDrop spectrophotometry. One μg of total RNA was used for reverse transcription using Thermo Scientific Verso cDNA Synthesis Kit for first-strand cDNA synthesis and was again quantified by NanoDrop spectrophotometry. All gene-specific primers used for quantitative real time PCR analysis were designed using the PrimerQuest (Intergrated DNA Technologies). For specificity, primers were designed from the C-terminal non-conserved regions to give a product size of 100–150 bp. Finally, 200 ng/μL cDNA was used as template to run qRT-PCR according to the manufacturer instructions for Mastercycler^R ep realplex (Eppendorf AG, Hamburg, Germany) with Absolute Blue qPCR SYBR Green Mix (Thermo Fisher Scientific, Surrey, UK). A complete list of primer sequences and the qRT-PCR amplification program can be found

in Appendix I. The total volume from the qRT-PCR was 20 μL and *actin-2* was used as a housekeeping gene for normalization. Relative quantity ($2^{-\Delta\Delta Ct}$ method) was then used to calculate relative gene expression level.[128]

2.2.10 Statistical analysis

A one-way analysis of variance (One-way ANOVA) followed by Duncan's multiple comparison test (IBM SPSS Statistics 20) was used to determine statistical significance of each parameter across treatments, except qRT-PCR assay, in which Student t-test was applied to determine statistical significance of each gene. In the tables and figures for each assay, values followed by different letters are significantly different at $p \leq 0.05$.

2.3 Results and Discussion

2.3.1 Nanoparticle characterization

Table 2.1 shows the hydrodynamic diameter and zeta potential of CeO_2 and In_2O_3 NPs dispersed in deionized water and 1/2X Hoagland's solution. Generally, the hydrodynamic diameters of CeO_2 and In_2O_3 NPs in the deionized water were significantly smaller than in 1/2X Hoagland's solution, suggesting that ion strength is one of the main factors that can determine the NP aggregation in solution. However, two different concentrations of both NPs had no impact on either hydrodynamic diameter or zeta potential regardless of solution types. Interestingly, as compared to the zeta potential values from the deionized water treatment, 1/2X Hoagland's solution altered the surface charges of both NPs from positive to negative.

2.3.2 *A. thaliana* phenotype grown on CeO_2 and In_2O_3 NPs

The growth of *A. thaliana* in the presence of 0-3000 ppm CeO_2 NP is shown in Figure 1; visible signs of phytotoxicity are evident at concentrations as low as 500 ppm (Figure 2.1 A). At 250 ppm of CeO_2 NPs, the total plant biomass was significantly increased ($p<0.01$), although root length was unaffected (Figure 2.1 B and C). At 500 ppm of CeO_2 NPs, fresh biomass was not significantly affected by exposure but the average root length was reduced by nearly 60%. In addition, exposure to CeO_2 at concentrations higher than 500 ppm yielded a classic dose-response effect, with higher concentrations resulting in biomass reductions of 75-90%. Morphologically, at concentrations of 500 ppm CeO_2 NPs and higher, *A. thaliana* roots were stunted and failed to penetrate the 1/2X MS medium; chlorosis of the leaves was also evident. At 3000 ppm, the plants did not survive exposure and biomass could not be determined. These findings deviate from some published work with this nanoparticle. Zhang et al. (2012) exposed cucumber to CeO_2 NPs at 2000 ppm and indicated that shoot and root biomass was unaffected by the nanoparticle.[50] Similarly, Ma et al. (2010) observed that CeO_2 NPs had no impact on root elongation of six out of seven plant species.[49] Alternatively, our findings are in line with those of García et al (2011), where 640 ppm of CeO_2 NPs almost completely inhibited the germination of cucumber, lettuce and tomato.[129] At concentrations of 64 ppm, phytoxicity was significantly reduced but for cucumber, the inhibition rate was still 90%. From the literature and based on our findings, it is clear that the phytoxicity will not only be species-specific but at low concentrations, growth enhancement may occur under some circumstances.

The effect of In_2O_3 NPs exposure on *A. thaliana* is shown in Figure 2.2. Because little is known about In_2O_3 phytotoxicity, a broader concentration range for exposure was

employed as compared to CeO_2. Notably, no visible signs of phytotoxicity were evident at exposure concentrations up to 2000 ppm. In terms of fresh biomass, NPs exposure resulted in significantly enhanced growth at 50 and 500 ppm and had no effect at the other concentrations. However, root length was significantly, although not dramatically, reduced at all exposure concentrations. On average, root length was reduced by 10-20% by In_2O_3 exposure but this effect clearly had no impact on overall plant mass. To our knowledge, this is the first report of NP In_2O_3 effects on plant growth. It is clear that under similar exposure conditions, CeO_2 NPs seem to exert much greater phytotoxicity than does In_2O_3.

2.3.3 Chlorophyll Content of *A. thaliana* exposed to CeO_2 and In_2O_3 NPs

The chlorophyll content of *A. thaliana* exposed to CeO_2 NPs is shown in Figure 2.3. Chlorophyll amounts in the 250 ppm and 500 ppm NPs treatments were unaffected by particle exposure. This is particularly interesting at 500 ppm, where although root elongation was significantly inhibited, shoot biomass and chlorophyll were equivalent to the control plants. At the 1000 ppm and 2000 ppm, chlorophyll content was reduced by 58 and 89%, respectively, relative to the control plants. Although the mechanism of phytotoxicity remains unresolved, it is clear that such a loss in photosynthetic potential would clearly compromise overall plant growth and vigor. A decrease in chlorophyll content upon exposure to metal nanoparticles has been reported by Jiang et al (2012)[130], Shi et al (2011)[131] and Oukarroum et al (2012).[132] Interestingly, In_2O_3 NPs treatment, even at levels of 2000 ppm, had no effect on the chlorophyll content of *A. thaliana* tissues. The total chlorophyll of control plants was approximately 2.4 mg/g, with the In_2O_3 NPs-exposed plants having values ranging from 2.2-2.5 mg/g. Notably, the data on

chlorophyll content is in good agreement with the biomass results; CeO_2 NPs clearly exert significantly greater phytotoxicity on *A. thaliana* than does NP In_2O_3.

2.3.4 Anthocyanin production in *A. thaliana* treated with CeO_2 and In_2O_3 NPs

Because of the significant membrane damage likely resulting from ROS production and associated toxicity of CeO_2 NPs exposure, the anthocyanin content of exposed tissues was determined (Figure 2.4). Significant anthocyanin production as evident by extract pigmentation in *A. thaliana* was observed at the 1000 and 2000 ppm exposure levels; no pigment production was evident at 250 ppm treatment. Quantitation of anthocyanin production confirms the results; the 250 ppm exposure level had no impact on anthocyanin production. However, exposure at 1000 ppm of CeO_2 NPs resulted in significantly greater ($p \leq 0.01$) anthocyanin content but the effect was somewhat reduced at the 2000 ppm level. Interestingly, anthocyanin levels were not significantly affected by In_2O_3 NPs exposure.

2.3.5 Effect of CeO_2 and In_2O_3 NPs on membrane integrity

Lipid peroxidation, which can be indirectly measured by MDA formation, is an indicative of abiotic stress, such as that of induced metal toxicity. Cell membrane damage generally results from reactive oxygen species (ROS) production, which then damage phospholipids. The formation of MDA in *A. thaliana* as a function of CeO_2 exposure is shown in Figure 2.5. CeO_2 NPs at 250 and 500 ppm had no impact on MDA production but at an exposure of 1000 ppm, the MDA levels were 4 fold higher than that observed in the control plants (significant at $p \leq 0.01$). Metal and metal oxide NPs have been known to induce dose-dependent increase in lipid peroxidation in a number of plant species.[47,133]

Interestingly, exposure to In_2O_3 NPs at concentrations up to 1000 ppm had no effect on *A. thaliana* lipid peroxidation. MDA production in control plants was approximately 0.37 µM and NPs-exposed plants had MDA levels of 0.37-0.42 µM. The lack of membrane damage upon In_2O_3 exposure suggests that either this particular NP does not induce ROS formation even at high exposure concentrations or perhaps that the plant's detoxification pathways are sufficient to address and remedy the induced stress. Similar to our findings, Zhao et al. (2012) showed the activation of plant defense response and subsequent lack of membrane damage by exposure to CeO_2 NPs.[117]

2.3.6 Analysis of ROS production in *A. thaliana* seedlings

ROS are common byproducts in plant metabolism.[87] However, under abiotic stress conditions, elevated levels of ROS can cause oxidative stress and lead to a series of adverse impacts on plant growth and development.[89] Confocal fluorescence microscopy was used to observe the induction of ROS in *A. thaliana* roots exposed to variable NP concentrations (Figure 2.6 A). Significantly higher levels of ROS (green fluorescence) were evident in the *A. thaliana* roots upon NP treatments relative to controls, with notably highest fluorescence response at the 1000 mg/L In_2O_3 NPs exposure. Quantitative analysis of ROS-derived fluorescence intensity (Figure 2.6 B) showed that the total ROS intensity across all NP treatments was 6-10 times higher than the control unexposed plants. ROS speciation (H_2O_2 and $O_2^{\bullet -}$) was assessed using histochemical staining (DAB and NBT) (Figure 2.7 A). Exposures of 250 and 1000 mg/L CeO_2 and In_2O_3 NPs induced higher amounts of H_2O_2 in *A. thaliana* leaves as compared with the control. Relative color intensities in both NPs treated leaves were approximately 2 to 3-fold of the control

(Figure 2.7 B). Conversely, negligible amounts of $O_2^{\bullet-}$ were only observed in the 1000 mg/L NP treatments of *Arabidopsis* leaves (images are not shown).

Previously, it was noticed that H_2O_2 content in Neptune, a medium amylose rice cultivar, exposed to 250 mg/L of CeO_2 NPs was similar to the control group.[51] As exposure concentration increased to 500 mg/L, significantly higher levels of H_2O_2 were found in Neptune but no changes were found in Cheniere, a high amylose rice cultivar.[79, 51] Although, 250 mg/L of both NPs induced higher ROS in *A. thaliana*, no oxidative damage was evident in terms of MDA, chlorophyll, or anthocyanin content at this NP concentration.[20] These findings aligned with Arora *et al.*, who found that Au NPs induced ROS in *Brassica juncea* but had no impact either on growth or total seed yield.[77] Other metal-based NPs can also cause oxidative stresses by inducing excessive amounts of ROS at even lower concentrations. Rice seedlings treated with 0.2 to1 mg/L Ag NPs showed that significantly high levels of ROS productions (H_2O_2 and $O_2^{\bullet-}$) resulted in cell death in root tips.[134] Similarly, elevations of H_2O_2 and $O_2^{\bullet-}$ in 250 mg/L ZnO NPs treated rice seedlings were also evident.[135] Taken together, these results indicate that at certain exposure dose of metal-based NPs, induced ROS may act as a signaling molecule and thus could bio-stimulate plant growth by manipulating cell wall elongation.[20, 61] However, excessive amounts of ROS production in NP treated plants could lead to oxidative stress. The underlying mechanisms in plants to defend/counteract the nanotoxicity need to be further characterized due to NP types, exposure doses, and plant species.

2.3.7 Analysis of activities of ROS scavengers

Based on the observation of increased ROS levels in NP-exposed *A. thaliana*, the activities of key ROS scavenging enzymes (SOD, CAT, APX and POD) were measured (Figure 2.8). SOD activities in *A. thaliana* exposed to both NPs were approximately 2- to 3-fold higher as compared to the control plants, with the exception of the 250 mg/L CeO_2 NP treatment (not significantly different from the controls, Figure 2.8 A). SOD is capable of converting $O_2^{\bullet-}$ to H_2O_2, but the increased H_2O_2 levels need to be reduced or scavenged by antioxidant enzymes such as CAT, APX and POD in order to protect the plants from oxidative stress. Although the activities of CAT and APX at both exposure concentrations of In_2O_3 were increased by approximately 2-fold, these increases were not statistically significant (Figure 2.8 B and C). Alternatively, CeO_2 NP exposure increased both CAT and APX activities by 3.5- to 4-fold, with the exception of 250 mg/L CeO_2 NP treatment. POD is another H_2O_2 scavenger that can catalyze compounds such as *L*-ascorbic acid and guaiacol to donate electrons and subsequently convert H_2O_2 to H_2O. Upon exposure to both NPs, POD activities were significantly increased, with the 1000 mg/L CeO_2 NP treatment showing nearly twice the POD activity in comparison to the untreated controls (Figure 2.8 D).

Faisal *et al.* reported significantly increased SOD levels in tomato exposed to 0 mg/L to1000 mg/L NiO NPs. However, as exposure concentrations further increased, the decreases of SOD activity indicated that the antioxidant defense system was compromised.[48] Exposure to 250 mg/L CeO_2 NPs caused elevated SOD activity in the rice cultivar Cheniere, but no change in enzyme activity was found at 500 mg/L.[51] Similar results were also reported in 1 μg/mL and 100 μg/mL Al_2O_3 NP-treated onion

root, respectively.[136] These studies demonstrate that the pattern of antioxidant enzyme response may depend on NP type, NP exposure concentration and plant species. For example, in the root of the rice cultivar Cheniere treated with 500 mg/L CeO_2 NP, CAT activities were 50% that of the control group, while the activities of APX and POD were increased by 2 fold and 4-fold, respectively.[79] Similarly, upon foliar treatment of 2.94 g/m^3 CeO_2 NPs, increases in cucumber APX levels were observed only in the root (foliar spray), but CAT activities were increased in both leaf and root tissue.[44] In our study, In_2O_3 NPs only increased POD activities in *A. thaliana*, whereas CeO_2 NP exposure, particularly at the 1000 mg/L treatment, increased the levels of CAT, APX and POD.

2.3.8 Analysis of activities of stress related antioxidant enzymes in response to CeO_2 and In_2O_3 NP exposures

In most plant species, glutathione (GSH) metabolic pathway plays a critical role in the detoxification of toxic compounds including heavy metals and xenobiotics. In this pathway, GST catalyzes the conjugation of GSH to xenobiotic substrates (CeO_2 and In_2O_3 NPs in this case) via sulfhydryl groups, which then subsequently lowers contaminant toxicity to the plant. GSH can also directly break down H_2O_2 in the ascorbate-glutathione cycle; here, GSH is converted to GSSG (the oxidized form GSH).[137] GR can reduce GSSG to GSH; an elevated GR activity can further enhance the efficiency of GSH-mediated detoxification of xenobiotic substrates.[138] Results from the measurement of GST and GR activity are shown in Figure 2.9 A and B. GST levels were generally unaffected by NP exposure, with the exception of a 40% increase in the GST level for the 1000 mg/L CeO_2 NP treatment. No statistically significant change was

evident in the other NP treatments. Conversely, GR activity was increased by approximately 15% and 51% in the 1000 mg/L CeO_2 NP and 1000 mg/L In_2O_3 NP treatments, respectively.

The importance of the GSH metabolic pathway in scavenging ROS has been well established in many studies.[139, 140] How the plant can reuse oxidized GSH (GSSG) and promote GSH efficiency upon NP exposure was unclear. To our knowledge, there are only few studies reported on the GR activity in response to NP exposures in living systems. Rico *et al*. demonstrated that GR activity was increased in the roots of rice cultivar (Neptune) upon exposure to 62.5 and 500 mg/L CeO_2 NPs, whereas the decreases in the GR activity was evident in both rice cultivar Cheniere roots and shoots across four concentrations of CeO_2 NPs.[79, 51] The reduction in GR activity may correlate with low levels of ROS production and lipid peroxidation. At the molecular level, the transcription of GST in ZnO NPs treated *A. thaliana* were increased by approximately 9 to 11-fold, [26] while this value was 3 to 4-fold for Ag NPs exposure.[86]

Flavonoids can act as non-enzymatic antioxidants and are able to provide defense against oxidative damages.[24] In the current study, we sought to further examine anthocyanin overproduction as a potential defense mechanism for NP detoxification. Phenylanine ammonialyase (PAL) is a key enzyme in the anthocyanin biosynthesis pathway,[141, 142] and its activity can directly determine anthocyanin levels in plants. Although, In_2O_3 had no effect on PAL activity, the 1000 mg/L CeO_2 NPs-exposed *A. thaliana* seedlings had levels that were 10-fold greater than the PAL activity levels in the control group (Figure 2.9 C). These findings are highly consistent with the results of

anthocyanin production, where anthocyanin levels were largely unchanged in response to In_2O_3 and but were significantly elevated in the presence of CeO_2 NPs.

Polyphenol oxidase (PPO), which converts phenols into quinones, is another antioxidant enzyme associated with ROS removal and metal detoxification.[125, 143] Upon treatment with In_2O_3 NPs, PPO activities were significantly increased at both doses (Figure 2.9 D). Although CeO_2 NPs at 250 mg/L had no impact, PPO activity was elevated by nearly 4-fold when exposed to 1000 mg/L CeO_2 NPs. PPO activities can be regulated during various biotic and abiotic stresses.[144] Additional studies are needed to fully understand how PPO and ROS levels in plants are correlated following NP exposures.

2.3.9 Distribution of cerium and indium in *A. thaliana* tissues

With CeO_2 NPs treatments, the Ce content in 1000 mg/L CeO_2 NP-treated root was increased by approximately 4.3 times relative to the Ce content in the 250 mg/L CeO_2 NP-treated root (Figure 2.10 A). Similarly, there was a dose-response increase of Ce content in the shoot. However, regardless of exposure doses, no difference of In content in root was evident while there was a slight increase in shoot In levels. (Figure 2.10 B). Dose-response fashion was showed in soybean seedlings exposed to 0-4000 mg/L CeO_2 NPs suspension.[64] Potting experiment conducted by Zhao *et al.* (2013) suggested that the concentrations of Ce in cucumber upon exposure to 800 mg/kg CeO_2 NPs decreased from root to fruits; approximately 200-fold higher Ce concentration in CeO_2 NPs treated fruits suggested that food safety could be of major concerns.[76] Another study demonstrated that Ce mainly accumulated in corn root and barely transported to the aboveground part (leaf

and corn cob).[145] These results suggest that the uptake and tissue distribution of NPs depends on the type of NPs and plant species.

2.3.10 Elemental analysis in CeO_2 and In_2O_3 NPs treated *A. thaliana*

Nutrient displacement caused by CeO_2 and In_2O_3 NP exposure could result in nutrient deficiency and abiotic stress. As shown in Table 2.2, both doses of CeO_2 NPs significantly reduced K levels in *A. thaliana* shoots, although the decreases noted in the roots were statistically insignificant. In_2O_3 NPs had no impact on K uptake. The levels of Mg were largely unaffected by NP treatment, except when the plants were exposed to 250 mg/L In_2O_3 NPs: the Mg levels in the roots were increased by approximately 20% relative to the control. The Ca content in the root at these exposure concentrations showed an average increase of 11.5% and 29% in the CeO_2 and In_2O_3 NP treatments, respectively, whereas the shoot concentrations of Ca were unaffected. The concentration of P in both root and shoot tissue was decreased significantly by exposure to 1000 mg/L CeO_2 NPs, although no other treatments had an effect on P content. Exposure to the NPs had no impact on the levels of total N and S in both shoot and root tissues (data are not given).

The levels of additional micronutrients were analyzed in *A. thaliana* shoot and root tissues (Table 2.3). Fe content was affected by the NP exposure; levels of this important element were decreased in a dose-dependent manner, with overall reductions of over 50% for the high CeO_2 NP treatment. Given the amount of plant biomass available, the levels of Fe in *A. thaliana* shoots were below the instrument detection limit (Analytical Solution Quantification Limit, ASQL is 270 ppb) and are thus not shown in

Table 2. The CeO_2 and In_2O_3 NPs had no impact on the levels of Zn and B. Exposure to both NPs at 1000 mg/L caused significant decreases in the root Mn levels; however no effects on the Mn levels were evident at the lower NP concentrations in the roots or in any of the treated shoot tissues. Metal-based NPs can disrupt nutrient uptake and assimilation in plants, which could directly impact plant growth, development, quality and yield at harvest.[146]

In the present study, the uptake of Fe, which is critical for plant growth photosynthesis,[147] was significantly decreased in the presence of both NPs. Similarly, Ag NPs significantly lowered the levels of Fe in *Crambe*.[148] However, upon exposure to 800 mg/kg CeO_2 NPs, the Fe content in corncobs was not changed relative to the control.[145] Low Fe accumulation could be ascribed to the impact of NPs on the relative expression of divalent cation transporters in *A. thaliana*. For example, down-regulations of both IRT1and IRT2 were evident in 25 mg/L Au NPs-treated *A. thaliana*.[81] Another iron transporter, FRO, in *A. thaliana* was also down-regulated in the presence of Ag NPs.[86]

Ca is a secondary messenger molecule, which is involved in response to both abiotic and biotic stresses.[149, 150, 151] The elevation of Ca in *A. thaliana* roots may indicate that NP-induced ROS trigger Ca^{2+} ion channels to increase the concentration of Ca, which could subsequently stimulate defense related gene expressions in response to NP-induced oxidative stress.[152] The decrease in P uptake in 1000 mg/L CeO_2 NPs treated *A. thaliana* root agrees with other studies that have shown that CeO_2 NPs can bind P and lower the nutrients bioavailability.[80] A long-term study on corn and CeO_2 NP interactions demonstrated no impact on the accumulation of mineral nutrients in corncobs; however, it altered the distribution and localization of nutrients, such as Ca, Fe, Cu and Zn, in the

edible portion.[145] Besides mineral nutrients, CeO_2 and In_2O_3 NPs could also reduce the protein content in plants (Figure 2.11). In addition to the abiotic stressor (metal-based NPs), there are many factors including soil pH, fertilizers, soil organic matter etc. that can determine the nutrient levels in plants. Based on these results in *A. thaliana* seedlings, it is concluded that these effects may also be evident in other terrestrial plants, especially for crop plants, and thus could result in lower food quality and crops yield.

2.3.11 Regulations of iron transporters genes in *A. thaliana* seedlings exposed to CeO_2 and In_2O_3 NPs

The transcript levels of genes encoding the three important iron transporters (IRT, FER, and FRO) in *A. thaliana* were measured in an attempt to explain the reduced levels of Fe in the root tissue (Figure 2.12). Under iron deficiency, the relative expressions of these root-specific iron transporters are known to increase in *A. thaliana*.[153, 154] In plant leaves, FER is essential for the synthesis of iron containing proteins;[155] the expression level of the gene encoding FER can be used as a good proxy to indicate iron levels in plant shoot tissues. Figure 2.12 shows the time-dependent transcript levels of these three iron transporters in *A. thaliana* shoots and roots upon exposure to 1000 mg/L CeO_2 and In_2O_3 NPs after 96 and 120 hours. These exposure durations correspond with the exposure period for analysis of nutrient displacement assays in *A. thaliana*. Although, slight but not significant increases in FER expression were found in *A. thaliana* shoots upon exposure to both NPs at 96 hours, but the significant decreases in both CeO_2 and In_2O_3 NP-treated *A. thaliana* shoots were evident at 120 hours. In the roots of *A. thaliana*, the relative expression of FRO in 1000 mg/L In_2O_3 NPs treatment was elevated approximately 1.5 and 2.5-fold at 96 and 120 hours, respectively. Similarly, the transcript levels of IRT

were also up-regulated in In_2O_3 NPs treatment. It is interesting to note that the exposure of 1000 mg/L CeO_2 NPs did not affect the FRO and IRT regulations at 96 and 120 hours.

Although the functions of these iron transporters in *A. thaliana* have been well characterized,[153, 154, 155] the explanation of Fe deficiency in the NP-treated *A. thaliana* is unknown. As discussed earlier for the low Fe content in *A. thaliana* root, differential regulation of the cation transporters might be part of the defense mechanism in response to abiotic stresses to prevent the plants from accumulating potentially toxic metals. Au NPs caused 132.3 and 38.4-fold decreases in IRT1 and IRT2 relative to the control in *A. thaliana*.[81] Similarly, relative expression of FRO4 was only 0.29-fold of the control in Ag NPs treated *A. thaliana*, while no change was found in Ag ions treatment.[86] Plants can adjust their metabolism to control the uptake of toxic metals by down-regulating the expression levels of metal-related transporters. Our study has demonstrated that CeO_2 NPs are more toxic to *A. thaliana* than In_2O_3 NPs under the same exposure doses.[20] Although both NPs can cause decreases in Fe content, the addition of CeO_2 NPs resulted in significantly low content of Fe in *A. thaliana*, compared to the In_2O_3 NPs treatment. One of the most possible reasons is that upregulation of FRO and IRT in the In_2O_3 NPs treatment is to compensate for Fe deficiency. Another possibility is that IRT may be co-transporting Ce along with Fe. Therefore, due to the toxicity of CeO_2 NPs to the plants, it is possible that *A. thaliana* avoided taking up Ce by downregulating IRT. Our hypothesis is supported by previous studies showing that IRT transporter can take up many different metal cations, including cadmium, copper, zinc, cobalt and manganese.[156, 157] Further studies are needed to explore the mechanistic explanation for the interactions between Fe uptake and NP accumulation in plants.

2.3.12 CeO_2 and In_2O_3 NPs effect on antioxidant and stress-related gene expression

To evaluate antioxidant and stress-related gene expression under 500 or 1000 ppm CeO_2 NPs exposure, *A. thaliana* transcript production was quantified with qRT-PCR (Figure 2.13). GSH is the major antioxidant molecule in cells and has been shown to protect plants from oxidative stress caused by toxic metals and other abiotic stressors. Therefore, our efforts were focused on the regulation of genes involved in the sulfur assimilation and the glutathione metabolic pathway in response to CeO_2 and In_2O_3 NPs exposure. The relative level of sulfate adenylytransferase (ATPS) gene expression was significantly enhanced by both concentrations of CeO_2 NPs (Figure 2.13 A). Adenosine-5′-phosphosulfate reductase (APR) can convert adenosine-5′-phosphosulfate (APS) to sulfite and then to biosynthesized sulfide, a precursor of cysteine, under the catalysis of sulfite reductase (SiR). Figure 2.13 B and 6C show the relative expression of APR and SiR as a function of CeO_2 NPs exposure. APR expression under 1000 ppm of CeO_2 NPs treatment was 4-fold higher than untreated control plants, whereas the relative expression of SiR at the same treatment level was dramatically reduced. This inhibition of SiR synthesis is likely due to less sulfide production and may explain the lack of cysteine synthase (CS) induction (Figure 2.13 D). Glutathione synthase expression was more than doubled in *Arabidopsis* exposed to 500 and 1000 ppm CeO_2 NPs (Figure 2.13 E). In plants, adenosine phosphosulfate kinase (APSK) plays a crucial role in a secondary metabolic pathway of sulfate assimilation.[158] As shown in Figure 2.13 F, treatment with CeO_2 NPs significantly increases APSK expression; at 1000 ppm of CeO_2 NPs, the gene was up-regulated by 3-fold over untreated plants.

The impact of In_2O_3 NPs exposure on these same genes is shown in Figure 2.14 and notably, the pattern of induction is somewhat similar to that observed with CeO_2 NPs. For example, the relative level of ATPS gene expression, which controls APS synthesis by catalyzing sulfate, was significantly increased by exposure to In_2O_3 NPs at both 50 and 500 ppm (Figure 2.14 A). However, unlike CeO_2 NP exposure, the upregulation of genes involved in sulfite and sulfide biosynthesis was far less significant (Figure 2.14 B and C), although NP exposure concentrations were intentionally lower for In_2O_3. Conversely, the glutathione metabolic pathway was significantly induced, with more than a 4-fold increase in GS transcript expression at 50 ppm of In_2O_3 NPs treatment (Figure 2.14 E). For CeO_2 NPs treatment, exposure to 500 ppm NP only doubled GS expression. Moreover, as precursor of glutathione, CS was also up regulated to a much higher extent upon In_2O_3 NPs treatment (Figure 2.14 D). It is presumed that significantly greater activation of the glutathione pathway (CS, GS) upon In_2O_3 NPs exposure is responsible for general lack of phytotoxicity (biomass, chlorophyll, anthocyanin, lipid peroxidation) observed with treated *A. thaliana*. The phenomenon of metal ion detoxification in plants through the glutathione metabolic pathway has been demonstrated previously.[159,160,161] In the field of nanoparticle phytotoxicity, others have recently begun to focus on tissue glutathione levels as an important parameter of study.[162]

Sulfur is a required cellular nutrient and is necessary for the biosynthesis of several important macromolecules.[163,164] After adenosine phosphosulfate (APS) formation under the catalysis of ATPS, subsequent sulfate assimilation can occur by two pathways in plants.[158,98] The primary pathway is that APS can be reduced to sulfite by sulfite reductase (SiR) and then channeled into cysteine synthesis, which is a precursor to

biosynthesize glutathione. The secondary sulfated metabolic pathway is controlled by APSK, which plays an important role in plant growth and viability.[158,98] The genes involved in both of sulfated metabolic pathways were induced under the stressful conditions caused by CeO_2 and In_2O_3 NPs exposure. The pathway involved in glutathione metabolism is part of the primary sulfated pathway. Figures 6 and 7 displayed that transcripts related to antioxidants were induced by both REE oxide NPs, suggesting an enhancement of plant defense to oxidative stresses through the glutathione pathway. Paulose *et al* (2010) reported gene expression of *Crambe abyssinica* in response to arsenate exposure and demonstrated that transcripts related to sulfated metabolism (SiR, ATPS) and glutathione synthase (GS) were induced under this abiotic stress.[104] Similarly, Zulfiqar *et al* (2011) noted that glutathione metabolism and amino acid synthesis were stimulated in *Crambe abyssinica* upon exposure to chromium.[165]

Clearly, the literature on REE metal oxide NP interactions with plants is under developed. Given the widespread and increasing use of this class of nanoparticles and the potential ecological and human health impacts through food chain contamination, it is clear that significant research into this area is necessary. This is the first report demonstrating differential regulatory response through altered expression of glutathione and sulfated metabolic pathways in response to REE oxide NPs exposure.

Table 2. 1 Characterization of CeO_2 and In_2O_3 NPs in DI water and 1/2X Hoagland's solution

Treatment	Solution	DLS (nm)	Zeta potential (mV)
250 mg/L	DI water	229±56.7	28.59±3.34
In_2O_3 NPs	1/2X Hoagland's solution	1795.9±57.5	-8.68±1.70
1000 mg/L	DI water	221.4±6.5	32.28±1.95
In_2O_3 NPs	1/2X Hoagland's solution	1779.5±73.4	-10.38±1.52
250 mg/L	DI water	249.4±2.5	43.09±2.11
CeO_2 NPs	1/2X Hoagland's solution	3352.8±691.5	-4.24±1.02
1000 mg/L	DI water	209.1±1.0	43.58±2.39
CeO_2 NPs	1/2X Hoagland's solution	3532.6±1075.9	-6.12±0.81

Table 2. 2 The levels of macronutrients in shoot and root of A. thaliana exposed to CeO_2 and In_2O_3 NPs for 5 d

Plant tissue	Macro-nutrient	Control	CeO_2 NPs (ppm)		In_2O_3 (ppm)	
			250	1000	250	1000
Shoot (mg/kg)	K	64799.0±3003.1B	56314.5±1683.8 A	55106.5±971.0 A	59535.8±2345.8 AB	60573.7±1665.0AB
	Mg	2431.3±65.2 A	2279.0±79.7 A	2348.5±88.9 A	2371.0±82.1 A	2288.1±63.0 A
	Ca	7302.1±533.2 A	6762.1±88.0 A	6642.4±166.1 A	7212.2±156.3 A	7579.5±403.4 A
	P	12056.2±721.6 B	10377.8±267.1 B	8138.7±811.5 A	11994.8±545.5 B	11200.3±99.8 B
Root (mg/kg)	K	32842.1±2813.5a	31482.0±1446.9 ab	26862.5±752.0 a	35321.8±3860.2 a	27945.2±2779.5ab
	Mg	1135.9±54.6 a	1159.7±18.5 a	1175.1±30.9 a	1354.8±26.6 b	1210.0±4.5 a
	Ca	5355. 6±269.6 a	5946.7±121.8 b	6295.9±181.2 bc	7014.8±168.2 d	6696.6±178.6 cd
	P	6931.5±345.5 bc	6942.0±229.2 bc	5872.3±178.2 a	7687.4±376.6 c	6356.6±318.4 ab

Note: Data are mean ± standard error of 4 or 5 replicates. Values of each element content followed by different letters indicate that the data points are significantly different at $p \leq 0.05$.

Table 2. 3 The levels of micronutrients in shoot and root of A. thaliana exposed to CeO_2 and In_2O_3 NPs for 5 d

Plant tissue	Micro-nutrient	Control	CeO_2 NPs (ppm)		In_2O_3 (ppm)	
			250	1000	250	1000
Shoot (mg/kg)	Fe	< 270	< 270	< 270	< 270	< 270
	Zn	139.4±10.2 AB	124.7±2.0 A	124.0±4.1 A	140.7±5.2 AB	149.0±7.9 B
	Mn	245.7±11.1 B	225.3±6.6 AB	216.9±6.6 A	238.5±3.1 AB	215.6±10.4 A
	B	100.3±6.8 A	103.7±5.6 A	102.9±6.6 A	99.5±12.3 A	91.7±2.4 A
Root (mg/kg)	Fe	3512.5±123.4 d	2745.9±74.5 bc	1448.7±196.6 a	3045.7±117.2 cd	2279.0±292.4 b
	Zn	339.8±16.9 ab	379.7±16.9 b	294.2±10.1 a	356.0±19.8 b	348.7±4.1 b
	Mn	107.4±6.4 c	75.9±1.4 a	83.2±5.8 ab	96.7±7.0 bc	90.4±4.6 ab
	B	159.7±24.6 ab	189.8±24.2 b	112.3±11.5 a	179.6±32.0 ab	113.4±17.1 a

Note: Data are mean ± standard error of 4 or 5 replicates. Values of each element content followed by different letters indicate that the data points are significantly different at $p \leq 0.05$. For Fe determination, analytical Solution Quantification Limit (ASQL) is 270 ppb.

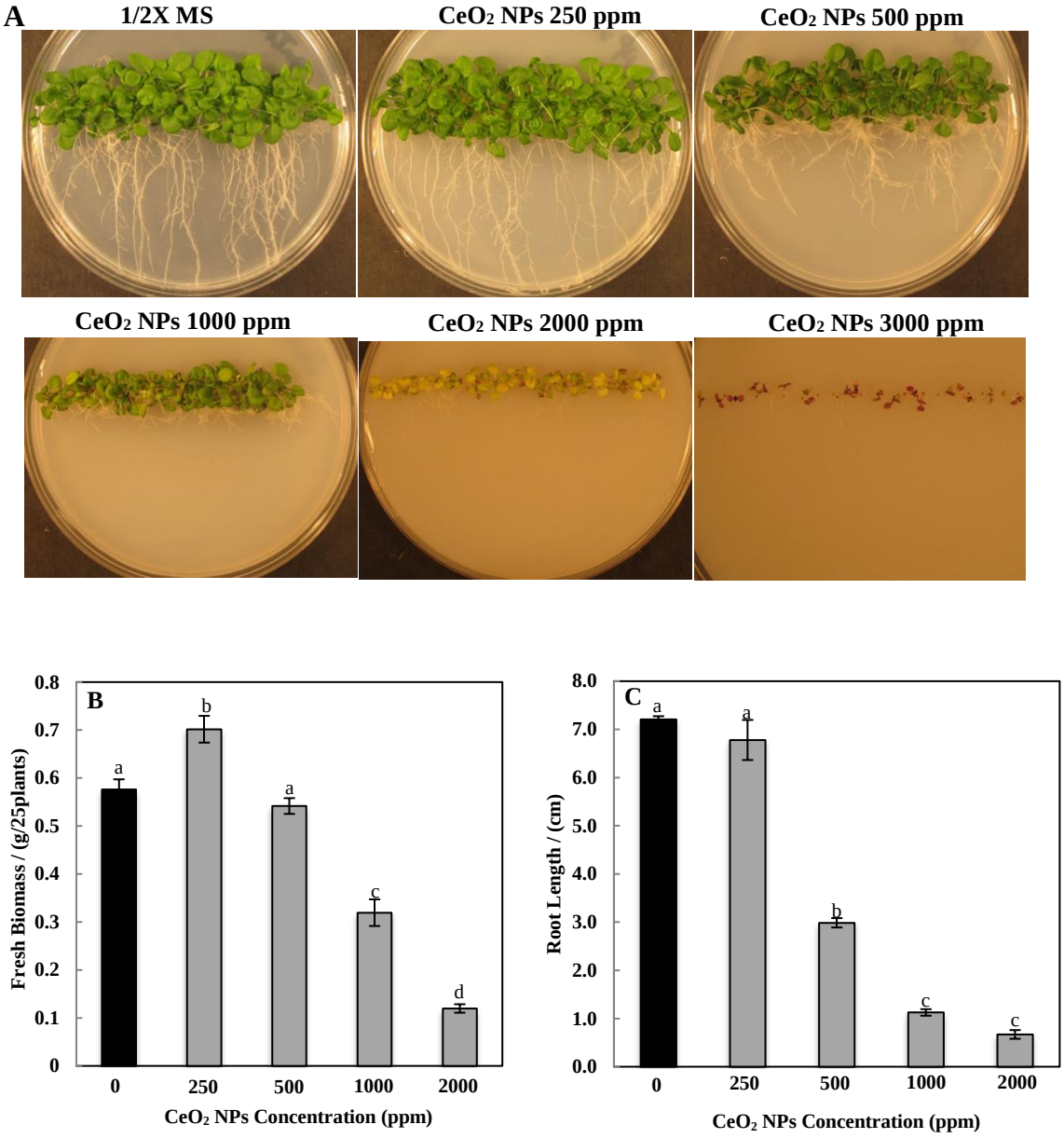

Figure 2. 1 *A. thaliana* treated with different concentrations of CeO_2 NPs. (**A**) Images of *A. thaliana* exposed to different nominated concentrations of CeO_2 NPs. (**B**) Fresh biomass of *A. thaliana* including roots and shoots. (**C**) Root length of *A. thaliana*. The means are averaged from 4 replicates and error bars correspond to standard error of mean. Values of fresh biomass or roots length followed by different letters are highly significant differences at $p<0.01$.

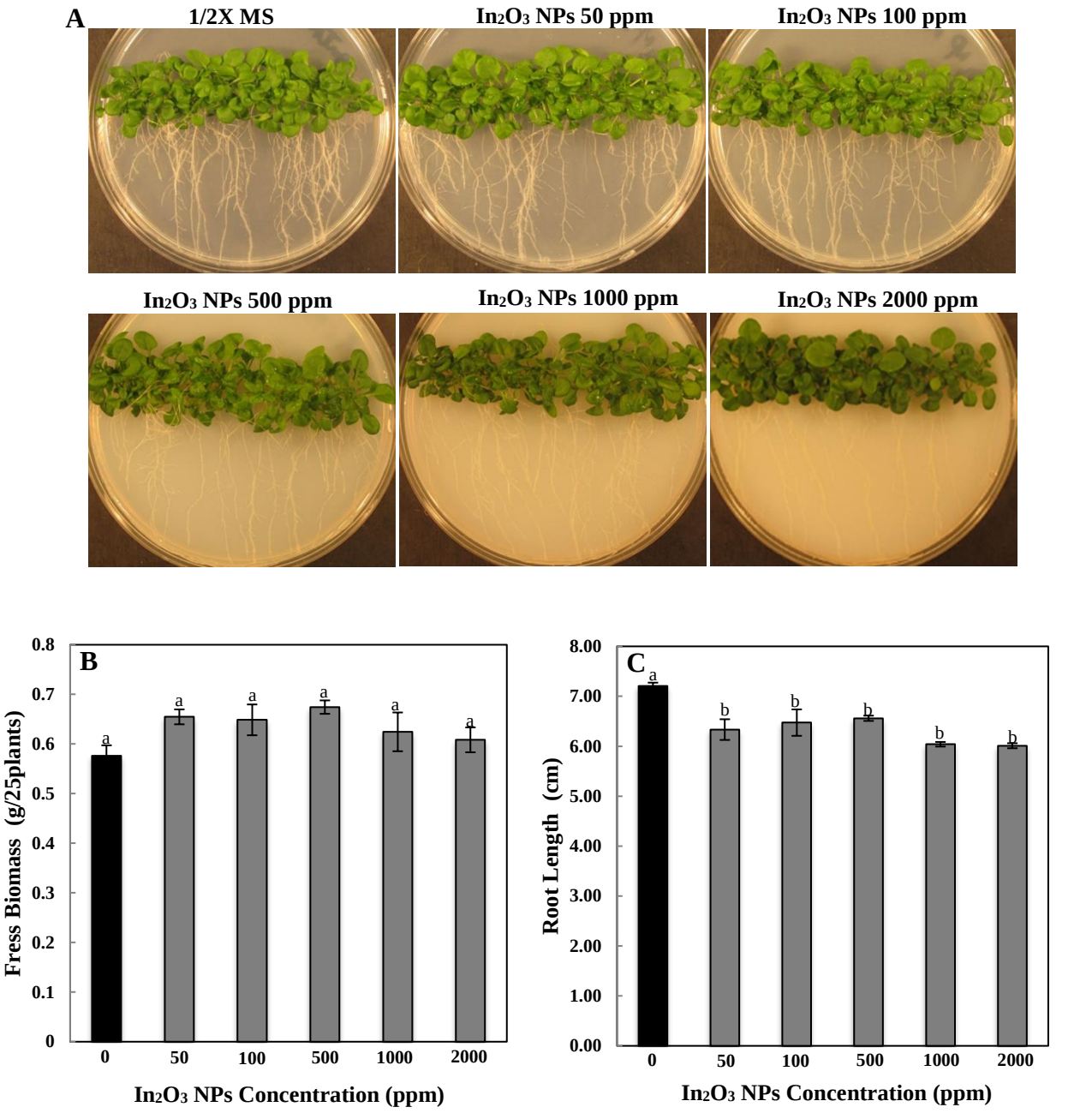

Figure 2. 2 *A. thaliana* treated with different concentrations of In_2O_3 NPs. (**A**) Images of *A. thaliana* exposed to different nominated concentrations of In_2O_3 NPs. (**B**) Fresh biomass of *Arabidopsis Thaliana* including roots and shoots. (**C**) Root length of *A. thaliana*. The means are averaged from 4 replicates and error bars correspond to standard error of mean. Values of fresh biomass or roots length followed by different letters are highly significant differences at $p<0.01$.

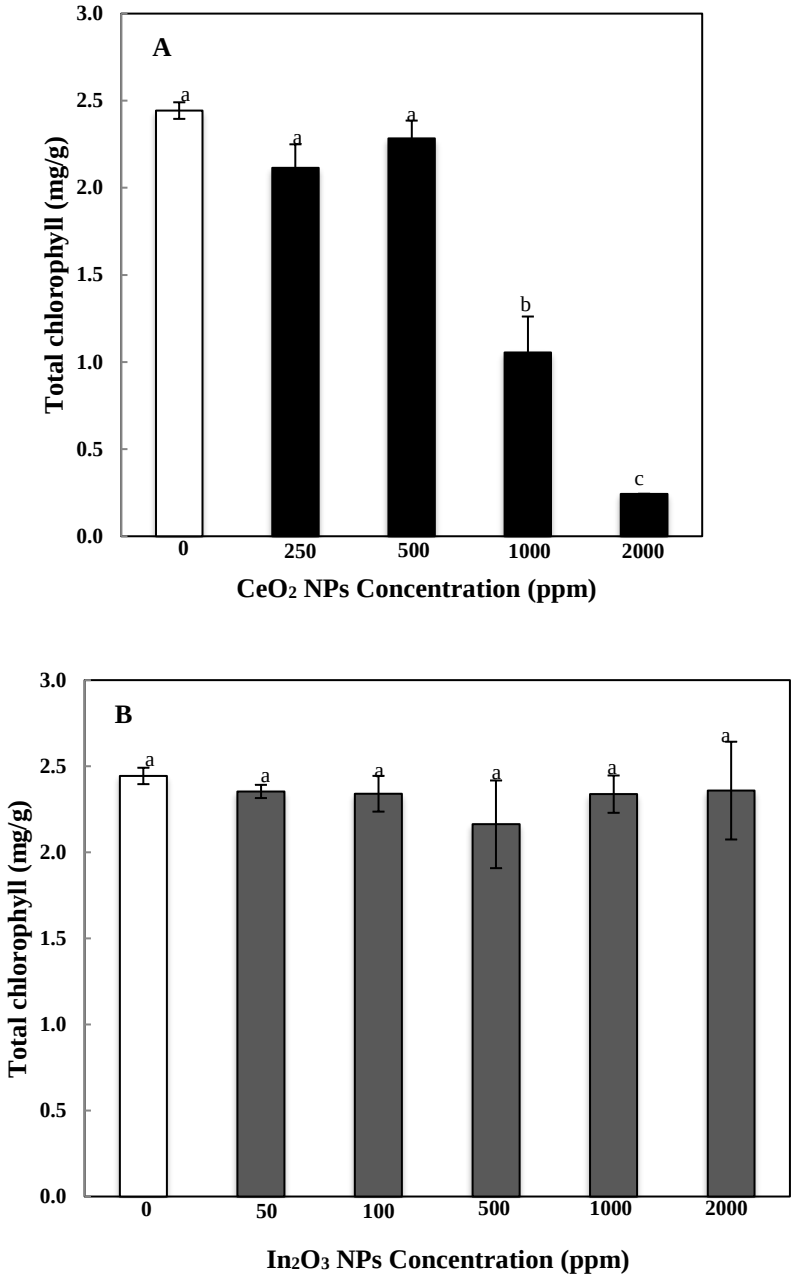

Figure 2. 3 Total chlorophyll of *A. thaliana* treated with different concentrations of CeO_2 (**A**) and In_2O_3 (**B**) NPs. The means are averaged from 4 replicates of *A. thaliana* leaves. The error bars correspond to standard error of mean. Values of total chlorophyll followed by different letters are highly significant differences at $p<0.01$.

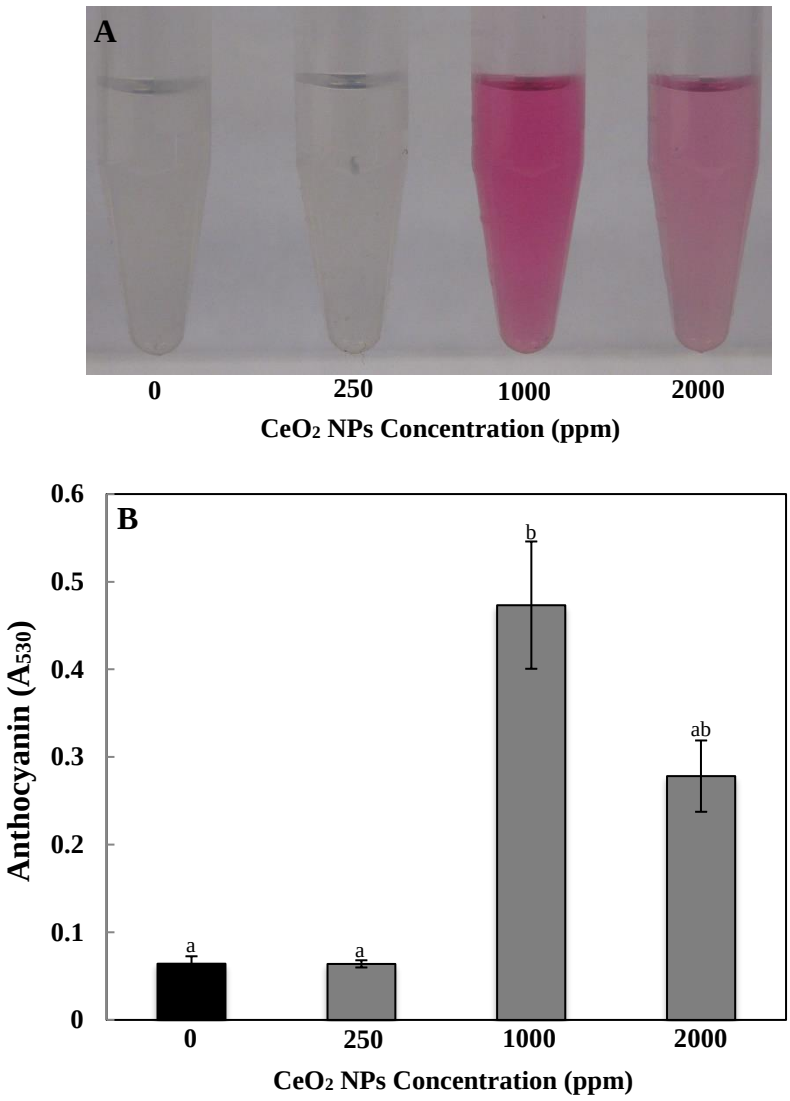

Figure 2. 4 Quantification of anthocyanin in the leaves of *A. thaliana* treated with different concentrations of CeO_2 NPs. (**A**) image of anthocyanin color in Arabidopsis leaves increased as exposure doses of CeO_2 NPs increased. (**B**) quantification of anthocyanin under different concentrations of CeO_2 NPs treatment. The means are averaged from 4 replicates of anthocyanin and the error bars correspond to standard error of mean. Values of anthocyanin followed by different letters are highly significant differences at $p<0.01$.

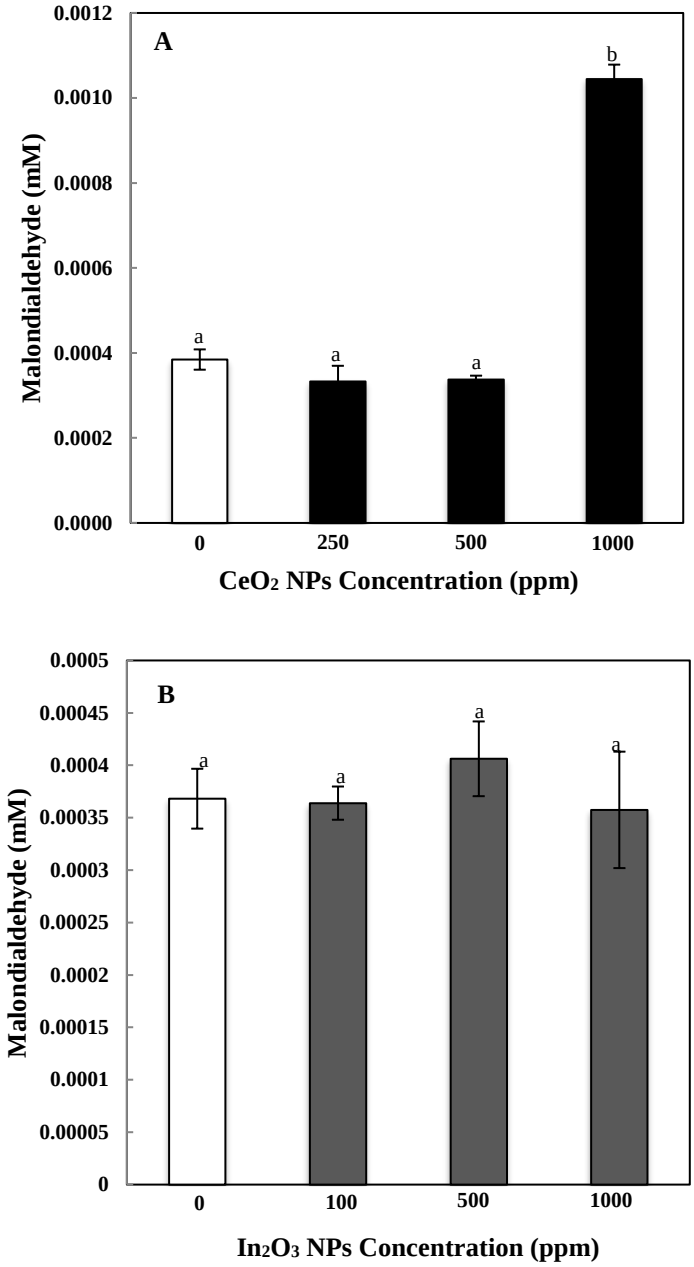

Figure 2. 5 Lipid peroxidation of *A. thaliana* treated with different concentrations of CeO_2 (**A**) and In_2O_3 (**B**) NPs. The means are averaged from 4 replicates of *A. thaliana*. The error bars correspond to standard error of mean. Values of Malodialdehyde followed by different letters are highly significant differences at $p<0.01$.

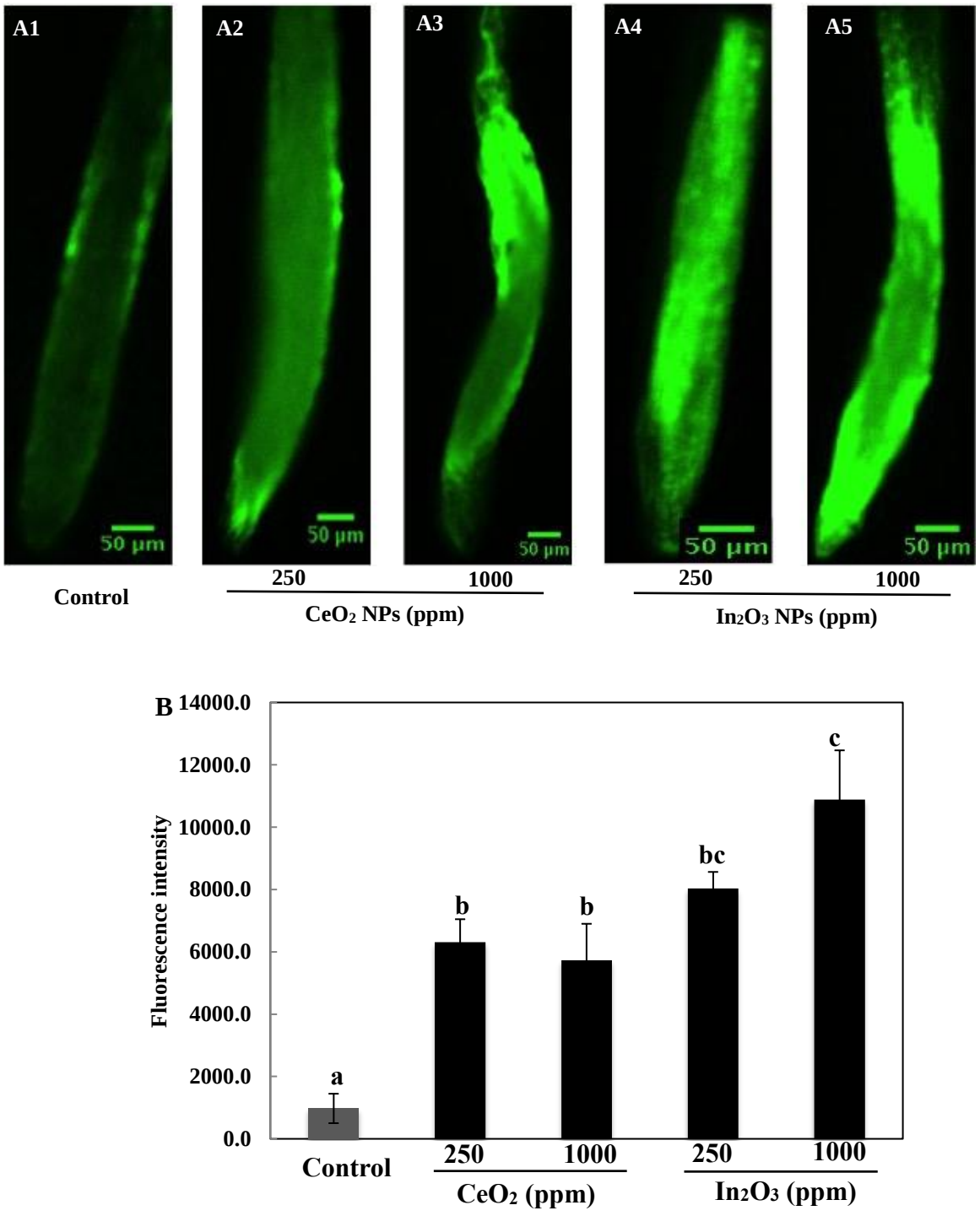

Figure 2. 6 Total ROS production in *A. thaliana* root treated with 250 and 1000 mg/L CeO_2 and In_2O_3 NPs at Day 7. Panels **A1-A5** represent the total ROS in control, 250 mg/L CeO_2, 1000 mg/L CeO_2, 250 mg/L In_2O_3, and 1000 mg/L In_2O_3 NPs treatment, respectively. Panel **B** represents fluorescence intensity corresponding to each treatment. Data are mean ± standard error of three replicates. Values of fluorescence intensity followed by different letters indicate that the data points are significantly different at $p \leq 0.05$.

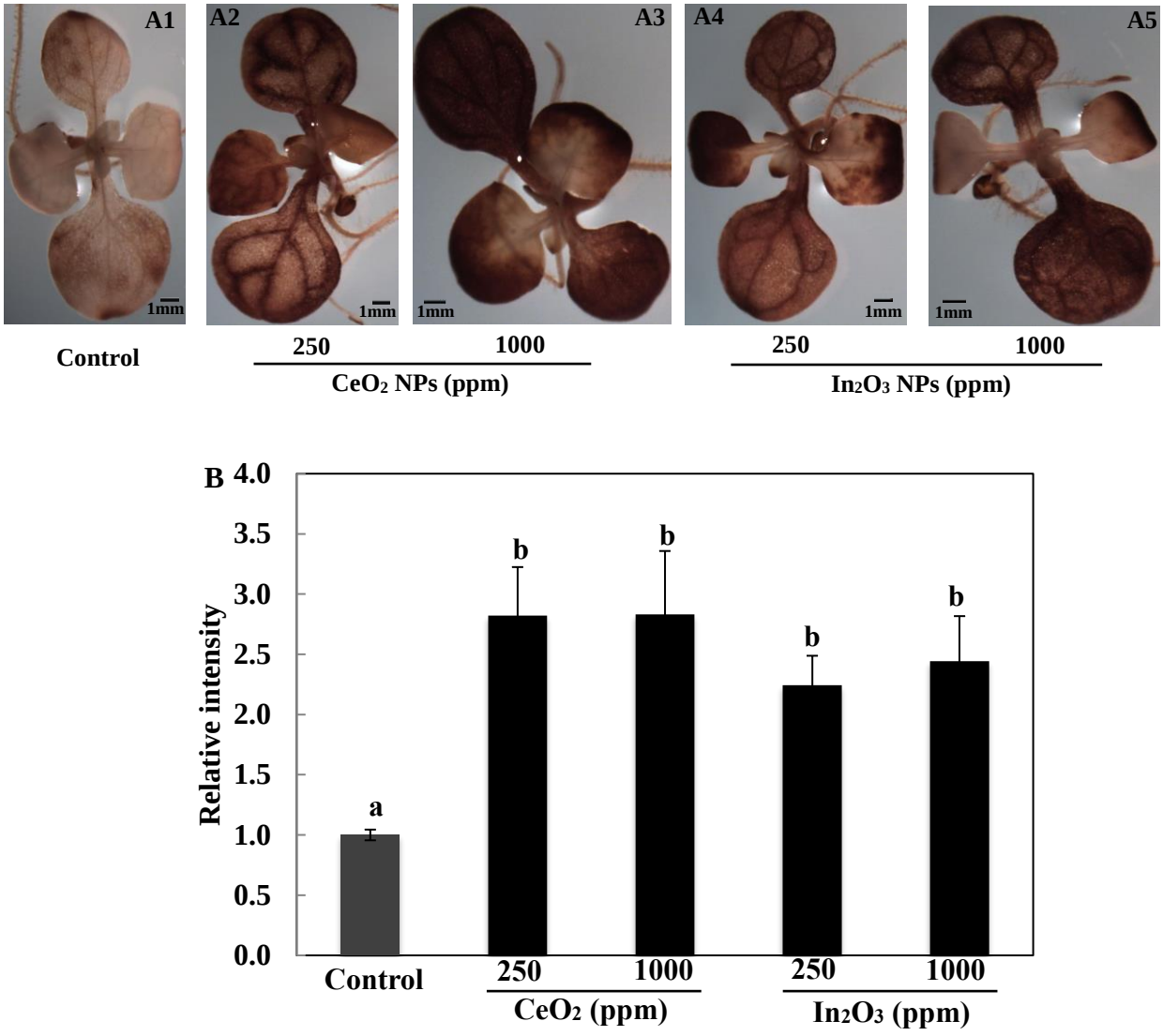

Figure 2. 7 H_2O_2 production in *A. thaliana* shoot treated with 250 and 1000 mg/L CeO_2 and In_2O_3 at Day 7. Panels **A1-A5** represent the H_2O_2 levels in control, 250 mg/L CeO_2, 1000 mg/L CeO_2, 250 mg/L In_2O_3, and 1000 mg/L In_2O_3 NPs treatment, respectively. Panel **B** represents relative intensity corresponding to each treatment. Data are mean ± standard error of three replicates. Values of fluorescence intensity followed by different letters indicate that the data points are significantly different at $p \leq 0.05$.

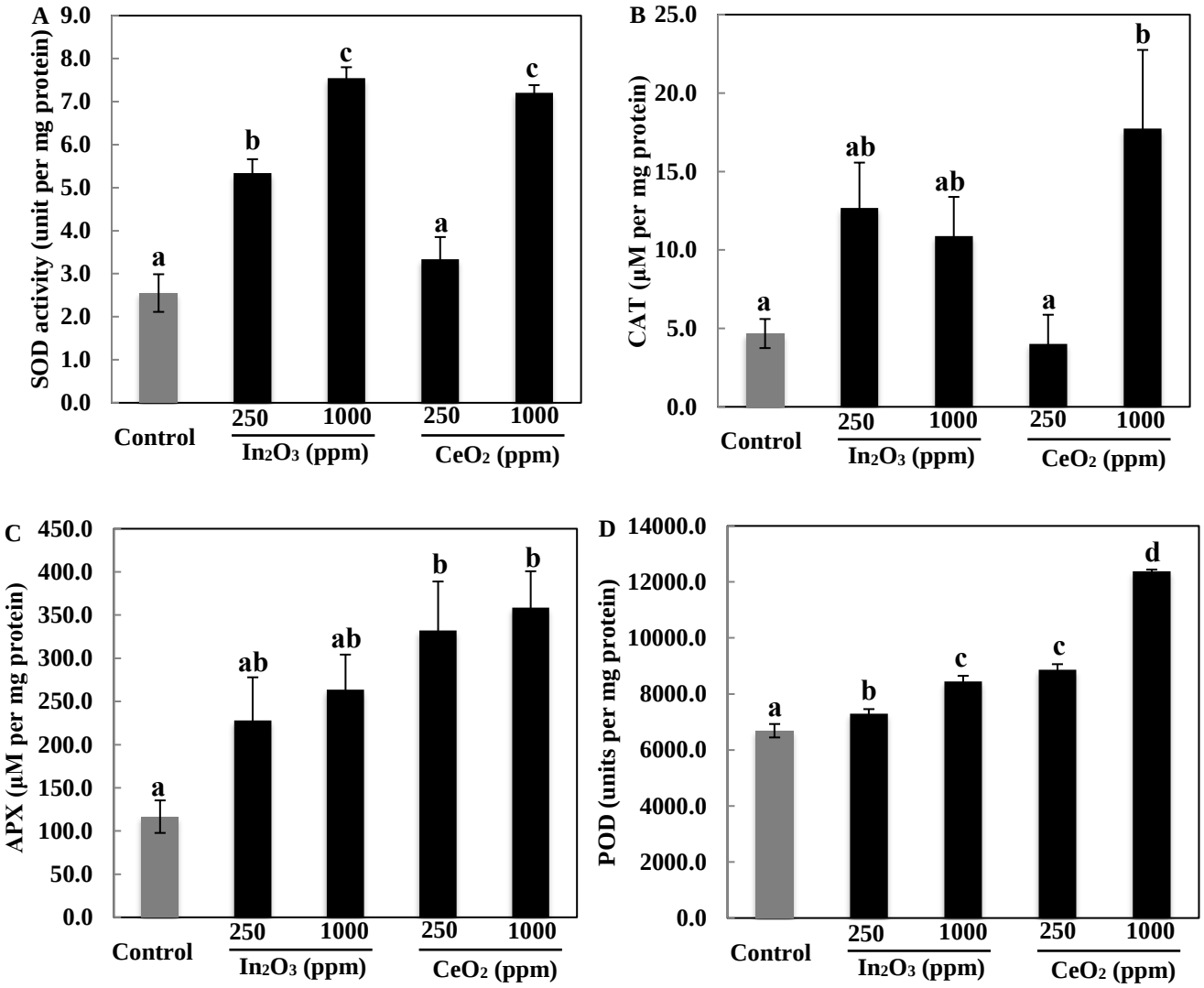

Figure 2. 8 Antioxidant enzyme activities in *A. thaliana* seedlings treated with 250 and 1000 mg/L In_2O_3 and CeO_2 NPs for 25 d. (**A**) SOD activities in *A. thaliana* in response to both In_2O_3 and CeO_2 NPs exposures; (**B**) differences of CAT activities in NP-treated *A. thaliana* seedlings; (**C**) responses of APX activities in *A. thaliana* seedlings to NP exposures; (**D**) POD activities in *A. thaliana* treated with NPs. Data are mean ± standard error of four or five replicates. Values of each antioxidant enzyme activities followed by different letters indicate that the data points are significantly different at $p \leq 0.05$.

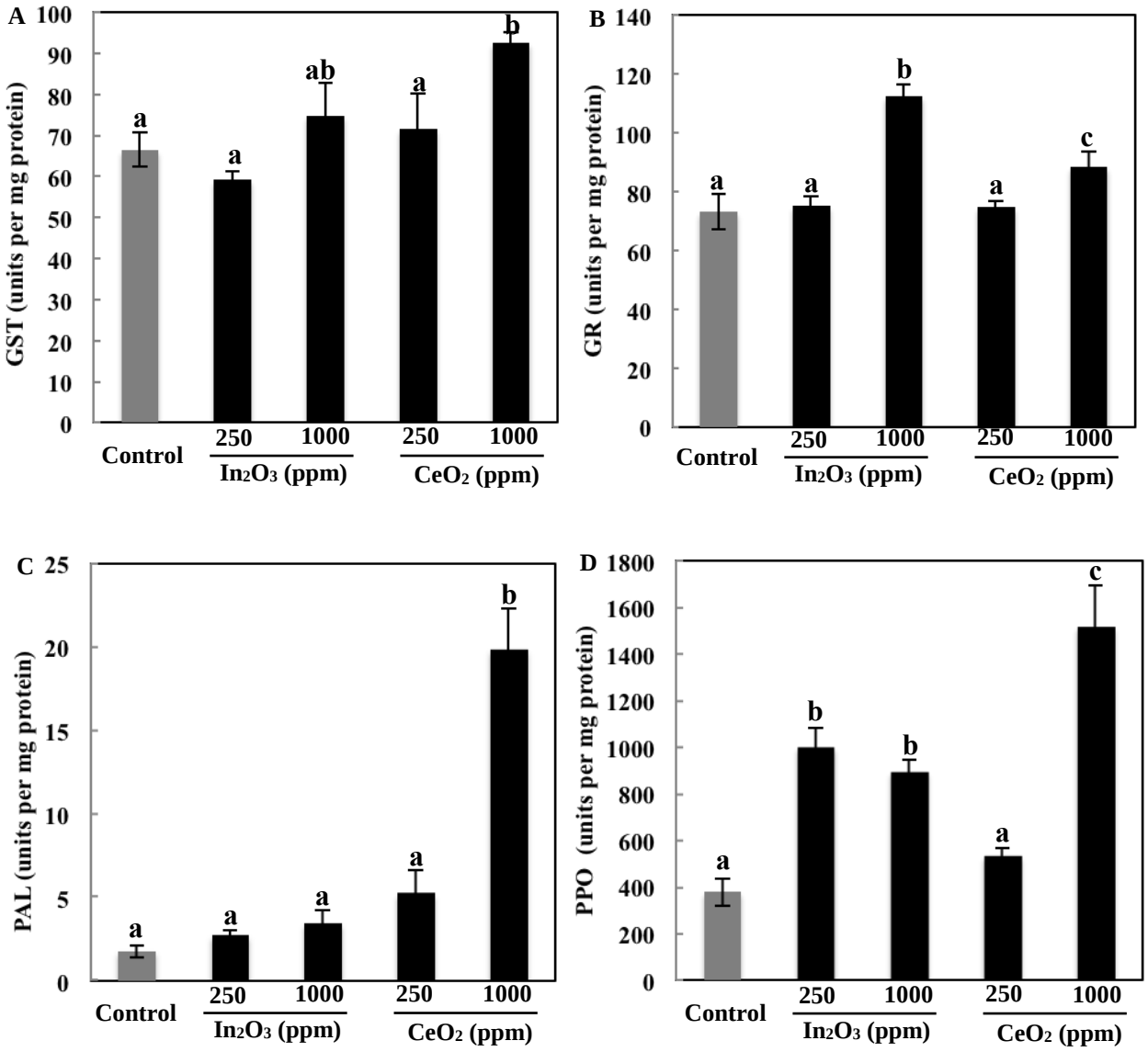

Figure 2. 9 Activities of stress related enzymes in *A. thaliana* seedlings treated with 250 and 1000 mg/L In_2O_3 and CeO_2 NPs for 25 d. (**A**) GST activities in *A. thaliana* seedlings treated with two concentrations of In_2O_3 and CeO_2 NPs; (**B**) responses of GR activities in *A. thaliana* to NP exposures; (**C**) PAL activities in in *A. thaliana* treated with NPs; (**D**) differences of PPO activities in NP-treated *A. thaliana* seedlings. Data are mean ± standard error of three replicates. Values of each enzyme activities followed by different letters indicate that the data points are significantly different at $p \leq 0.05$.

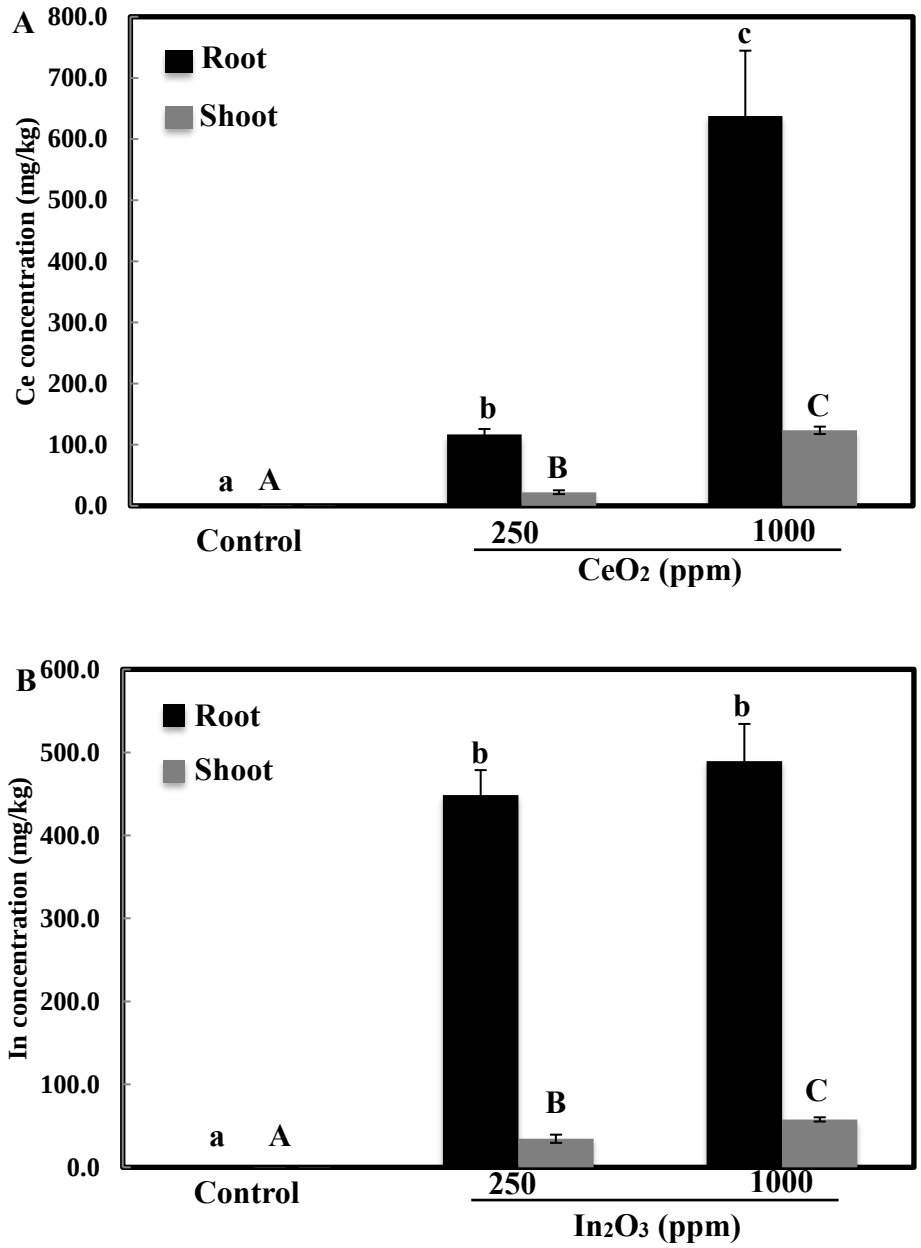

Figure 2. 10 Ce and In content in shoot and root of *A. thaliana* after 5 d exposure. (**A**) Ce content in shoot and root of Arabidopsis treated with 250 and 1000 mg/L CeO_2 NPs; (**B**) In content in shoot and root of Arabidopsis treated with 250 and 1000 mg/L In_2O_3 NPs. Data are mean ± standard error of 4 or 5 replicates. Values of metal uptake followed by double asterisks indicate statistically significant differences at $p \leq 0.01$ compared to control group.

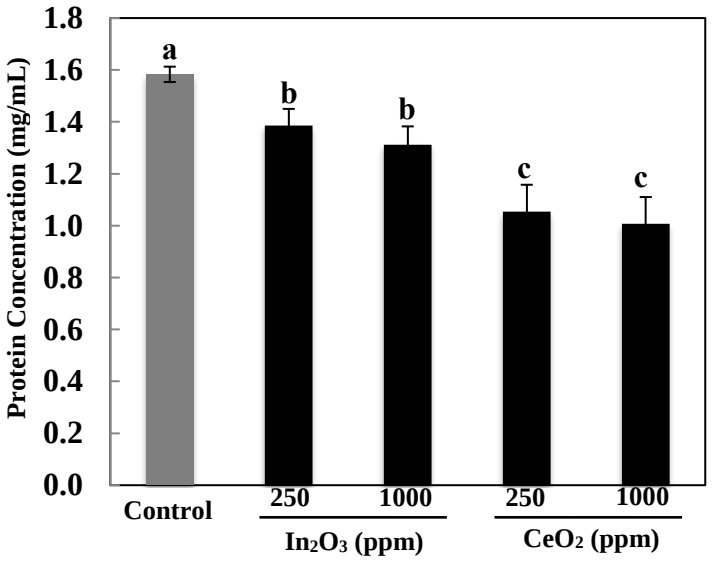

Figure 2. 11 Total protein content in *A. thaliana* seedlings treated with different concentrations of In_2O_3 and CeO_2 NPs. Data are mean± standard error of 3 replicates. Values of total protein content followed by different letters indicate that the data points are significantly different at $p \leq 0.05$.

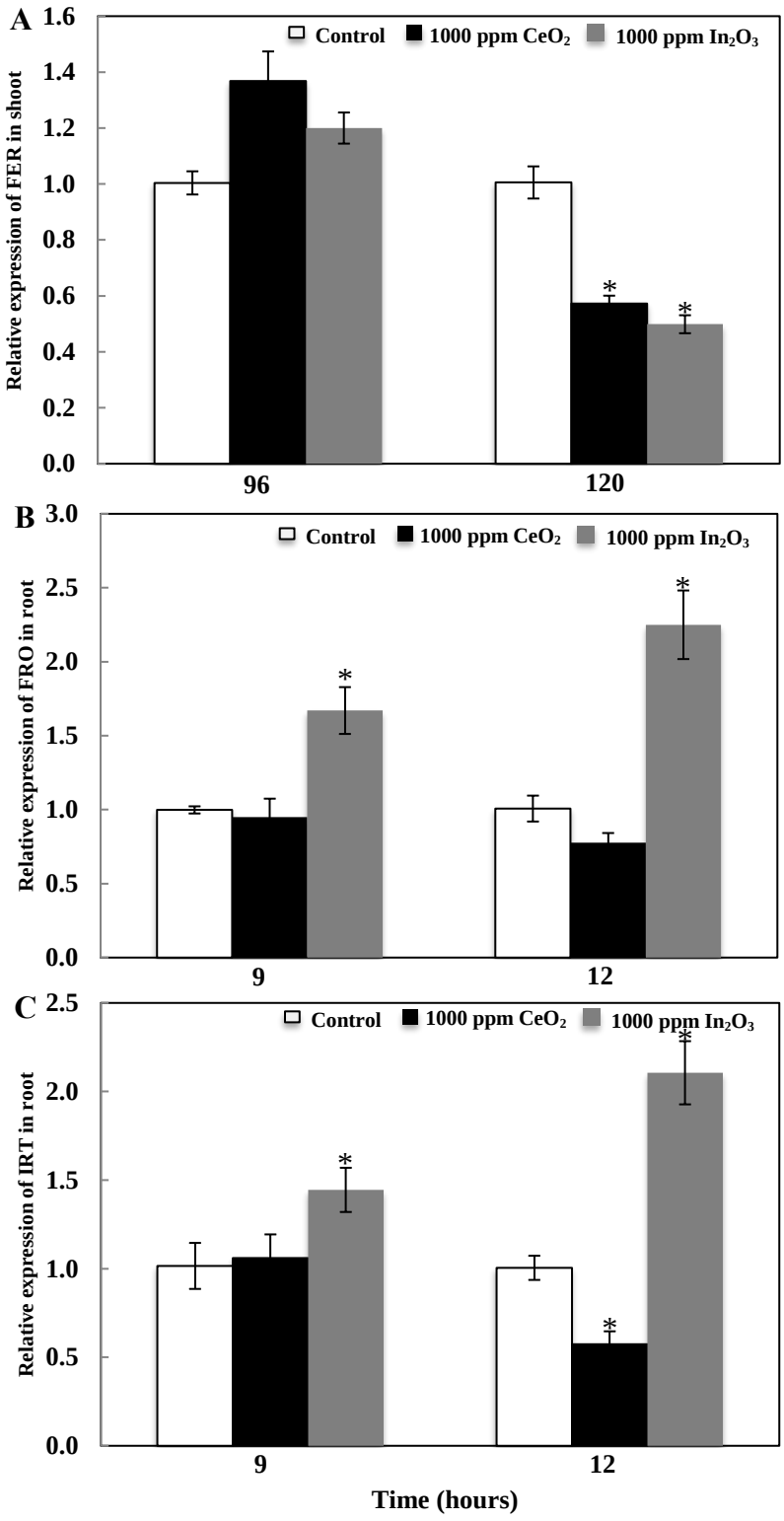

Figure 2. 12 Relative expressions of iron transporter in *A. thaliana* treated with 1000 mg/L CeO_2 and In_2O_3 NPs at 96 and 120 hours. **A**, **B**, and **C**- expression levels of FER, FRO and IRT in *A. thaliana* treated with both NPs, respectively. Data are mean ± standard error of three replicates.

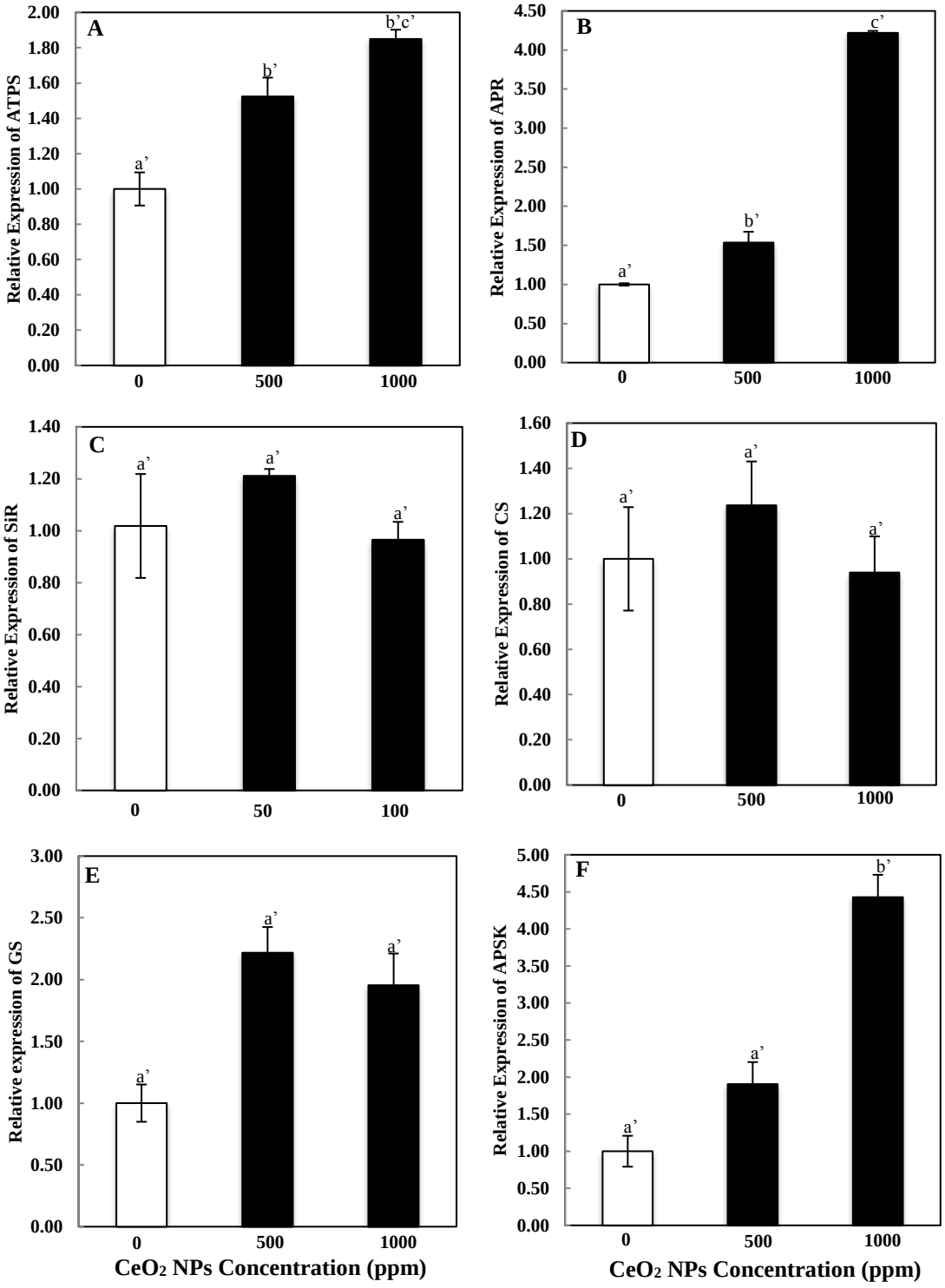

Figure 2. 13 Relative expression of antioxidant related genes in responses to CeO_2 NPs in *A. thaliana*. **Figure A-F** represent ATPS, APR, SiR, CS, GS, and APSK, respectively. The means are averaged from 3 replicates of *A. thaliana*. The error bars correspond to standard error of mean. Values of each gene followed by different letters with apostrophe are significant differences at $p<0.05$.

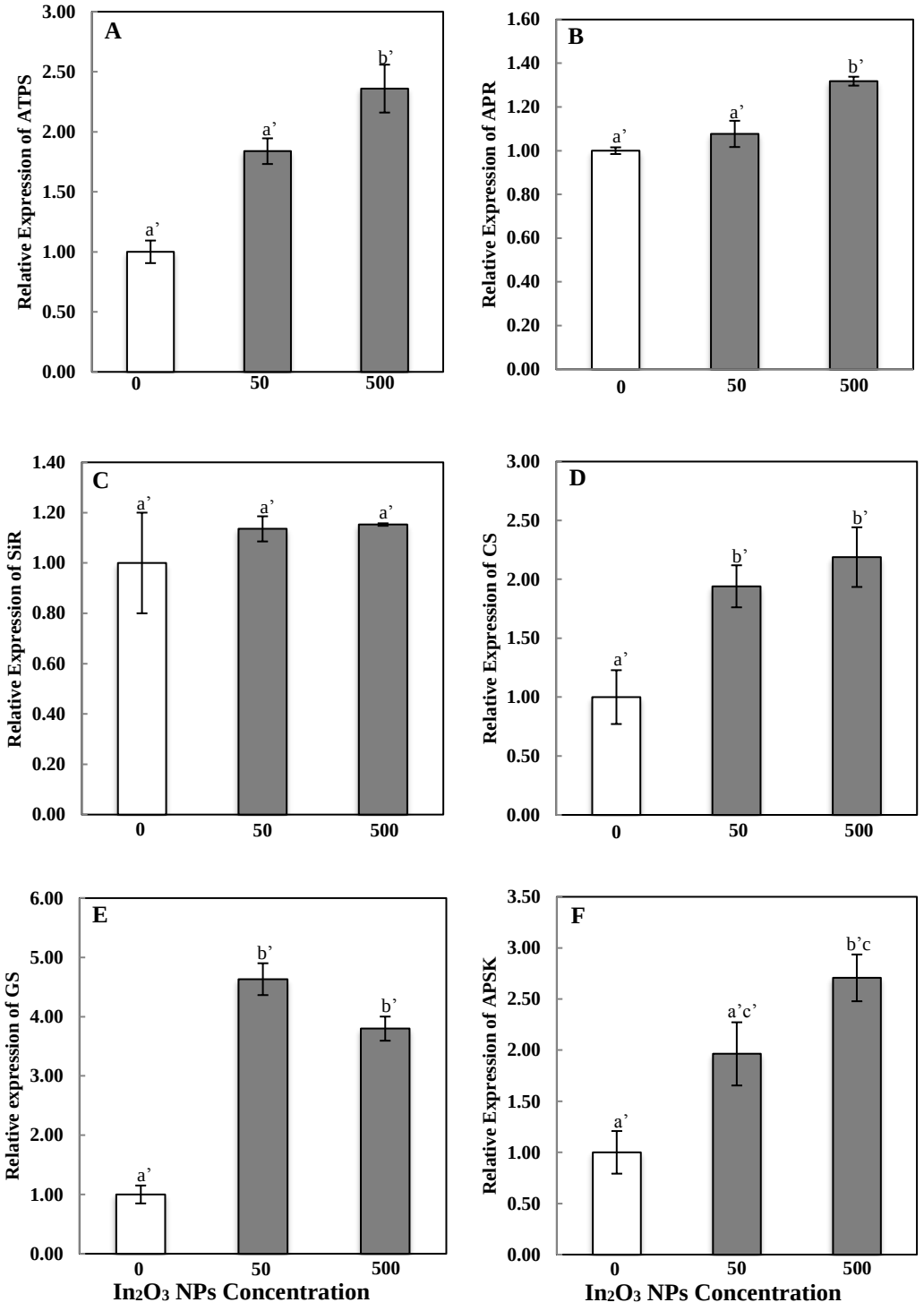

Figure 2. 14 Relative expression of antioxidant related genes in responses to In_2O_3 NPs in *A. thaliana*. **Figure A-F** represent ATPS, APR, SiR, CS, GS, and APSK, respectively. The means are averaged from 3 replicates of *A. thaliana*. The error bars correspond to standard error of mean. Values of each gene followed by different letters with apostrophe are significant differences at $p<0.05$.

CHAPTER 3

REDUCED SILVER NANOPARTICLE PHYTOTOXICITY IN *CRAMBE ABYSSINICA* WITH ENHANCED GLUTATHIONE PRODUCTION BY OVEREXPRESSING BACTERIAL Γ-GLUTAMYLCYSTEINE SYNTHASE

3.1 Introduction

Nanotechnology has been applied in a diverse range of industries, including pharmaceuticals, cosmetics, electronics, and agriculture.[166, 167, 168] It is widely known that at size dimensions of the nanoscale (<100nm), physical and chemical properties of materials can change dramatically, and that much of this change is driven by the higher ratio of surface to volume. It is the usefulness of many of these unique size-dependent properties that has driven the exponential growth in nanotechnology.[1, 169, 68, 170] However, it is also widely recognized that there is an insufficient understanding of nanomaterial fate, transport and effects in the environment.[171, 172] A number of recent studies have been published demonstrating that upon nanoparticle exposure, toxicity to plants, microorganism, and animals may occur.[173, 29, 174, 37, 64 175] Clearly, further work, particularly at the mechanistic and molecular scale, is necessary to fully characterize the risk of nanomaterial use and exposure.

Silver nanoparticles (Ag NPs) are among the most widely used nanomaterials in consumer products,[176] largely due to the observed antimicrobial activity, and as such, concerns over Ag NPs impacts on non-target biota have increased. Zheng *et al.* demonstrated that Ag-SiO_2 shell nanoparticles displayed antimycotic activity to phytopathogenic fungi at doses as low as 0.5 ppm.[177] Savithramma *et al.* observed that Ag NPs synthesized from *Shorea tumbuggaia* were highly effective at inhibiting both bacterial and fungal growth.[178] Similarly, *Escherichia coli* exposed to Ag NPs

experienced growth inhibition but importantly, sulfidation of Ag NPs, as may be common in wastewater treatment, lessened the observed nanotoxicity.[179]

Although numerous reports have recently been published on the fate and toxicity of nanomaterials to terrestrial plants species, a critical knowledge is still lacking. Mechanisms of nanoparticle toxicity remain elusive but due to the increased reactivity and small size, nanoparticle entry into and accumulation within plants cells may be significant. A growing body of evidences has demonstrated that Ag NPs at a wide range of concentrations can result in oxidative stress, leading to observed phytotoxicity, although low exposure doses of Ag NPs from 0.01 to 0.1 mg/L could stimulate *A. thaliana* growth.[180] Ravindran *et al.* and Stampoulis *et al.* noted that Ag NPs in a wide range of exposure doses from 10 to 1000 ppm inhibited seed germination, root elongation, biomass/growth and transpiration rate in tomato (*Lycopersicum esculentum*), corn (*Zea mays*) and summer squash (*Cucurbita pepo*).[181, 182] Upon exposure to Ag NPs (20nm and 100nm) for 14 days, duckweed (*Lemna minor L.*) exhibited a linear dose-response relationship, as exposure doses increased, both frond number and relative growth rate of duckweed were significantly decreased.[183] Lee *et al.* evaluated the phytotoxicity of Ag NPs to mung bean (*Phaseolus radiates*) and sorghum (*Sorghum bicolor*) under both agar and soil conditions.[72] Interestingly, the phytotoxicity of Ag NPs in soil was markedly less, presumably to the lower bioavailability of the particles in natural media. It is noteworthy that the majority of the nanoparticle phytotoxicity data is confined to physiological endpoints and that few studies have addressed toxicity at the molecular level. Kaveh *et al.* demonstrated that transcripts involved in thalianol biosynthetic pathway (one of plant defense mechanism) were highly up-regulated in Ag NPs treated *A. thaliana*.[86] Panda *et*

al. described the genotoxicity of Ag NPs to *Allium cepa* when compared to other Ag forms, noting that the NPs caused cell death and DNA damage by inducing reactive oxygen species (ROS) generation.[21]

Crambe abyssinica, a member of *Brassicacea*, is naturally tolerant to abiotic stresses such as cold, salt and heavy metals.[184] Crambe is a high biomass, high oil content (35-40%) crop with a short life cycle, making it an ideal industrial crop for both biofuel production and phytoremediation.[104] Previously, we engineered Crambe to overexpress the *E. coli* γ-ECS gene, which yields high levels of glutathione (GSH), as compared to wild type (WT) Crambe.[184] GSH is widely recognized as one of the most important redox buffer in living cells for the detoxification of oxidative stress and damage caused as a result of high ROS levels production under stress conditions. In this study, two independent γ-ECS transgenic Crambe lines were exposed to Ag NPs and Ag^+ ions to evaluate the potential tolerance of genetically modified Crambe to nanoparticle and ionic Ag. Measured physiological parameters included biomass, transpiration rate, and chlorophyll content, as well as Ag shoot and root content. In addition, to gain a perspective on toxicity and tolerance, three main thiol compounds involved in the entire GSH metabolic pathway along with soluble nutrient elements were evaluated. To our knowledge, this study represents the first report of simultaneous physiological and biochemical effects of nanotoxicity to genetically engineered plant.

3.2 Materials and Methods

3.2.1 Seed sterilization

C. abyssinica cultivar BelAnn was transformed with *γ-ECS* gene as described by Chhikara *et al.*[184] Two transgenic lines (γ-ECS1 and 16) showing high transgenic expression were selected for this study.[184] γ-ECS16 showed higher expression level of γ-ECS transcripts as well as γ-ECS protein level compared to γ-ECS1.[184] Seeds of WT and two independent homozygous transgenic Crambe were surface sterilized with 70% ethanol for 10 min, twice soaked in 25% (v/v) commercial bleach solution for 15 min, and washed 5 times with autoclaved DI H_2O for 5 min rinsing.[118] The seeds were inoculated on half-strength Murashige and Skoog medium (1/2x MS medium: 2.22 g MS Basal medium/vitamins, 20 g sucrose and 8 g phytoblend in 1 L DI H_2O, pH 5.7) in magenta boxes.[185] The plants were incubated in a growth chamber at 22 °C with 16h/8h (light/dark) cycle, the light intensity is 250 μmol $m^{-2}s^{-1}$.

3.2.2 Determination of inhibitory Ag concentrations

An initial screening study was conducted to characterize the dose-dependent nature of toxicity and to enable determination of optimum Ag exposure concentrations for additional physiological and biochemical studies. The initial concentrations were 25, 50, 100 and 200 mg/L Ag NPs (particle size 20 nm; purchased from US Research Nanomaterials, Inc); 500, 1000, 2000 and 3000 mg/L for bulk Ag (particle size: 44 μm; Strem Chemicals); and 25, 50, 100 and 200 μM for Ag^+ ions (Fisher Scientific). Ag NPs were twice dispersed by ultrasonic treatment for 30min each time prior to storage in the dark place at room temperature overnight.[29] Hydrodynamic diameters of Ag NPs in DI

water and Hoagland's solution were measured by Dynamic Light Scattering (DLS), as shown in Figure 3.1. For each treatment, fifteen seeds of WT Crambe per box were planted into Ag-amended 1/2x MS medium. All experiments were conducted in triplicates. These magenta boxes were maintained in a growth chamber as described above for 25 days prior to biomass determination.

Based on the preliminary dose-response assay (Figure 3.2), 200 and 250 mg/L were selected as the Ag NP exposure levels, and 200 and 250 μM were chosen for Ag^+ ions. However, no significant difference of fresh biomass was found among bulk Ag treatments (even at 3000 mg/L exposure dose) as compared to Ag NPs and Ag^+ ions treatments. Thus, additional work in this study will exclude bulk Ag treatment. Using identical exposure conditions, both WT and transgenic Crambe were exposed to Ag for 25 days.

3.2.3 Phytotoxicity of Ag NPs to Crambe in hydroponic systems

To determine the impact of Ag exposure on transpiration and metal uptake, WT and transgenic Crambe were germinated in a magenta box with 1/2x MS medium containing phytoblend as described above. After 25 days, the plants were carefully removed from solid medium, and were rinsed gently with DI water to remove attached media on the roots. Both WT and transgenic Crambe were transferred to half-strength Hoagland's solution (Hoagland Modified Basal Salt Mixture purchased from Phytotechnology Laboratories) and allowed to acclimatize for 7 days prior to 5 days exposure to the Ag NPs and Ag^+ ions treatments. The transpiration was measured by the volume of solution

lost; fresh solution without Ag was added daily to maintain a consistent volume. After exposure, plant tissues were harvested to evaluate Ag content, GSH, and nutrient levels.

3.2.4 Measurement of chlorophyll content

Chlorophyll content was determined by modified protocol as described in Lichtenthaler.[120] Briefly, 50 mg fresh tissue was harvested and cut into pieces (< 1 cm), and added to 15 mL centrifuge tubes amended with 10 mL 95% ethanol. The tested tubes were kept in the dark for 3-5 days and the chlorophyll content was measured by a UV-Vis spectrophotometer (Spectronic Genesis 2). Chlorophyll a, chlorophyll b and total chlorophyll were determined by the following equations: $Chla=13.36A_{664.2}-5.19A_{648.6}$, $Chlb=27.43A_{648.6}-8.12A_{664.2}$ and Total chlorophyll=Chla+Chlb.

3.2.5 Measurement of Ag accumulation and nutrient uptake in Crambe

Harvested root tissue was rinsed with DI H_2O three times to remove surface retained Ag. All shoot and root samples were oven-dried at 65 °C for 3 days and then 30 mg of tissue was transferred to 15 mL centrifuge tubes amended with 3 mL of HNO_3. The samples were digested at room temperature for 48 hrs. Five hundred microliters of H_2O_2 were then added to complete the tissue digestion. The digests were diluted 35 folds with DI H_2O prior to determination of Ag content by inductively coupled plasma mass spectroscopy (ICP-MS, Agilent 7500ce).[35] Ag NPs and $AgNO_3$ amended ½ X Hoagland's solution was centrifuged at 5000 rpm for 1 hr. Supernatant was passed through 0.45μm filter then used for determination of Ag content.

For extraction of soluble fraction of nutrient shoot and root 200 mg tissue samples were extracted in I mL of 5% perchloric acid (PCA). Samples were again frozen and thawed 3 times and kept frozen at -20°C until analyses.[186] For quantitation of nutrients PCA extracts were diluted 100 fold and analyzed using a simultaneous axial inductively coupled plasma emission spectrophotometer (ICP-AES, Vista CCD, Varian, Palo Alto, CA, USA) and Vista Pro software (Version 4.0). National Institute of Standards and Technology (NIST, Gaithersburg, MD, USA) standards for Eastern white pine needles (SRM 1575A) and apple leaves (SRM 1515) were used since no standards are available for fresh foliar tissues. We did use an in-house ground wood reference sample for quality control and assurance. For all samples, a standard curve was repeated after every 20 samples, and check standards were run after every recalibration and after every 10 samples.

3.2.6 Measurement of lipid peroxidation in Crambe

Lipid peroxidation was determined by measuring malondialdehyde (MDA) content in shoot and root of Crambe. 200 mg of plant tissues were homogenized in 4 mL of 0.1% (w/v) of tricholoroacetic acid (TCA). The extracts were used for measuring MDA content following the method described in Jambunathan (2010).[187]

3.2.7 Measurement of levels of γEC, GSH and PC3 in Crambe

A pool of approximate 200 mg fresh tissue (homogenous mix of shoot and root) was collected in 1.5 mL containing 1 mL extraction buffer (6.3mM diethylenetrianmine pentacetic acid, DTPA, mixed with 0.1% trifluoroacetic acid, TFA). The extracts were used for derivatization and analysis of thiol compounds (Cysteine, γEC, GSH and PC3)

as described in Minocha *et al.*[188] 250 μL of sample extract or standard was mixed with solution containing 615 μL of 200 mM 4-(2-hydroxyethyl)-piperazine-1- propane sulfonic acid (HEPPS) buffer and 25 μL of 20 mM Tris(2-carboxyethyl)phosphine hydrochloride (TCEP). 0.5 mM *N*-acetyl-l-cysteine (NAC) was used as an internal standard. The mixture was incubated at 45 °C for 10 min, and 10 μL of 50 mM monobromobimane (mBBr) was added before placing all samples in the dark place at 45 °C for 30 min. 1M methanesulfonic acid (MSA) was used to terminate the reaction. All samples were passed through 0.45 μm filters and stored at -20 °C until analysis of thiol compounds using high performance liquid chromatography (HPLC).

3.2.8 Statistical analysis

For each assay, the means are averaged from 4-5 replicates and error bars correspond to standard error of mean. One-way analysis of variance (One-way ANOVA) followed by Duncan multiple comparison test was used to determine statistical significance of each parameter among treatments. Values of each assay followed by different letters are significantly different at $p \leq 0.01$ or 0.05.

3.3 Results and Discussion

3.3.1 Determination of inhibitory Ag concentrations for Crambe growth

Wild type Crambe was exposed to different concentrations of NPs, Ag^+ ions as well as Ag bulk particles (Figure 3.2). Exposure to 25 mg/L Ag NPs resulted in a significant decrease in plant biomass relative to unexposed controls but the observed phytotoxicity was not significantly different at 25, 50, and 100 mg/L. At 200 mg/L Ag NPs, the

biomass reductions were significantly greater than other exposure concentrations and were 60% less than that of unexposed controls. Although 50 μM of Ag^+ ions had no impact on plant biomass, exposure to higher concentrations resulted in dose-dependent phytotoxicity (Figure 3.2). Bulk Ag exposure at 200-2000 mg/L resulted in 18-32% biomass reductions relative to unexposed controls; high variability in biomass at 3000 mg/L exposure resulted in statistical ambiguity with regard to toxicity (Figure 3.2). It is notable that for exposure at equivalent concentrations of 200 mg/L (μM for Ag^+ ions), Ag NP results in 20% more biomass reduction, indicating greater toxic response with Ag NPs exposure. In addition, Ag NP exposure at 25 mg/L induced significantly greater toxicity than much higher levels of ionic or bulk particles. Based on these findings, concentrations of 200 and 250 mg/L for Ag NPs and 200 and 250 μM for Ag^+ ions were selected for additional study. High concentrations of bulk Ag were used to select inhibitory concentration for this study, however, bulk Ag treatment did not show higher phytotoxicity compared to other two treatments. Therefore, we stopped using bulk Ag in further experiment.

3.3.2 Analysis of fresh biomass in Ag-exposed Crambe

As described in Material & Methods sections, transgenic γ-ECS and wild type (WT) plants were exposed to 200 and 250 mg/L Ag NPs and 200 and 250 μM Ag^+ ions. After 25 days of Ag exposure, the biomass (roots and shoots) of WT and two independent γ-ECS transgenic Crambe lines was determined at harvest. There were no significant differences in the biomass of WT and transgenic plants in the non-exposed control. Ag exposure in any form significantly reduced the biomass of all plant types (Figure 3.3). However, across all four Ag-exposure scenarios, γ-ECS Crambe lines achieved

significantly higher biomass than respective WT plants. WT Crambe biomass was 28-33% and 44-46% less than the transgenic lines at 200 mg/L and 250 mg/L Ag NPs, respectively. Similarly, transgenic Crambe lines attained significantly greater biomass under Ag^+ ions exposure as compared to WT; at 200 and 250 µM, the WT mass was reduced by 39-43% and 27-33%, respectively, relative to γ-ECS Crambe. Collectively, Ag NPs exposure resulted in more damages to both WT and transgenic Crambe as compared to Ag^+ ions treatment, nanoscale effects might be the main reason beyond the toxicity caused by Ag^+ ions.

The exposure dose for Ag NP and Ag^+ ions in our study is higher than that used in a number of other studies, including annual ryegrass (*Lolium multiflorum*) (0-40 ppm) in solutions, [28] wheat (*Triticum aestivum L.*) (2.5 ppm) in sand matrix,[189] *P. radiatus* and *S. bicolor* (0-40 ppm) in agar test [72] and rice (*Oryza sativa L.*) (0-60 ppm) in N6 growth cultivation media.[22] Transgenic Crambe lines exhibited greater tolerance and were noticeably healthier than WT after exposure to Ag NPs and Ag^+ ions (Fig. 1). In accordance with a number of recent studies, Ag NPs caused greater phytotoxicity than corresponding bulk and ion treatments. Hawthorne *et al.* reported significantly less zucchini biomass upon exposure to 250 ppm Ag NPs relative to an equivalent bulk Ag control.[173] Dimpka *et al.* illustrated that the inhibition of wheat root and shoot tissue was significantly greater for Ag NPs (2.5 mg/kg) than an equivalent amount of Ag^+ ions.[189] In addition to Ag, other metal NPs such as CuO,[71, 190, 131] CeO_2 (0-4000 ppm) [66] and Al_2O_3 [191] have been reported to induce oxidative stress and reduce the biomass of plants such as *Z. mays*, cucumber (*Cucumis sativus*), dotted duckweed (*Landoltia punctata*) and tobacco (*Nicotiana tabacum*).

3.3.3 Analysis of chlorophyll content in Ag-exposed Crambe

As the critical photosynthetic pigment, chlorophyll levels can be a significant indicator of toxicity to plants. In the control plants, there were no significant differences in the chlorophyll content between WT and transgenic Crambe (Figure 3.4). The chlorophyll content of all plants was decreased upon Ag exposure, regardless of concentration and Ag types. However, similar to the biomass data above, across all four Ag-exposure scenarios the chlorophyll levels in the γ-ECS Crambe lines were significantly greater than the respective WT plants. WT Crambe chlorophyll content was 47-49% and 34-42% less than the transgenic lines at 200 mg/L and 250 mg/L Ag NPs, respectively. Similarly, transgenic Crambe produced significantly greater chlorophyll content under Ag^+ ions exposure as compared to WT; at 200 and 250 μM, the WT mass was reduced by 47-49% and 39-40%, respectively, relative to γ-ECS Crambe.

Similarly, Jiang *et al.* reported a time-dependent decrease in giant duckweed (*Spirodela polyrhiza*) chlorophyll content upon exposure to 0-10ppm Ag NPs. [192] Oukarroum *et al.* investigated the impact of 0-10 ppm Ag NPs exposure on green algae (*Chlorella vulgaris* and *Dunaliella tertiolecta*) at two temperatures. The study reported not only dose dependent decreases in chlorophyll content but also described a nanoparticle-induced disruption of photosynthetic electron transport. [193] Although other metal oxide nanoparticles such as CuO NPs [131] have also been shown to decrease chlorophyll production, it is worth noting that both TiO_2 [194] NPs and Au NPs [77] were reported to increase the production of the pigment in *T. aestivum spp.* and *Brassica juncea*. Additional studies are being planned to characterize the mechanism of Ag NPs-induced decreases in chlorophyll levels, which may occur by inhibition of chloroplast

formation or by direct interaction with and degradation of chlorophyll. From the aspect of molecular response to Ag NPs treated *A. thaliana*, down-regulation of transcription levels of protochlorophyllide reductases, which are responsible for chlorophyll sysnthesis, were observed. [86] This result could further lead us to understand the mechanism of chlorophyll degradation occurred in the presence of Ag NPs.

3.3.4 Analysis of Ag-exposure on transpiration in Crambe

In order to understand the effects of Ag NPs on plant transpiration rate, hydroponic system was set up as shown in Appendix II. The transpiration rate was determined by calculating water loss by volume for each replicate over 24 h interval for 5 days period (Figure 3.5). Similar to biomass and chlorophyll, the transpiration rate after 5 days exposure was reduced by Ag NPs exposure, regardless of concentrations, but both γ-ECS Crambe lines consistently transpired more solution than the respective WT individuals. The transpiration rates of WT Crambe treated with 250 mg/L Ag NPs were significantly reduced by 35-46% relative to the transgenic lines (Figure 3.5). Similar results for transpiration rate were obtained when plants were exposed to 200 mg/L Ag NPs (data not shown). Interestingly, the exposure to Ag^+ ions at 250 □M concentration had no effect on solution transpiration rates, regardless of plant types. Also, at lower concentration of 200 □M Ag^+ ions, no difference in transpiration rate was observed (data not shown).

Our findings are in agreement with Stampoulis *et al.* where Ag NPs decreased *C. pepo* transpiration volume by 75% as compared to bulk-exposed and untreated plants.[182] Conversely, transpiration rate was not impacted in corn and radish plants grown in CeO_2 NPs amended soil.[145, 195] Another study demonstrated that TiO_2 NPs could notably

elevate transpiration rate in Elm tree (*Ulmus elongata*) hydroponically.[196] This finding is highly significant that, in spite of the well-known phytotoxicity of Ag NPs, the γ-ECS Crambe lines yielded significantly greater growth (biomass, transpiration) at equivalent exposures, strongly implicating GSH metabolism in the defense of NP-induced abiotic stress.

3.3.5 Analysis of lipid peroxidation in Ag-exposed Crambe

Membrane integrity in both WT and transgenic Crambe was assessed by MDA formation (Figure 3.6). MDA content in shoot of Crambe showed that significantly high level of MDA was produced in WT Crambe compared to both transgenic lines regardless of Ag forms. At 200 mg/L Ag NPs and 200 μM Ag^+ ions, MDA content in both γ-ECS Crambe was reduced by 27.3 - 32.5% and 20.6 - 33.6%, respectively, relative to WT. Similarly, in the root of both WT and transgenic Crambe, significantly low MDA content in both transgenic lines indicated that γ-ECS engineered plants showed high tolerance to metal stresses, regardless of metal forms. Other NPs could also induce excess amounts of MDA production in plants, indicating oxidative stress occurred in plants in the presence of metal-based NPs. As exposure doses of CuO NPs increased, MDA content in root of mung beans was significantly elevated.[197] High level of MDA was measured in CeO_2 NPs treated *A. thaliana*.[20] However, CeO_2 NPs could not induce lipid peroxidation in either corn plants or kidney beans.[23, 198] Up-regulations of relative expression of genes, including glutathione S-transferase, peroxidase, superoxide dismutase, all of which can scavenge excess amounts of ROS, were evident in Ag NPs treated *A. thaliana*.[86]

3.3.6 Analysis of γEC, GSH and phytochelatins in Ag-exposed Crambe

Cysteine is the primary precursor molecule in glutathione (GSH) biosynthesis in plants. In the unexposed plants, cysteine levels were similar for the WT and transgenic Crambe. However, upon exposure to Ag NPs and Ag^+ ions, cysteine production was significantly greater for the γ-ECS transgenic Crambe lines (Figure 3.7 A), clearly demonstrating the enhanced GSH metabolic pathway enabled by γ-ECS gene overexpression. γ-Glutamylcysteine (γ-EC) and GSH play essential roles in metal detoxification through thiol group (-SH) chelation. In Figure 3.7 B, transgenic plants produced significantly higher levels (up to four-fold) of γ-EC under the catalysis of γ-glutamylcysteine synthetase (γ-ECS), regardless of Ag presence. Glutathione synthetase (GS) converts γEC into γ-Glu-Cys-Gly (GSH) and in Figure 3.7 C, significantly greater GSH synthesis is evident in both transgenic lines without any treatments. Notably, GSH levels in WT and transgenic plants were decreased after exposed to Ag NPs and Ag^+ ions compared to the respective untreated control groups. PC synthetase (PCS) can effectively convert GSH into phytochelatins- PCs $(\gamma\text{-Glu-Cys})_{2\text{-}8}$-Gly, which results in depleting GSH levels. As shown in Figure 3.7 D, PC3 levels in both transgenic lines were overproduced compared to WT upon exposure 250 mg/L Ag NPs.

Cysteine is an effective antioxidant and could counteract Ag-induced stress because of the thiol group (-SH). Li *et al.* found that a significant increase in cysteine could be induced through overexpression of γ-ECS in Arabidopsis upon arsenic treatment because the great demand to synthesize GSH.[103] In addition, cysteine can be converted into GSH rapidly under the catalysis of γ-ECS and GS. Additionally, under the abiotic stress caused by Ag, reactive oxygen species (ROS) can be produced in plants, especially

superoxide anion (O_2^-) and hydrogen peroxide (H_2O_2).[21] Due to the direct toxicity of ROS in plant cells, GSH redox cycles are frequently activated for plant defense. In the GSH-mediated defense pathway, GSH peroxidase (GPx) can detoxify hydrogen peroxide by oxidizing GSH to GSSG.[199] GSH, also through its redox activity, can directly reduce Ag^+ ions through the conversion of GSH to the GSSG.[200] This may explain the reduction in overall GSH levels upon Ag NPs and Ag^+ ions treatment as compared to the control group. Dimkpa *et al.* demonstrated that GSSG in *T. aestivum* was increased significantly after treating with 2.5 ppm Ag NPs and 2.5 ppm Ag^+ ions.[189] Highly induced transcription levels of glutathione synthase (GS) were evident in both In_2O_3 and CeO_2 NPs treated Arabidopsis.[20] Another reasonable pathway to explain the GSH depletion is through phytochelatin biosynthesis. [201, 103] GSH is the precursor for the synthesis of phytochelatins catalyzed by phytochelatin synthase (PCS). [201] It has been reported that PCS in plants can be activated by metal ions such as Cd^{2+}, Hg^{2+}, Ag^+, Zn^{2+} and Cu^{2+}, [202] which could yield high levels of phytochelatins for detoxification of toxic metals. Li *et al*. observed that in transgenic Arabidopsis by overexpressing AtPCS1, Cd exposure enhanced phytochelatins levels by several fold over the control group. [203] Our results agree with these findings in that Ag NPs treatment increased PC3 levels in both WT and transgenic Crambe (Fig. 5D). Another possible pathway for GSH depletion is that GSH can directly bind/complex with Ag via –SH group.

3.3.7 Ag distribution and nutrient displacement in Crambe

The Ag content in each of the non-Ag exposed Crambe plants was below 0.5 μg/kg (not shown in the figure). The shoot Ag content of transgenic Crambe under Ag NPs treatment was significantly higher than WT. Notably, the Ag content in γ-ECS 16 shoots

reached to 50.5 mg/kg, which is 5-fold higher than WT plants (Figure 3.8 A). Under Ag^+ ions exposure, the shoots of γ-ECS transgenic Crambe also contained significantly higher Ag levels than WT plants, although the size of the increase was not as dramatic as observed with the NP treatment. Contrary to shoot, Ag content in the roots of both γ-ECS 1 and γ-ECS 16 Crambe exposed to Ag NPs were lower than WT. However, the Ag content of plant roots exposed to Ag^+ ions did not vary significantly among the γ-ECS and WT Crambe plants (Figure 3.8 B). Additional studies will be conducted to explore the decreased Ag content in transgenic root tissue. The shoot-to-root translocation factor (TFs; shoot concentration divided by root concentration) is shown in Figure 3.8 C. Regardless of Ag type, the transgenic Crambe translocation had significantly greater quantities of the element to the shoot tissue than WT. The centrifuged Hoagland's solution supernatant of $AgNO_3$ exposed plants had similar Ag levels across all plant types (Figure 3.8 D). Similarly, for the γ-ECS 16 Crambe, the solution Ag content of the Ag NPs treatment did not vary from that of the WT. However, for unknown reasons, the γ-ECS 1-8 treated with 250 ppm Ag NPs had nearly 3 fold higher Ag levels in the supernatant than WT. Notably, the root Ag content of these plants did contain significantly lower Ag levels than WT.

This observation is particularly noteworthy given the markedly decreased phytotoxicity observed with the γ-ECS Crambe but may have been a function of the significantly greater transpiration exhibited by the transgenic plants relative to WT. This observation may suggest that the higher levels of GSH and PC3 synthesis in transgenic plants may result in greater chelation of Ag or potentially differential storage in vacuoles or the cell wall. The findings of higher metal NP translocation than equivalent ions agree

with the work of De L Torre-Roche *et al*., where soybean (*Glycine max*) and *C. pepo* accumulated more shoot Ag under NP exposure (500 and 2000 ppm) relative to bulk or ions.[204] Similarly, Dimpka *et al.* reported that Ag levels in *T. aestivum* shoots were greater under 2.5 ppm Ag NPs treatment than equivalent bulk metal.[189] Others have reported on a dose-dependent accumulation of Ag NPs in organisms such as *L. multiflorum* [28] and *Chlamydomonas reinhardtii*.[205] In fact, similar dose-dependent nanoparticle accumulation has been noted for various concentrations of CuO, ZnO and Au NPs in *C. sativus* [71], *Z. mays* [206] and *B. juncea*.[77] Although our study only investigated a limited concentration range of Ag NPs and Ag^+ ions in WT and transgenic Crambe, the data clearly suggest phytochelation of Ag^+ with PC3, GSH and cysteine, along with subsequent transport from roots to shoots. In related work, we observed that engineered *A. thaliana* overexpressing the γ-ECS gene could also accumulated higher levels of cadmium and mercury than WT.[201]

Along with Ag distribution, nutrient elements were also determined in both WT and transgenic Crambe (Table 3.1). The levels of most soluble nutrient elements, such as Ca, K, Mg, Zn and Mn, were similar regardless of Ag presence and plant types, indicating that either Ag NPs or Ag^+ ions could not disrupt nutrient transport in Crambe. However, Fe level in WT Crambe, as one exception, was significantly lower in either Ag NPs or Ag^+ ions treatment than WT control group. Similar phenomenon was not found in γ-ECS Crambe lines as Fe levels in these lines were higher than WT plants under Ag NPs or Ag^+ ions. In addition, our results showed that P level in Ag^+ ions treated transgenic Crambe was significantly elevated compared to untreated transgenic controls, although the difference between WT and transgenic lines treated with Ag^+ ions was not significant.

Both Zhao *et al.* and Gao *et al.* studies suggested that CeO_2 and TiO_2 NPs could not disrupt nutrient levels in corn and *U. elongata*, respectively.[145, 196] Further studies are necessary to understand how plants respond to nutrient elements uptake in the presence of NPs and whether there is a defense mechanism (such as stomatal closure, transpiration rate reduction) in plants to avoid excess elements uptake, which subsequently causes nutrient displacement.[207]

In conclusion, we showed that enhanced level of GSH in transgenic Crambe expressing γ-ECS is involved in protecting plants from phytotoxicity caused by Ag NPs and Ag^+ ions. Further, exposure to Ag NPs caused significant decrease in Fe uptake only in wild type plants and not in γ-ECS lines. Since Fe is the most deficient nutrient for plant growth, our results holds significant importance to prevent crop yield loss as a results of Ag NPs and Ag^+ ions-induced phytotoxicity and Fe deficiency. This study is highly helpful to understand the fate, transport and toxicity of NPs in plants and role of GSH in counteracting the Ag NPs phytotoxicity, which could prove useful for mitigating the threat of NPs in the food chain and the environment.

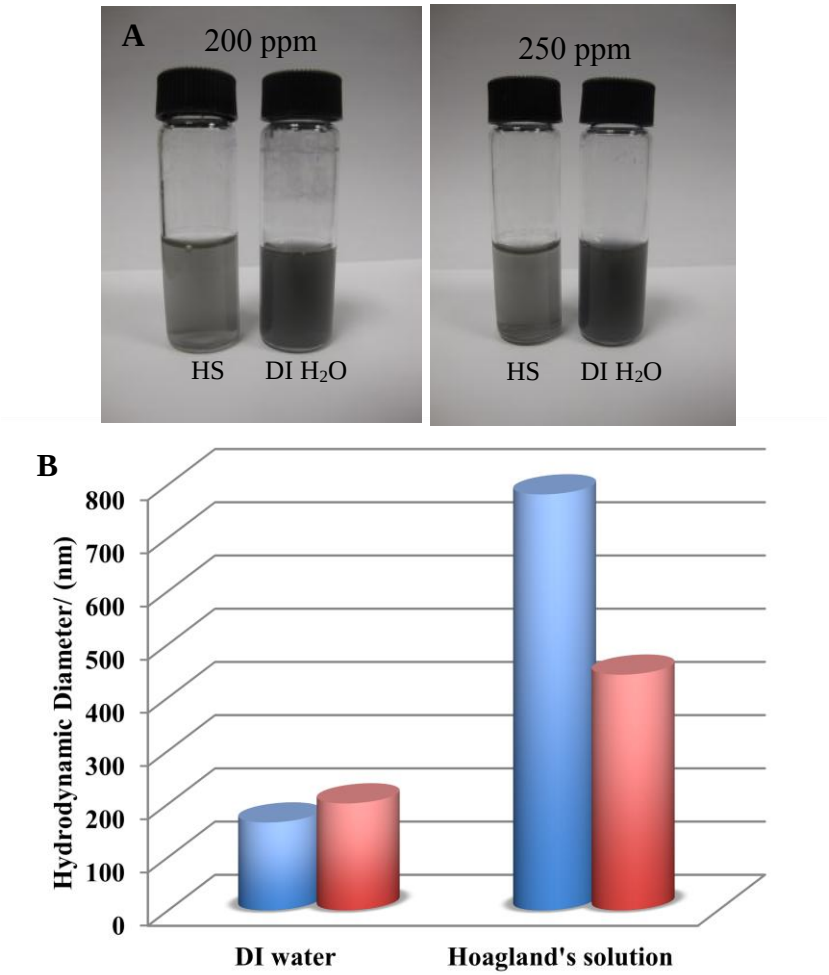

Figure 3. 1 Hydrodynamic diameter analysis of Ag NPs by DLS. (**A**) Images of two different concentrations of Ag NPs dispensed in DI water and Hoagland's solution (HS). (**B**) Hydrodynamic diameter analysis of Ag NPs in DI water and HS respectively. The means are averaged from 7 replicates. Hydrodynamic diameter of Ag NPs dispensed in HS was significantly higher than that of in DI water because of high ion strength in HS. Nanoparticle could be forced to agglomerate together in the solution with high ion strength.

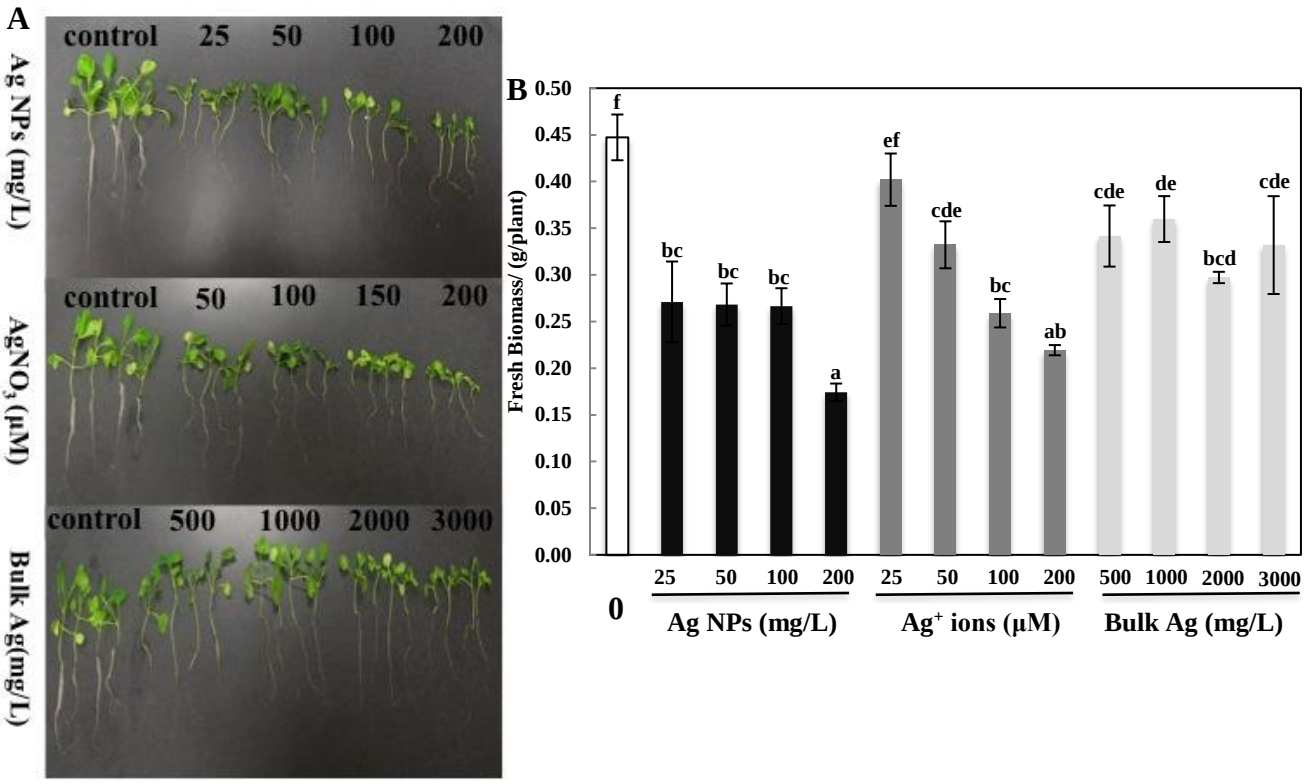

Figure 3. 2 Phenotypes of WT Crambe versus different forms of Ag. (**A**) In Ag NPs treatment, WT Crambe was exposed in the range of 25-200 ppm; In Ag^+ ions treatment, a series of doses were used from 50 to 200 µM to test Ag^+ ions toxicity on WT Crambe; In Bulk Ag treatment, no significant differences were observed in a wide range from 500 to 3000 mg/L. (**B**) Effects of various of Ag on fresh biomass of WT Crambe. Bulk Ag caused less damages to plants compared to other two forms of Ag. Data are mean ± standard error of three replicates of 15 plants each. Values of total fresh biomass followed by different letters are significantly different at $p \leq 0.05$.

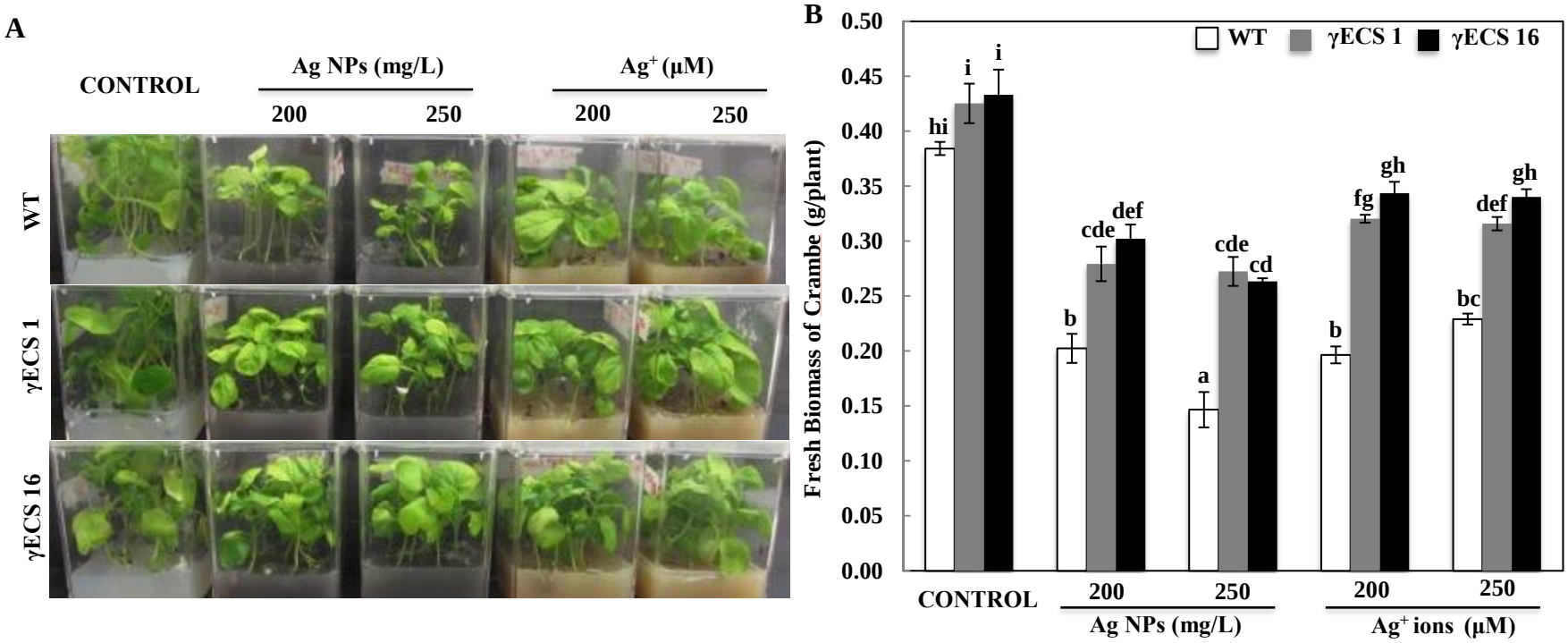

Figure 3. 3 Growth analysis of WT and γ-ECS lines treated with Ag NPs and Ag^+ ions. Plants were exposed to the indicated concentrations of Ag NPs and Ag^+ ions, respectively, for 25 days. (**A**) Images of WT and γ-ECS lines grown on Ag NPs and Ag^+ ions amended 1/2 x MS media after 25 day of growth. (**B**) Total fresh biomass of Ag NPs and Ag^+ ions treated WT and two γ-ECS lines. Data are mean ± standard error of 3 replicates of 15 plants each. Values of total fresh biomass followed by different letters are significantly different at $p \leq 0.01$.

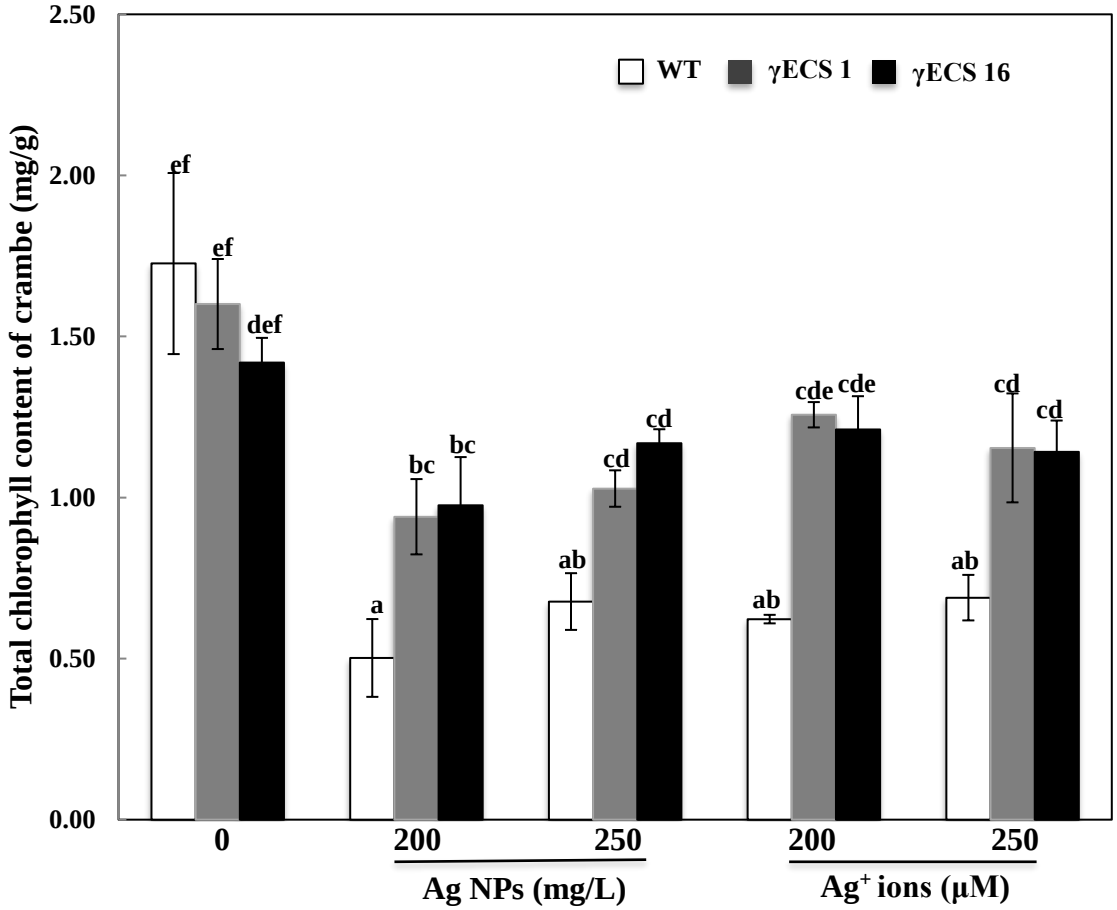

Figure 3. 4 Analysis of total chlorophyll content in WT and γ-ECS lines treated with Ag NPs and Ag^{+} ions. Data are mean ± standard error of three replicates of 15 plants each. Values of total chlorophyll contents followed by different letters are significantly different at $p \leq 0.05$.

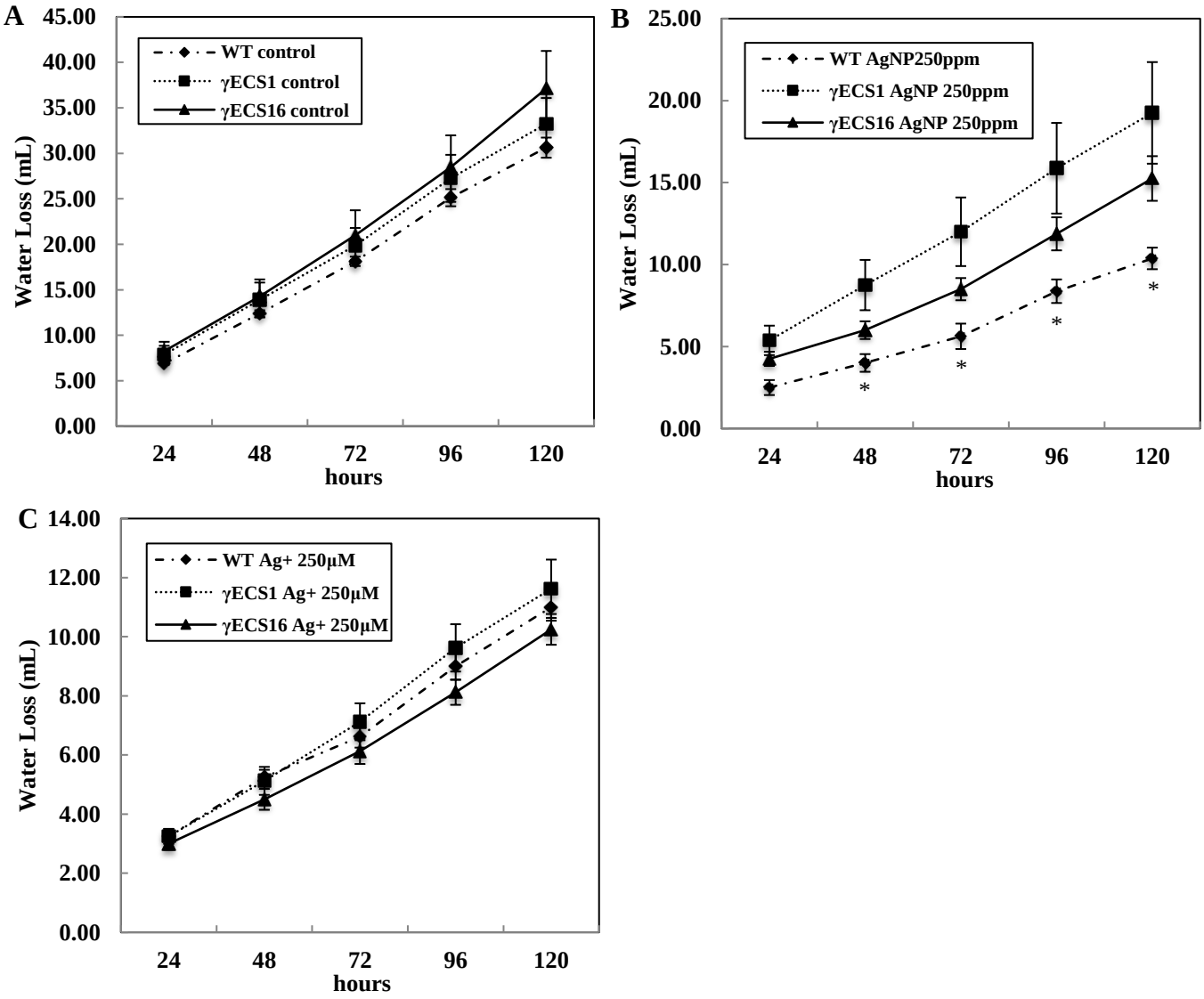

Figure 3. 5 Analysis of transpiration rate between WT and transgenic Crambe treated with 250 ppm Ag NPs and 250 µM Ag^{+} ions for 5 days. Water loss was calculated in 24 hours intervals. Data are mean ± standard error of 5 replicates. Values of transpiration rate marked with asterisks (*) are significantly different at $p \leq 0.05$.

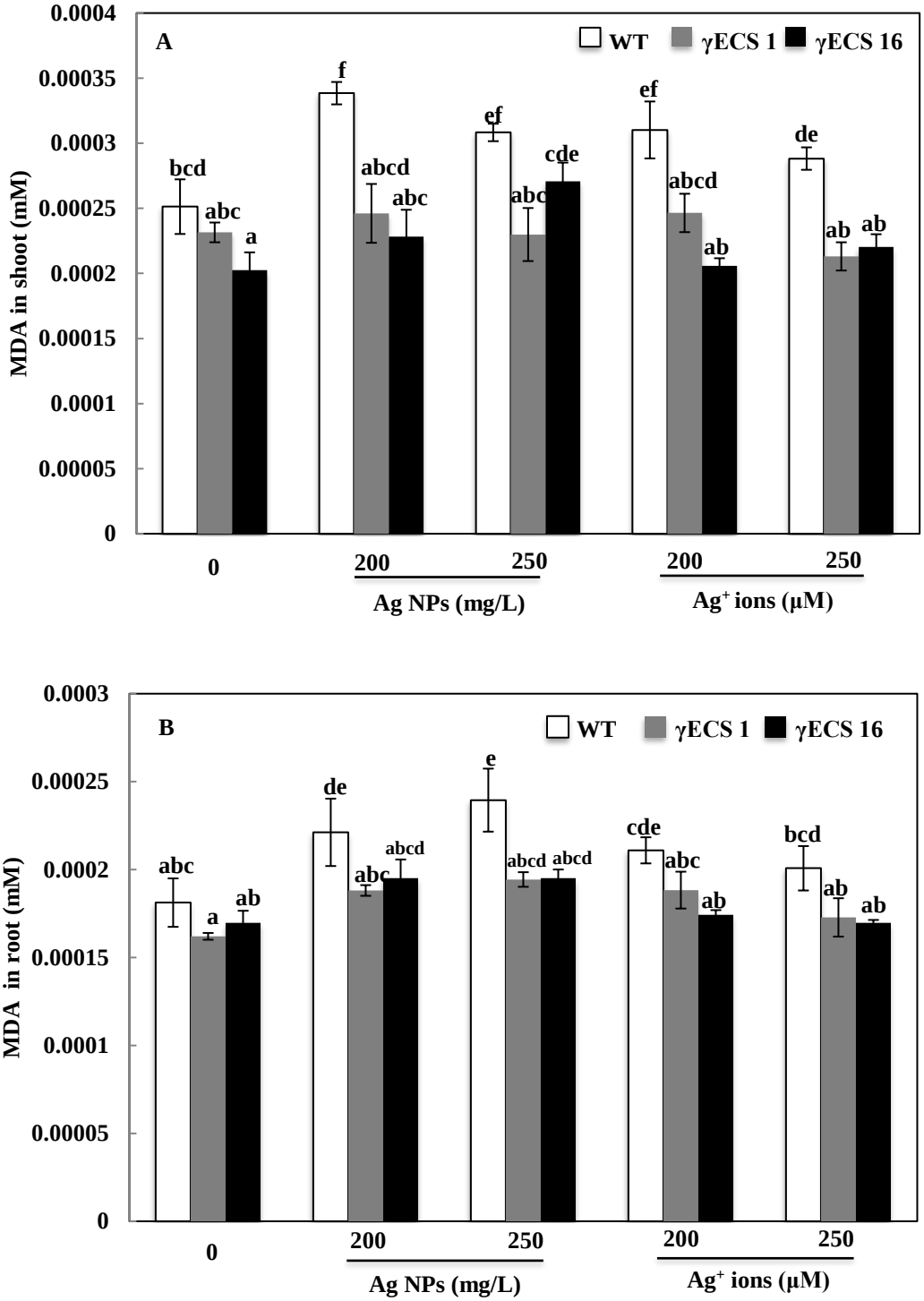

Figure 3. 6 Lipid peroxidation in shoot and root of WT and γ-ECS Crambe. MDA contents in shoot (**A**) and root (**B**) of WT and transgenic Crambe treated with 250 mg/L Ag NPs and 250 µM Ag^+ ions, respectively, for 25 days. Data are mean ± standard error of 4 replicates of 15 plants each. Values of MDA content followed by different letters are significantly different at $p \leq 0.05$.

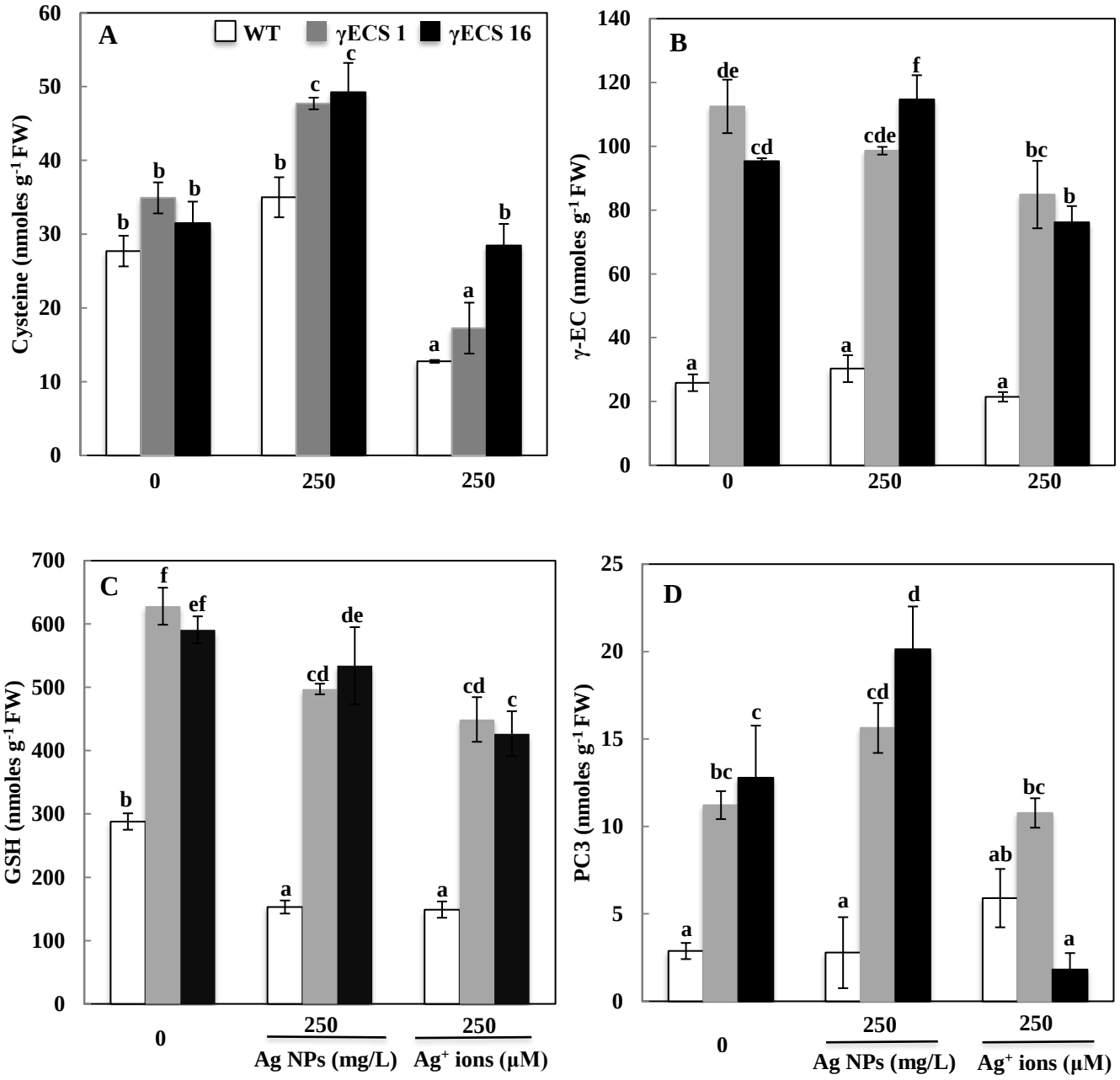

Figure 3. 7 Analysis of total cysteine, γ-EC, GSH and PC3 levels in WT and γ-ECS Crambe treated with 250 mg/L Ag NPs and 250 µM Ag^{+} ions. The individual component above were extracted from homogenous mix of shoots and roots tissues. **Figure A**, **B**, **C**, and **D** represent different levels of cysteine, γ -EC, GSH and PC3 between WT and transgenic Crambe, respectively. Data are mean ± standard error of 4 replicates. Values of each component followed by different letters are significantly different at $p \leq 0.05$.

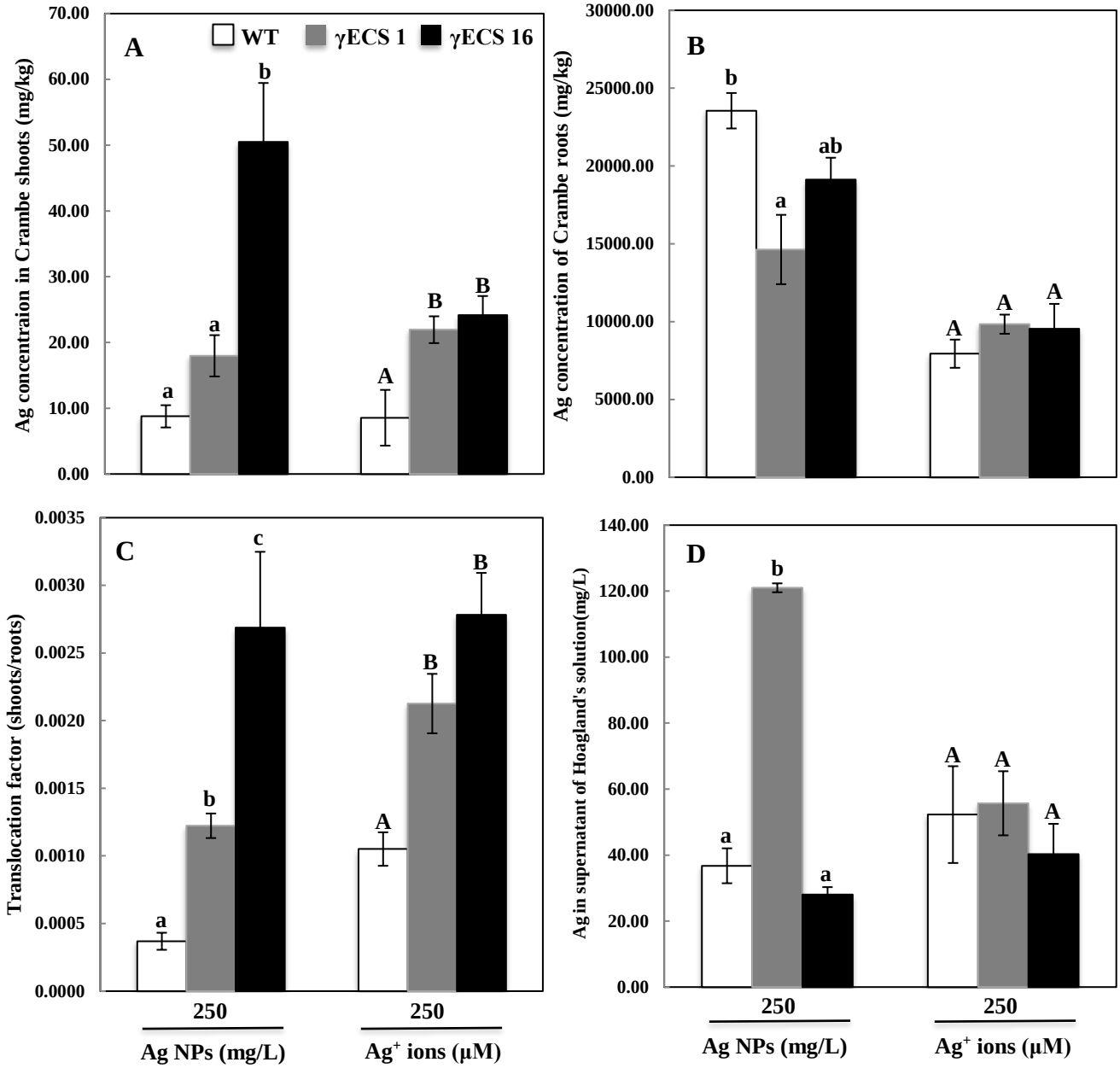

Figure 3. 8 Ag uptake and distribution in WT and γ-ECS lines treated with 250 mg/L Ag NPs and 250 µM Ag^+ ions. Panels **A**, **B**, **C**, and **D** represent Ag content in shoots, roots, TFs (shoots/roots), and supernatant of 1/2 x Hoagland's solution, resrectively. Data are mean ± standard error of 4 replicates. Values of Ag concentration in Ag NPs and Ag^+ ions treatment followed by different lowercase and uppercase letters, respectively, are significantly different at $p \leq 0.05$.

Table3. 1 Soluble elements (extracted in 5% perchloric acid) in Ag NPs and Ag^+ ions treated WT and γ-ECS Crambe lines

Soluble Nutrient element (µmoles g^{-1} FW)	Treatment	WT Crambe	γECS 1 Crambe	γECS 16 Crambe
Ca	Control	36.55±1.30 b	35.48±1.52 b	36.71±4.51 b
	250 mg/L Ag NPs	26.97±1.62 a	32.64±2.56 ab	29.61±1.45 ab
	250 µM Ag^+ ions	31.87±1.74 ab	33.15±2.61 ab	35.05±1.87 b
K	Control	62.60±1.85 ab	62.28±3.06 ab	64.68±2.18 ab
	250 mg/L Ag NPs	65.47±1.01 abc	68.83±0.70 bc	74.35±3.62 b
	250 µM Ag^+ ions	58.98±5.09 a	68.09±2.89 abc	66.85±1.66 abc
Mg	Control	5.36±0.30 ab	4.92±0.31 ab	4.67±0.38 ab
	250 mg/L Ag NPs	4.13±0.30 a	4.39±0.33 ab	4.91±0.57 ab
	250 µM Ag^+ ions	5.21±0.41 ab	5.19±0.35 ab	5.56±0.40 b
Mn	Control	0.169±0.051 a	0.158±0.023 a	0.167±0.025 a
	250 mg/L Ag NPs	0.146±0.029 a	0.168±0.019 a	0.115±0.012 a
	250 µM Ag^+ ions	0.166±0.021 a	0.207±0.034 a	0.184±0.040 a
Fe	Control	0.406±0.025 c	0.289±0.062 abc	0.211±0.003 ab
	250 mg/L Ag NPs	0.135±0.034 a	0.220±0.076 ab	0.170±0.053 ab
	250 µM Ag^+ ions	0.261±0.042 ab	0.340±0.075 bc	0.147±0.057 a
Zn	Control	0.051±0.007 ab	0.048±0.004 a	0.053±0.001 ab
	250 mg/L Ag NPs	0.048±0.004 a	0.044±0.003 a	0.065±0.007 c
	250 µM Ag^+ ions	0.054±0.003 ab	0.069±0.007 c	0.071±0.003 bc
P	Control	3.01±0.51 a	3.34±0.34 a	3.52±1.00 a
	250 mg/L Ag NPs	3.22±0.37 a	4.16±0.27 ab	5.02±1.17 ab
	250 µM Ag^+ ions	4.22±0.80 ab	6.40±0.92 b	6.16±1.01 b

Data are mean ± standard error of 4 replicates. Values of each element level followed by different letters are significantly different at $p \leq 0.05$.

CHAPTER 4

THE IMPORTANT ROLE OF GLUTATHIONE IN DETOXIFICATION OF SILVER NANOPARTICLES AND ENHANCEMENT OF NITROGEN ASSIMILATION IN SOYBEAN (*GLYCINE MAX*)

4.1 Introduction

Nanomaterials (NMs) are applied as nanocapsules for delivery of pesticides, fertilizers, and growth hormones; as nanosensors for detecting plant pathogens and monitoring soil conditions; and as carrier for delivering targeted gene to plants.[208] For example, Ag NPs is one of commonly used metal-based NMs in agriculture and industries. Beside direct application in agriculture, the released Ag NPs could also end up in agricultural filed via sewage sludge application. Due to their specific properties, NMs may pose potential risks in agricultural systems with low exposure doses despite positive impacts on the crops. Sustainable management of natural resource is the aim in agriculture.[209] Thus, it is very important to assess the nanoparticles (NPs) safety in agriculture.

Legume plants, belonging to *Leguminosae* family, are grown for purpose of good grain seed (such as beans) and major source of protein and edible oils in agriculture. It is well known that legume plants are capable of establishing a symbiotic relationship with *Rhizobium* species through forming nodules in the root system. Then, the atmospheric nitrogen (N_2) can be trapped and converted into ammonia (NH_4^+), which is bioavailable for plants compared with other nitrogen forms, by nitrogen fixing bacteria inside the nodules. The *Rhizobia*-legume symbiosis is considered as one of the most important mutualistic evolution in agriculture.[210] However, a major concern is that introducing NPs into agricultural system may pose phytotoxicity to both the legume plants and N fixing *Rhizobia Sp.*, which subsequently disrupt nodules formation in the root system, and

eventually compromise nitrogen cycle in agriculture. This could cause significant loss of crop yield and seriously affect the global food security. Recent studies have demonstrated that Ag NPs could inhibit root length, decrease plant biomass, alter transpiration rate, and delay plant development.[17, 71, 72, 73, 74] Also, NPs could lower nitrogen-fixation potential in soybean nodules, although no effect on nodules formation (dry weight of nodules) in the presence of NPs was evident.[32] Related research is still in the initial stage. Thus, the question regarding the effect of NPs on N fixation, how NPs disrupt nodules formation in legume plants that is critical to crop yield and food safety in full life cycle analysis of plants remains unanswered.

Soybean, one of the dominant crop legumes, can fix 16.4 Ton N annually, which represents 77% of the N fixed by the crop legumes.[211] Moreover, soybeans rank second, after corn, among the most-planted field crops in the USA, and soybean oil represents approximately 65% of all edible oil consumed in the United States (http://www.epa.gov/agriculture/ag101/cropmajor.html). The possible reasons that the applications of Ag NPs incorporated products in agriculture could potentially comprise N fixation in legume plants are: (1) the presences of NPs can inhibit *Rhizobium* species activity in soil[212], which will result in decreasing the chances of establishing symbiotic relationship with soybean; (2) In the early phase of legume-*Rhizobia* symbiosis establishment, soybean can biosynthesize some flavonoids such as genistein and daidzein to recognize specific *Rhizobia* in the early phase of legume.[213] Upon exposure to Ag NPs, the phase of recognition can be compromised due to disorder of flavonoid secretion. Together, failure to establish the legume-*Rhizobia* relationship could directly results in decreases of nitrogen-fixation efficiency in nodules, which may significantly affect crop

yield. Additional fertilizers have to be applied in the field with regard to this matter, which are not only costly, but also bring in some environmental concerns as nitrogen run-off from agriculture fields are major cause of N pollution in soil and ground water. Thus, in order to avoid these foreseeable concerns, how to alleviate NPs impacts on nitrogen-fixation efficiency in soybean becomes one of critical problems that need serious consideration and warrant further studies.

GSH is involved in plant defense against abiotic stresses such as heavy metals, drought and extreme temperature. It also plays an essential role in the development of the root nodules during the symbiotic interaction. On one hand, previous studies have demonstrated that introducing buthionine sulphoximine (BSO), an inhibitor of GSH, in legume plant could alter nodule formation.[214] Low level of GSH production could directly result in decreasing the numbers of root nodules. On the other hand, in order to bio-convert N_2 into NH_4^+, nodules are required to create a reducing condition accompanied by ROS production. Thus, GSH may also scavenge ROS through glutathione-ascorbate cycle in order to avoid disruption of nitrogen-fixation potential induced by ROS.[215] Glutathione S-transferases (GSTs) are ubiquitous enzymes, which are capable of catalyzing GSH conjugation to xenobiotic substrates for the purpose of detoxification. GST9 is the most prevalent one out of 14 forms of GST in nodules of soybean. Downregulation of transcript levels of GST resulted in decrease of nitrogenase activity and increase of oxidative stress. Thus, GSTs are also crucial to nitrogen-fixation potential in nodules [139]. Collectively, GSH is involved in nitrogen-fixation potential, which is directly linked to fertilizer usage and crop quality. Thus, in this study the role of GSH will be characterized in soybean upon exposure to Ag NPs.

In this study, we investigated the physiological effects of Ag NPs on soybean growth, including fresh biomass, nodule numbers and biomass, net photosynthetic rate, transpiration rate, and stomatal conductance. At harvest, total Ag content and nutrient contents were determined in nodule, root, and shoot of soybean. Synchrotron based X-ray fluorescent microscopy was applied to differentiate Ag speciation in plant tissues. Total N in nodule, root, and shoot was measured as well. In addition, we characterized the role of GSH in detoxifying Ag nanotoxicity and enhancing N assimilation in soybean. All of these results can help us understand how NPs interact with legumes and potentially lower the nitrogen-fixing potential. These questions directly link to crop yield and food quality in the sustainable agriculture.

4.2 Materials and Methods

4.2.1 Experimental design

Substrate optimization. Prior to conduct the exposure experiment, we optimized the soil substrate by mixing with different types of commonly used amendments (vermiculite and potting mix). 25% or 50% (v/v) vermiculite and potting mix was mixed with field soil collected from the Agronomy Research Farm of the University of Massachusetts in South Deerfield. Soybean was grown for 3 weeks under greenhouse conditions. At harvest, we chose physiological parameters, including plant biomass, shoot height and total number of nodules to determine the soil substrate used in this study.

Concentration selection of Ag NPs. Ag NPs was mixed with optimized soil substrate thoroughly, according to the desired exposure concentrations in each treatment (0-62.5 mg/kg). Pots were filled with 250 g soil and 50 mL of tap water was added into each pot

from the bottom. After 24 hours, soybean was seeded in the surface soil at 1 cm depth. Plants were maintained under the greenhouse conditions for 4-5 weeks. Fresh biomass and number of nodules were used to determine the selected concentrations.

Concentration selection of GSH. Soybean was seeded in each pot containing 250 g soil without any addition of Ag NPs. 50 mL of different concentrations (0, 5, 10, and 20 mM) of GSH solution was applied to each pot every week for 4 weeks. The optimized concentration of GSH was determined based on results of fresh biomass, total number of nodules.

4.2.2 Chlorophyll content

Chlorophyll content will be determined by the procedure modified by Lichtenthaler (1987).[120] Briefly, 50 mg fresh tissue will be harvested and cut into pieces (< 1 cm), and added to 15 mL centrifuge tubes amended with 10 mL 95% ethanol. The tested tubes will be kept in the dark for 3-5 days and the chlorophyll content will be measured by a UV-Vis spectrophotometer (Spectronic Genesis 2). Chlorophyll a, chlorophyll b and total chlorophyll will be determined by the following equations: $Chla=13.36A_{664.2}-5.19A_{648.6}$, $Chlb=27.43A_{648.6}-8.12A_{664.2}$ and Total chlorophyll=Chla+Chlb.

4.2.3 Net photosynthesis rate, transpiration rate, stomatal conductance

Photosynthesis rate (Pn), stomatal conductance and transpiration rate were measured right after the first trifoliate leaves fully developed. LI-6400XT Portable Photosynthesis System was used to measure all the parameters in both control and Ag NPs treated soybean. For instrument setup, CO_2 in reference chamber was 400 μmoles; relative

humidity was between 50-65%; light intensity was 750 μmoles; flow was 200 μmoles. In order to obtain stable reading, the machine was matched every ten samples.

4.2.4 Metal uptake and nutrient displacement

Dry shoot or root tissues were ground to fine powder and approximately 50 mg was transferred into a glass tube containing 3 mL concentrated HNO_3. All samples were digested at 105 °C for 40 min in a heating block and then 500 μL H_2O_2 was added for 20 min to complete the digestion. All digests were diluted with deionized (DI) H_2O to 50 mL prior to elemental analysis for Ce and In by inductively coupled plasma mass spectroscopy (ICP-MS) and for macro- and micronutrients by inductively coupled plasma optical emission spectrometry (ICP-OES).[35]

4.2.5 Ag biotransformation in soil and plant tissues

Soybean tissues were harvested and stored at -80 °C until further analysis. The root and nodule were axially sectioned to 30 micron thickness using a cryomicrotome. The thin sections were mounted onto slides and were stored in the freezer. Synchrotron X-ray fluorescence maps were collected at an energy higher than Ag K-edge (25523 eV). At Ag hot spots, micro X-ray absorption near edge structure (μXANES) was collected at Ag K-edge. Bulk X-ray absorption spectroscopy (XAS) was collected for representative Ag model compounds (e.g. Ag NPs, Ag_2S, AgCl, $AgNO_3$, Ag_3PO_4, Ag-GSH, and Ag-citrate). Principle component analysis and linear combination fittings (LCF) were conducted on the unknown and reference compounds to determine the structure and relative composition of the unknown samples.

4.2.6 Total nitrogen analysis

Soybean tissues (leaf, root and nodule) were freeze-dried using Lyophilizer (FREEZONE 4.5, LABCONCO). All tissues were ground to fine powder before Kjeldahl digestion for determining total nitrogen. Briefly, 0.2g tissue and 1.625 g of mixture of potassium sulfate and cupric sulfate were mixed in kjeldahl flask. 3.5 mL sulfuric acid was added into each sample and digested at medium heat till clear solution was observed. Then, sample was further digested at high heat for 40 min after solution had turned to green. All digests were cooled down in the hood before adding 46.5 mL deionized distilled H_2O into each flask. Total nitrogen was measured using the QC8500 analyzer.[216]

4.2.7 Growth curve of Ag NPs treated Bradyrhizobium in HM medium w/ or w/o the presences of GSH

Previously, it was shown that *Bradyrhizobium* abundance was the highest as compared to *Frankia* and *Rhizobium* in the field soil.[217] As the same soil used in the soybean work here, *Bradyrhizobium japonicum* (USDA 110) was chose to test Ag NPs effects on rhizobium growth in HEPES-MES (HM) medium with or without the additions of GSH (Appendix III). A series of exposure concentrations of Ag NPs were prepared in autoclaved deionized H_2O. 5 mM of GSH was used to study whether the presences of GSH could reduce Ag NPs toxicity to rhizobium. *Bradyrhizobium* was inoculated in HM medium and when OD_{600nm} reached to approximately 1.0 in each flask, different concentrations of Ag NPs suspension and GSH solution were added into the culture. The experiment lasted for one week, and the culture was sampled at Day 1, 2, 3, 5 and 7. A fixed amount of culture were spread on growth media plate and the changes of total

number of colonies in each Ag NPs treatment over 7 days was determined.

Dehydrogenase activity was used to determine *Bradyrhizobium* activities upon exposures to different concentrations of Ag NPs. At Day 7, a volume of 2 mL culture in each treatment was transferred into Eppendorf tube and centrifuged at 4000 rpm, 4 °C for 15 min. The cell pellet was re-suspended in 2 mL deionized H_2O, then 2mL 0.2% triphenyl tetrazolium chloride (TTC) was added into the suspension. The mixture was inoculated at 37 °C overnight. The red formazan was extracted by 4 mL acetone, and then OD value was determined at 484 nm.[218]

4.2.8 Analysis of γEC and GSH

The contents of GSH and γEC in Ag NPs treated soybean with or without the additions of GSH were determined by following the identical protocols described in section 3.2.7.

4.2.9 Analysis of amino acid

Approximately 200 mg fresh soybean tissues were placed in 1 mL of 5% (v/v) ice cold perchloric acid and were stored at -20 °C until further analysis. Detailed information regarding sample preparation, HPLC conditions, as well as sample separation can be found in Minocha et al. (2004).[219]

4.3 Results and Discussion

4.3.1 Effects of different types of soil amendments on soybean nodules

As shown in Figure 4.1, soybean was grown in natural soil amended with 25 or 50% (v/v) vermiculite or potting mix. There was not much visible difference among all the

treatment, except the vermiculite alone treatment, in which soybean was relative small as compared to other treatments (Figure 4.1 A). Root length and whole plant height did not exhibit the significant different among all the treatments (Figure 4.1 B). However, due to the low contents of organic matter and nutrient in the vermiculite, the lowest shoot biomass was evident in the vermiculite alone treatment (Figure 4.1 C).

At harvest, the image of soybean root system is shown in Figure 4.2 A. Interestingly, no nodule was evident in both vermiculite and potting mix alone treatments. Two types of amendments had different impact on total numbers of nodules. The highest numbers of nodules were found in the treatment of 25% vermiculite + 75% soil. The additions of 25 or 50% potting mix significantly decreased the nodule numbers relative to the control (natural soil alone treatment). The possible reason might be that the organic matter content in the potting mix was notably high as compared with the vermiculite, and could provide the relatively sufficient nitrogen source and thus, plant might need less help from the symbiotic relationship with rhizobium, which can fix N from the atmosphere and convert N_2 to NH_4^+.

4.3.2 Physiological effects of Ag NPs on soybean

4.3.2.1 Effects of Ag NPs on soybean growth and nodule formation

The additions of different concentrations of Ag NPs can severely impact soybean growth as shown in Figure 4.3 A. Low exposure doses of Ag NPs did not impact on soybean growth in term of fresh biomass. As exposure doses of Ag NPs increased to 62.5 mg/kg, the fresh biomass of soybean root and shoot were decreased by more than 50% relative to the control group (Figure 4.3 B). Although the exposure dose of 31.2 mg/kg Ag NPs had

no impact on plant biomass, the total numbers of nodules were significantly lower than the control and other Ag NPs treatments (Figure 4.3 C).

It is well known the fact that metal-based NPs are unstable and can release certain amounts of ions to the environment. In order to figure out which form of Ag contributes the most on inhibition of soybean growth, Ag ions (in form of Ag NO_3) and bulk Ag (in micro-size) were also applied as Ag controls in this study. Both Ag ions and bulk Ag had no impact on soybean growth in terms of plant phenotype, fresh biomass and total numbers of nodules (Figure 4.4 A-C). Thus, nano-size effect might be the main reason that caused phytotoxicity to soybean.

4.3.2.2 Effects of Ag NPs on photosynthesis system in soybean

Photosynthesis system plays the essential role in plant growth and development. Net photosynthetic rate (Pn), stomatal conductance (Sc), transpiration rate (Tr) and total chlorophyll content in Ag NPs treated soybean are shown in Figure 4.5. The lowest Pn were evident in 62.5 mg/kg Ag NPs treatment, and low concentrations of Ag NPs had no impact on Pn (Figure 4.5 A). Similarly, the lowest Sc and Tr were only evident in 62.5 mg/kg Ag NPs treated soybean (Figure 4.5 B and C). Total chlorophyll content in Ag NPs treated soybean further confirmed that Ag NPs could compromise the photosynthesis system in soybean and subsequently result in low plant biomass (Figure 4.5 D). Our previous study also demonstrated that the presences of 200 and 250 mg/L Ag NPs could significantly reduce the total chlorophyll content in Crambe grown in medium.[220] Compared to the Crambe work, Ag NPs could cause phytotoxicity to soybean at the exposure dose as low as 62.5 mg/kg, indicating soybean is really sensitive to Ag NPs.

Interestingly, the additions of Ag ions and bulk Ag had no impact on Pn, Sc and Tr, but slight elevations of Sc and Tr were evident in the treatments of two different concentrations of bulk Ag.

4.3.2.3 Ag distribution in nodule, root, and shoot of soybean

Figure 4.6 shows Ag uptake in nodule and root of soybean treated with different concentrations of Ag NPs. The Ag contents in soybean nodule were increased as exposure doses of Ag NPs increased (Figure 4.6 A). The dose-response fashion was also evident in soybean root. The Ag accumulation in 62.5 mg/kg Ag NPs treated soybean root was more than 4-fold higher as compared with the one in 31.2 mg/kg Ag NPs treatment. No Ag accumulation was found in the aboveground tissue (data is not shown).

4.3.2.4 Analysis of Ag speciation in soil and soybean tissues

Metal-based nanoparticles (NPs) transformation can help us further understand the toxicity and biological fate of NPs to living organisms. As discussed above, phytotoxicity caused by Ag NPs can be mainly ascribed to nano-size effect. Thus, it is of importance to figure out whether metal biotransformation could occur in soybean tissue, as the Ag uptakes in nodule and root were evident. The related results could provide comprehensive understand on metal detoxification in soybean plant.

Figure 4.7 A-D represent Ag speciation in soil, nodule, cross section of root, and whole root, respectively. Ag speciation in 31.2 mg/kg Ag NPs soil was analyzed at harvest and LCF indicated that approximately 77.8% Ag remained in the form of Ag NPs, 18.3% Ag converted to Ag_2S, and very tiny amounts (4.8%) of Ag-GSH were also

evident (Table 4.1). In 31.2 mg/kg Ag NPs treated nodule, we found that the majority of Ag was still in the form of Ag NPs (83.6%) and only 16% of Ag existed in the form of Ag-GSH. However, Ag speciation exhibited the opposite results in soybean root tissues. We conducted the mapping on both cross section of roots and whole root (the root surface) in the treatment with 62.5 mg/kg Ag NPs. Two hot spots in each mapping were select to differentiate Ag speciation using XANES. Highly identical results were found in different positions of Ag NPs treated soybean roots that almost 60% of Ag were in form of Ag-GSH and the rest part remained in Ag NPs. Foliar exposure study demonstrated that Ag NPs in lettuce leaf were mainly in the form of oxidation of Ag NPs and complexation of Ag^+ by thiol molecules.[221] Another study suggested that biotransformation of gum arabic (GA) and polyvinylpyrrolidone (PVP) coated Ag NPs was different in aquatic microcosms. The plant derived dissolved organic matter could biotransform part of GA-Ag NPs to oxidized Ag (5-14%) and Ag complexation associated with thiol molecules (22-28%).[222] Biotransformation of other NPs such as CeO_2 NPs and ZnO NPs were also reported previously. Evidence on the presence of CeO_2 NPs in edible portion of soybean was reported using Synchrotron X-ray Fluorescence Mapping, suggesting that food safety caused by NPs should receive more attention than ever.[55]

4.3.2.5 Analysis of macro- and micro-nutrient displacements in soybean

The contents of macro and micronutrients in nodule, root and shoot of Ag NPs treated soybean are shown in Table 4.2 and 4.3, respectively. In the nodule, the presences of 31.2 mg/kg Ag NPs notably elevated the macronutrient contents, including K, P, S, Ca and Na, by 1.7-, 1.8-, 1.44-, 1.57-, and 1.65-fold of the control, respectively. In the root,

elevations of K, P, and Mg were evident in 31.2 mg/kg Ag NPs treatment. As exposure dose of Ag NPs increased to 62.5 mg/kg, significant decrease of Mg in the root was found. In the shoot, 62.5 mg/kg Ag NPs severely disrupt the macronutrient contents. For example, 28%, 22%, 38%, and 76% decreases in K, P, Ca, and Na contents were found in soybean shoot treated with 62.5 mg/kg Ag NPs as compared with the control group.

Similar to the macronutrient contents, the presences of Ag NPs could also impact on micronutrient contents in soybean tissues. For example, the Fe and Zn contents in 31.2 mg/kg Ag NPs treated nodule were increased by approximately 90% and 100% relative to the control, respectively. In the shoot, the addition of 62.5 mg/kg Ag NPs severely reduced the Fe, Cu, and Zn contents when compared to the control group.

Metal-based NPs could disrupt nutrient uptake and assimilation in plants, which could directly impact plant growth, development, and yield at harvest. In our previous study, uptake of Fe, which is required for plant growth, especially for photosynthesis, [147] in *Arabidopsis* root was significantly decreased in the presences of CeO_2 and In_2O_3 NPs. Ag NPs significantly lowered the levels of Fe in both Ag NPs and Ag^+ ions treated wild type *Crambe*.[220] Ca is a versatile second messenger, which is involved in responding to both abiotic and biotic stresses. [149, 150, 151] However, the presences of high concentration of Ag NPs severely reduced the Ca uptake in soybean shoot. In addition, Mg is also involved in chlorophyll synthesis.[223] Taken together, nutrient displacement might be another possible reason that resulted in adverse effects on photosynthesis system in soybean.

4.3.2.6 Effects of Ag NPs on total N in soybean roots, shoots and nodules

Total N in shoot and root system of Ag NPs treated soybean are shown in Figure 4.8. In soybean shoot, the lowest total N was evident in 62.5 mg/kg Ag NPs treatment, which was approximately 50% less than the control. Low exposure doses of Ag NPs such as 3.9 and 7.8 mg/kg Ag NPs had no impact on total N in soybean shoot (Figure 4.8 A). Similar decreases in total N of soybean nodule are shown in Figure 4.8 B. Interestingly, the exposure dose of Ag NPs as low as 7.8 mg/kg could notably lower the total N in the nodule. The decrease in total N in the root system was only evident in 62.5 mg/kg Ag NPs treatment. A recent study demonstrated that N_2 fixation potential was significantly reduced in CeO_2 and ZnO NPs treated soybean relative to control group. Scanning electron microscopy images further demonstrated that absence of rhizobia in CeO_2 NPs treated nodule was evident, which directly resulted in decrease of N_2 fixation potential.[32]

4.3.2.7 Effects of Ag NPs on Bradyrhizobium growth in HM medium

Figure 4.9 shows growth curve of Bradyrhizobium in Ag NPs amended HM medium for 7 days. Low exposure doses of Ag NPs, such as 5 and 10 mg/L, had significant impact on inhibiting Bradyrhizobium growth. As Ag NPs concentrations increased to 25-75 mg/L, severe inhibitions in the treatments with 50 and 75 mg/L Ag NPs were evident. For example, the number of CFU in 75 mg/L Ag NPs treated culture was only 6% of the control after 24 hours. In this experiment, the range of exposure doses of Ag NPs is consistent with the plant exposure study. Thus, the related results could provide the solid evidence that Ag NPs inhibited rhizobium growth in the environment could be one of possibilities that compromises the symbiotic relationship between legume plants and

rhizobium and subsequently results in low N assimilation in plants.

4.3.3 The presences of GSH significantly alleviate Ag nanotoxicity to soybean

4.3.3.1 GSH concentration selection

Phenotypic image of different concentrations of GSH treated soybean is shown in Figure 4.10 A. The additions of 5 and 10 mM GSH significantly enhanced the fresh biomass. However, as the concentration of GSH increased to 20 mM, the fresh biomass was decreased to the control level (Figure 4.10 B). Interestingly, the presences of GSH could severely decrease nodule formation. For example, the total number of nodules in the 5 mM GSH treatment was extremely low as compared to the control (without the addition of GSH). As concentrations of GSH increased to 10 and 20 mM, no nodule was evident in soybean root system. Thus, in the following experiment, only 5 mM GSH was applied to characterize the role of GSH on alleviation of Ag NPs toxicity to soybean.

4.3.3.2 Physiological effects of GSH on Ag NPs treated soybean

Figure 4.11A and B show phenotypic difference between Ag NPs alone and (Ag NPs + 5mM GSH) treatments. The additions of 5 mM GSH notably increased fresh biomass in both treatments with 31.2 and 62.5 mg/kg Ag NPs. The presences of 5 mM GSH significantly elevated the total biomass in 31.2 and 62.5 mg/kg Ag NPs treatments by approximately 100% as compared with the control without the GSH presences (Figure 4.11 C).

However, the additions of 5 mM GSH inhibited nodule formation in terms of number of nodules and nodule biomass. As shown in Figure 4.11 C and D, the total

number of nodules in GSH control group was only one fifth of the control (without the additions of GSH). Similar result was also evident in nodule biomass.

Thus, we hypothesized that the presences of GSH might interact with Ag NPs to lower its toxicity and bioavailability to soybean, and the extra GSH might be used as nitrogen source for plant growth and subsequently reduce the nodule formation in the root system.

4.3.3.3 Effects of GSH on photosynthesis system in Ag NPs treated soybean

Figure 4.12 shows effects of GSH on the total chlorophyll content and net photosynthetic rate in Ag NPs treated soybean. Across all four scenarios, the additions of GSH did not significantly alter the photosynthesis system in soybean. For example, the values of Pn, Sc, and Tr in (Ag NPs + 5 mM GSH) treatment were not statistically different as compared with either the control group or the GSH control. In the following study, we put the main effort on figuring out the reason that GSH enhanced plant growth and reduced the Ag nanotoxicity.

4.3.3.4 Effects of GSH on total N in Ag NPs treated soybean

Figure 4.13 A shows total N in shoot and root of soybean treated with 5, 10, 20 mM GSH. The presences of 5 mM GSH significantly elevated the total N level in soybean shoot as compared with the control group. No difference between the treatments of 10 and 20 mM GSH was evident. In the root, the total N in 10 and 20 mM GSH treatments were approximately 2-fold higher than the control root.

Figure 4.13 B-D represent total N in shoot, nodule, and root system of Ag NPs

treated soybean with or without the additions of GSH. The consistent results that high concentration of Ag NPs (62.5 mg/kg) decreased the total N in soybean shoot and root were evident. Interestingly, the presence of GSH notably increased the total N in shoot in both 31.2 and 62.5 mg/kg Ag NPs treatments, which was 46 and 69% higher than the GSH control, respectively (Figure 4.13 B). Similar results were also evident in the root system (Figure 4.13 D). However, the presences of GSH severely reduced the total N in the nodule as shown in Figure 4.13 C. The possible reasons might be that (1) GSH could inhibit rhizobium activities in soil and subsequently resulted in low nodule numbers and biomass; (2) GSH was used as nitrogen source to maintain plant growth and soybean probably needed no help from rhizobium to assimilate N from atmosphere. Thus, in order to figure out how the additions of GSH impact the rhizobium growth, we measured growth curve of Ag NPs treated Bradyrhizobium with the presences of 5 mM GSH.

4.3.3.5 Growth curve of Ag NPs treated *Bradyrhizobium* with the presences of GSH

Figure 4.14 exhibits activities of Ag NPs treated Bradyrhizobium in the presences of 5 mM GSH. Without the presences of Ag NPs, 5 mM GSH severely reduced the total CFU as compared with the control group. However, when introducing 50 and 70 mg/L Ag NPs into the culture, we found that the additions of 5 mM GSH enhanced Bradyrhizobium growth in term of total CFU number as compare with its respective Ag NPs control (Figure 4.14 A). In addition, we also measured dehydrogenase activities (DHA) in each treatment, as this enzyme activity can represent microorganism activities upon exposure to pollutants in the environment. The DHA results were consistent with the CFU number in the culture (Figure 4.14 B). In the GSH control group, 5 mM GSH severely inhibited the DHA activities by 44.4%, and subsequently resulted in significantly low CFU number

in the culture relative to the control group. In the Ag NPs treatments, the presences of GSH notably increased the DHA activity in 50 mg/L Ag NPs treatment, but only slightly higher DHA activity was evident in 75 mg/L Ag NPs treatment as compared to its respective control.

4.3.3.6 γEC and GSH contents

Figure 4.15 shows the contents of thiol compounds, including cysteine, γEC, and GSH, in Ag NPs treated soybean shoots, roots, and nodules with or without 5 mM GSH additions. As shown in Figure 4.15 A1-A3, the addition of 5 mM GSH significantly elevated the levels of cysteine, γEC, as well as GSH in 31.25 mg/kg Ag NPs treated shoots. However, no elevation among all three thiol compounds was obversed in 62.5 mg/kg Ag NPs treatment, regardless of the presence of 5 mM GSH. In soybean roots, the addition of 5 mM GSH notably increased the levels of three thiol compounds among all treatments when compared to their respective non-GSH controls. It is worthwhile to notice that extremely low content of GSH was evident in 62.5 mg/kg Ag NPs treated soybean roots and there was no GSH detected in 31.25 mg/kg Ag NPs treated soybean roots (Figure 4.15 B3). Interestingly, the GSH levels were similar between control and 31.25 mg/kg Ag NPs treatment with or without the GSH additions. In order to figure out where GSH went after taken up by soybean, the contents of amino acids were measured among all treatments in section 4.3.3.7.

4.3.3.7 Analysis of amino acid

The contents of amino acids involved in nitrogen assimilation pathway, including alanine, glutamate, and glutamine, were measured in Ag NPs treated soybean with or

without the addition of 5 mM GSH (Figure 4.16). As expected, the contents of all three amino acids were significantly increased in the GSH treatments as compared to the non-GSH treatments regardless of the presence of Ag NPs. For example, in 31.25 mg/kg Ag NPs treated soybean shoots, the contents of alanine and glutamate were 5-6 folds higher relative to the non-GSH treatments (Figure 4.16 A1 and A2). Additionally, the presence of Ag NPs further induced the amino acid contents as compared to the control group. Similar results were also evident in soybean roots (Figure 4.16 B1 and B2). Interestingly, there was no significant difference at the amino acid contents in soybean nodules among all treatments, although slight increases of all three amino acids were found in the GSH control relative to the non-GSH control (Figure 4.16 C1-C3).

Taken together, soybean plant is sensitive to Ag NPs exposure. The presences of Ag NPs could severely inhibit plant growth, alter the photosynthesis system, and disrupt the nutrient contents in soybean. When introducing GSH into plant-soil system, we found that the additions of GSH could significantly alleviate the Ag nanotoxicity to soybean and further enhance plant growth in term of fresh biomass. GSH had no impact on the photosynthesis system in soybean but inhibited the nodule formation in the root system. We conducted the separated experiment to investigate the interactions between *Bradyrhizobium* and GSH or (Ag NPs + GSH) under the laboratory conditions. The results suggested that GSH could inhibit *Bradyrhzobium* growth in terms of the CFU number and DHA activities. However, with the presence of Ag NPs, GSH could alleviate Ag NPs toxicity and increase the CFU number as compared with the Ag NPs alone treatments. Thus, we speculated that GSH might coat on the surface of Ag NPs or form the complexation of Ag with the thiol molecules to alleviate Ag NPs toxicity to

Bradyrhizobium. This process could decrease the GSH level in the culture and subsequently reduce the negative effect of GSH on rhizobium growth. Significantly high levels of total N were evident in either the GSH control or (Ag NPs + GSH) treatments. We currently put our main effort on investigating the underlying mechanism how soybean utilizes GSH as nitrogen source for its own growth in the presences of Ag NPs. The related experiments including analysis of cysteine and GSH contents, amino acid contents, as well as gene expression involved in GSH degradation pathway in soybean, are currently underway.

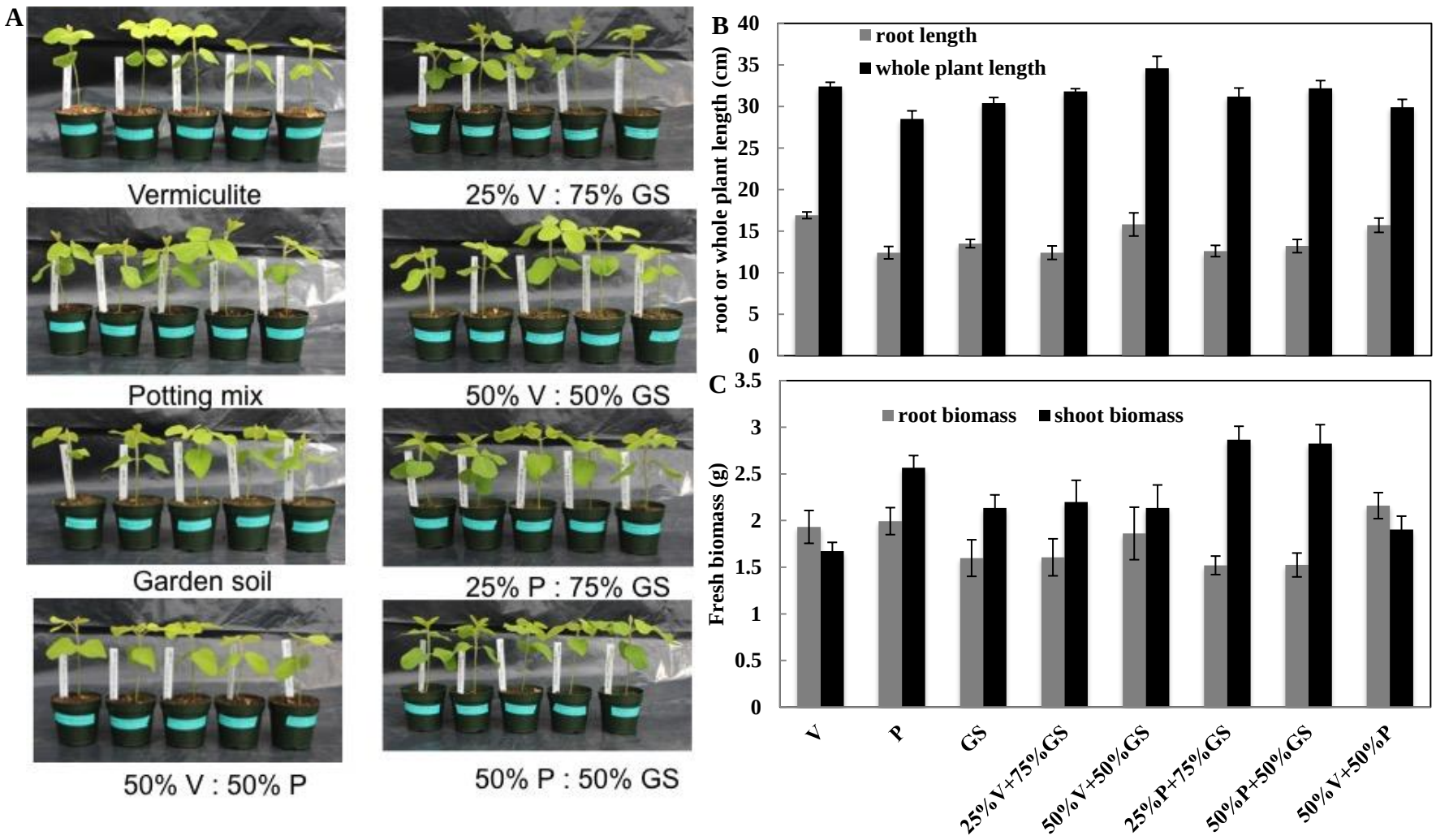

Figure 4. 1 Effects of different types of amendments on soybean growth. (**A**) phenotypic images of soybean grown in soil amended with different percentages of vermiculite and potting mix; (**B**) root length and whole plant length; (**C**) fresh biomass of root and shoot. V: vermiculite; P: potting mix; GS: garden soil.

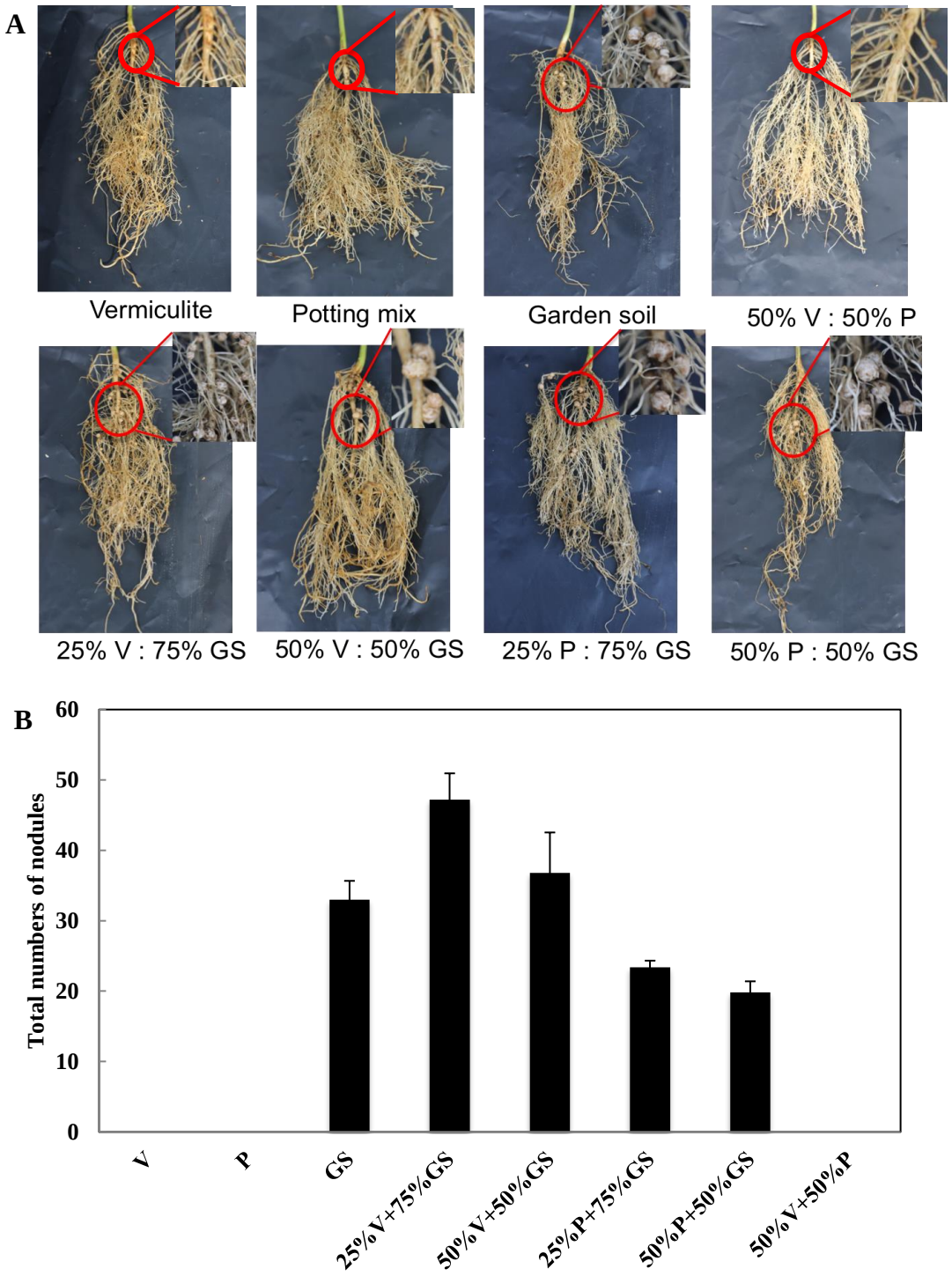

Figure 4. 2 Effects of different types of amendments on total numbers of nodules. (**A**) phenotypic images of soybean nodules grown in soil amended with different percentages of vermiculite and potting mix; (**B**) total numbers of nodules. V: vermiculite; P: potting mix; GS: garden soil.

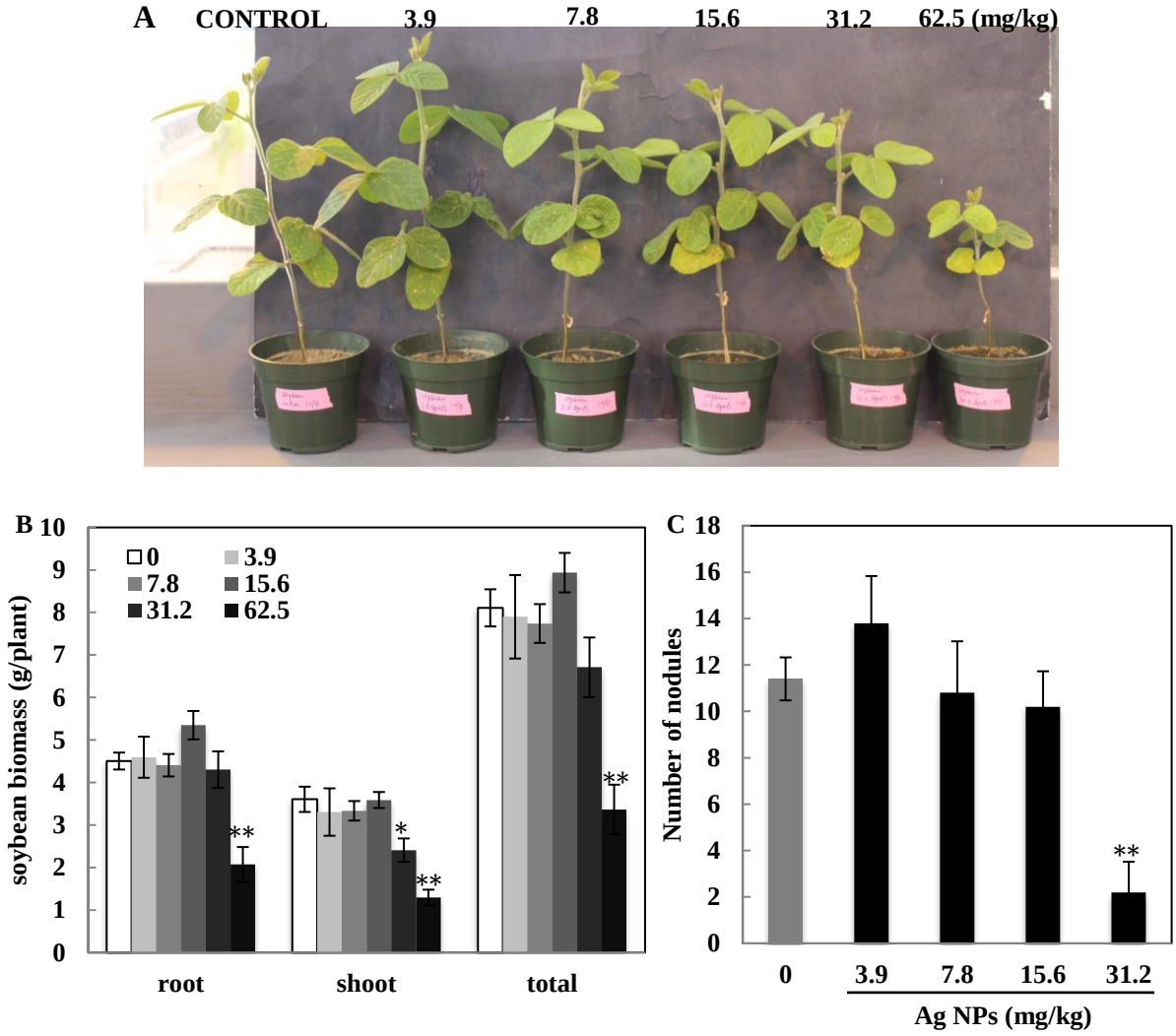

Figure 4. 3 Physiological effects of Ag NPs on soybean growth. (**A**) phenotypic images of soybean grown in different concentrations of Ag NPs amended soil; (**B**) fresh biomass of soybean; (C) total numbers of nodules.

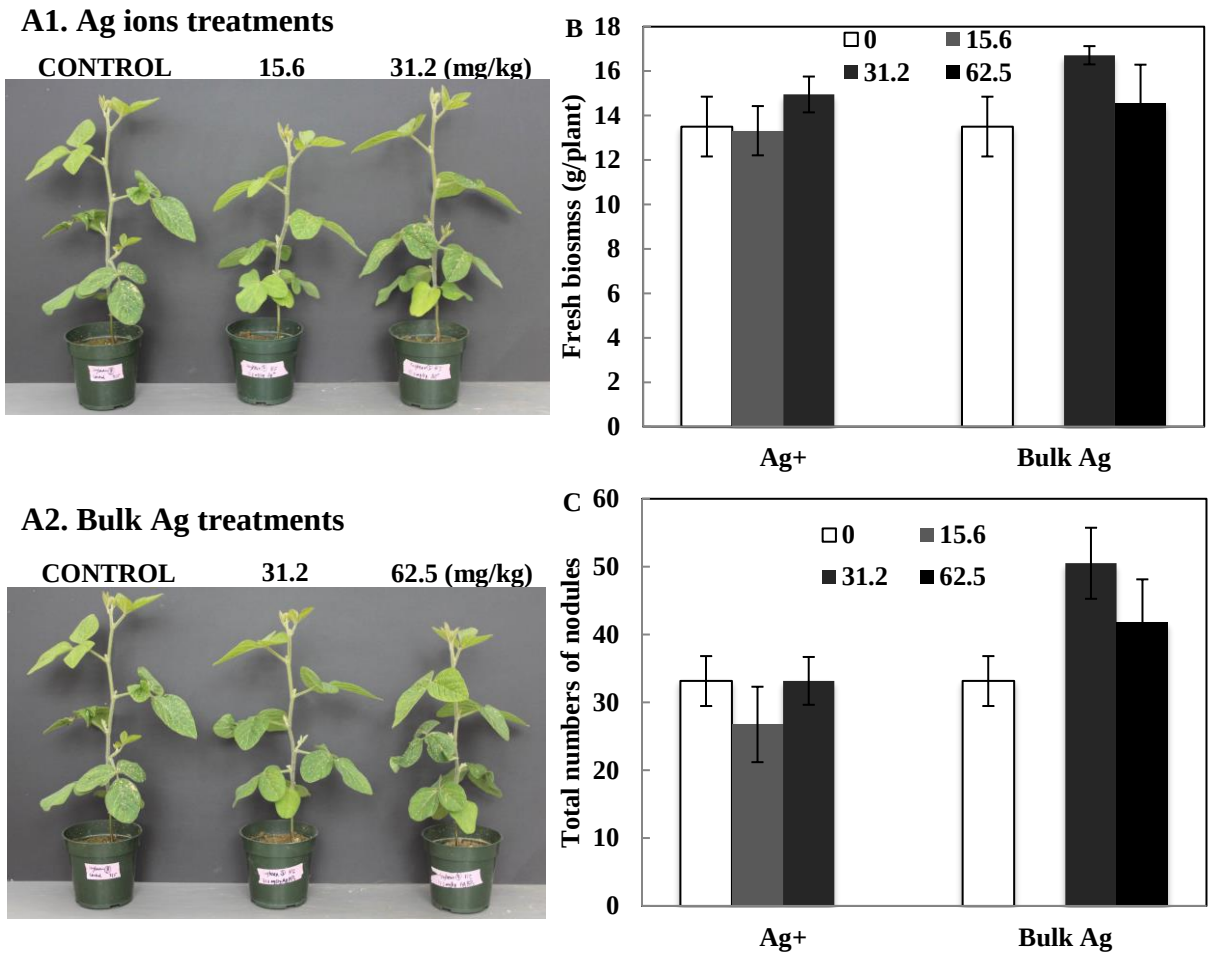

Figure 4. 4 Physiological effects of Ag^{+} ions and bulk Ag on soybean growth. (**A1-2**) phenotypic images of soybean grown in Ag ions and Bulk Ag amended soil, respectively; (**B**) fresh biomass of soybean; (**C**) total numbers of nodules.

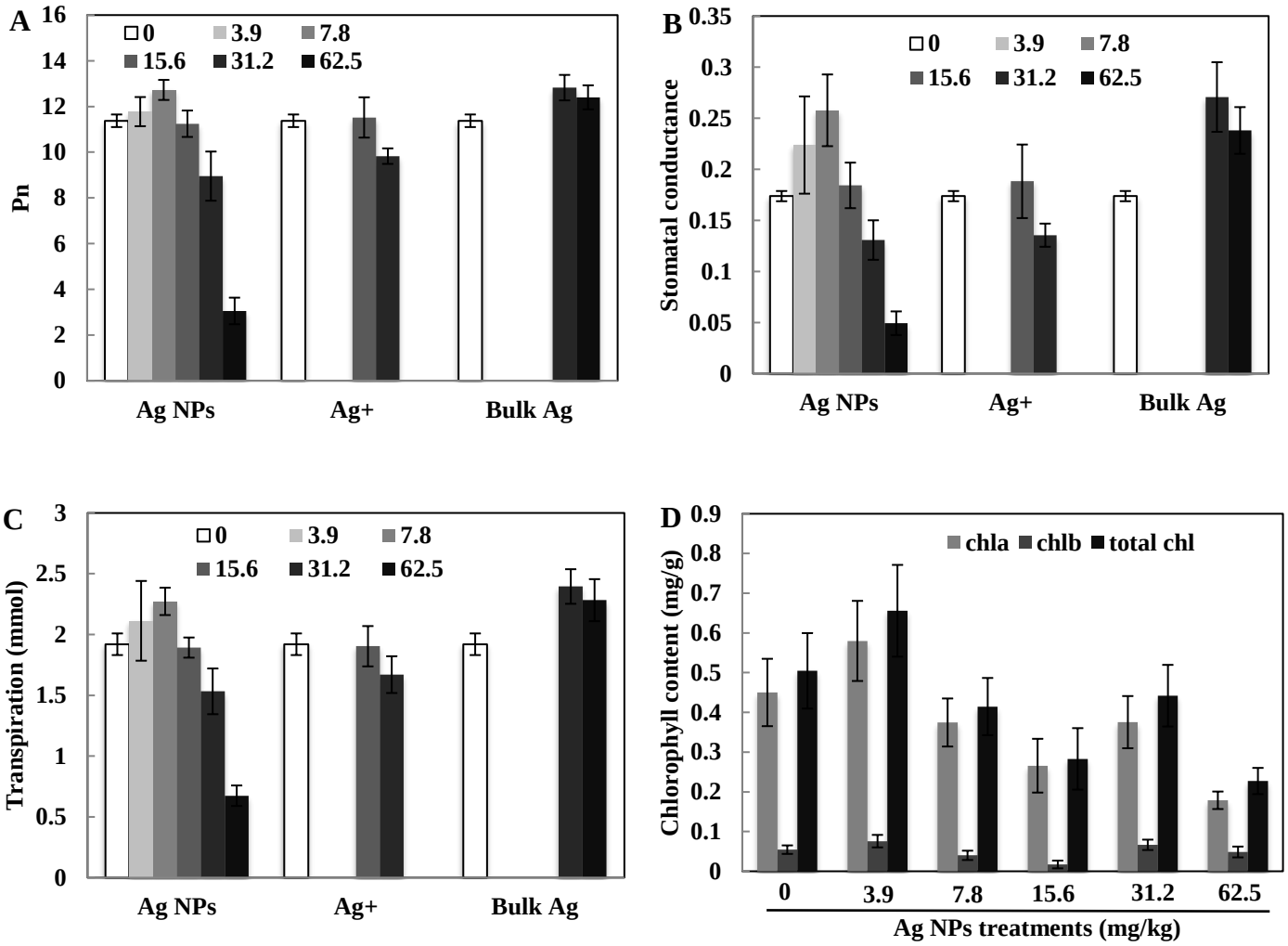

Figure 4. 5 Effects of Ag NPs on photosynthesis system in soybean. **Figure A-D** represent net photosynthesis rate, stomatal conductance, transpiration and chlorophyll content, respectively.

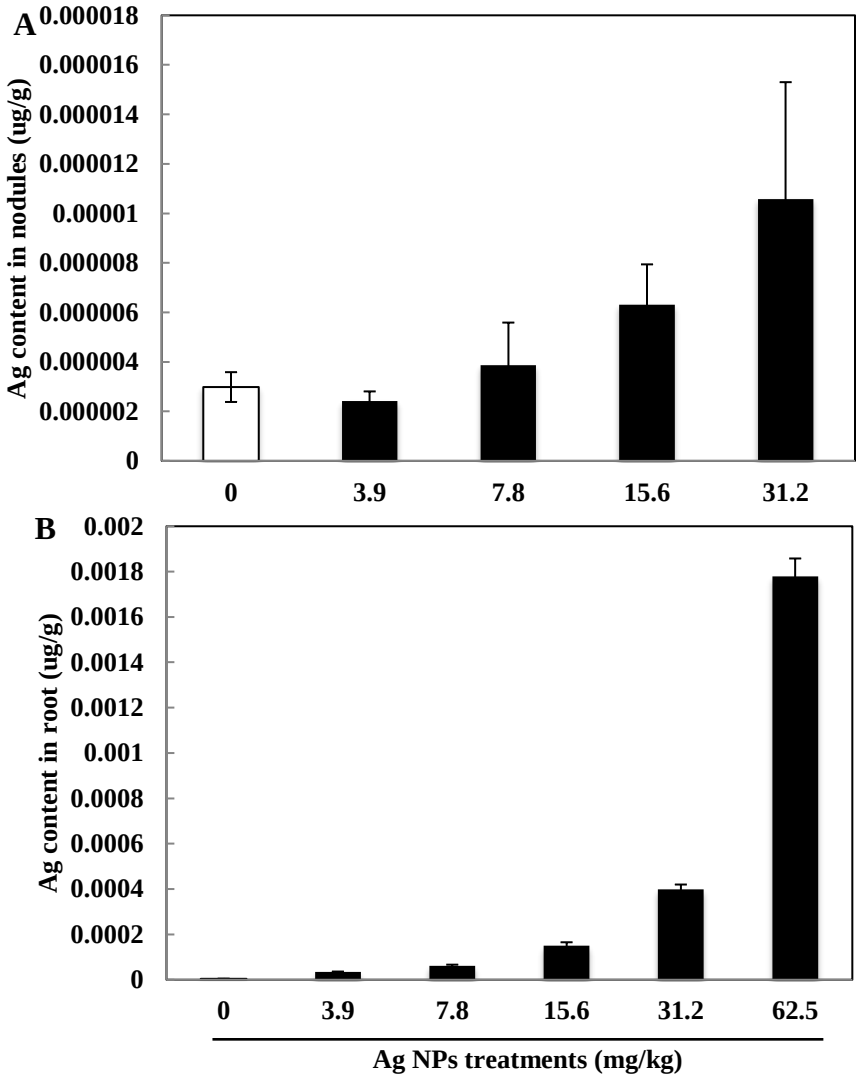

Figure 4. 6 Ag distribution in soybean grown in different concentrations of Ag NPs amended soil. **Figure A** and **B** represent Ag content in nodules and roots, respectively.

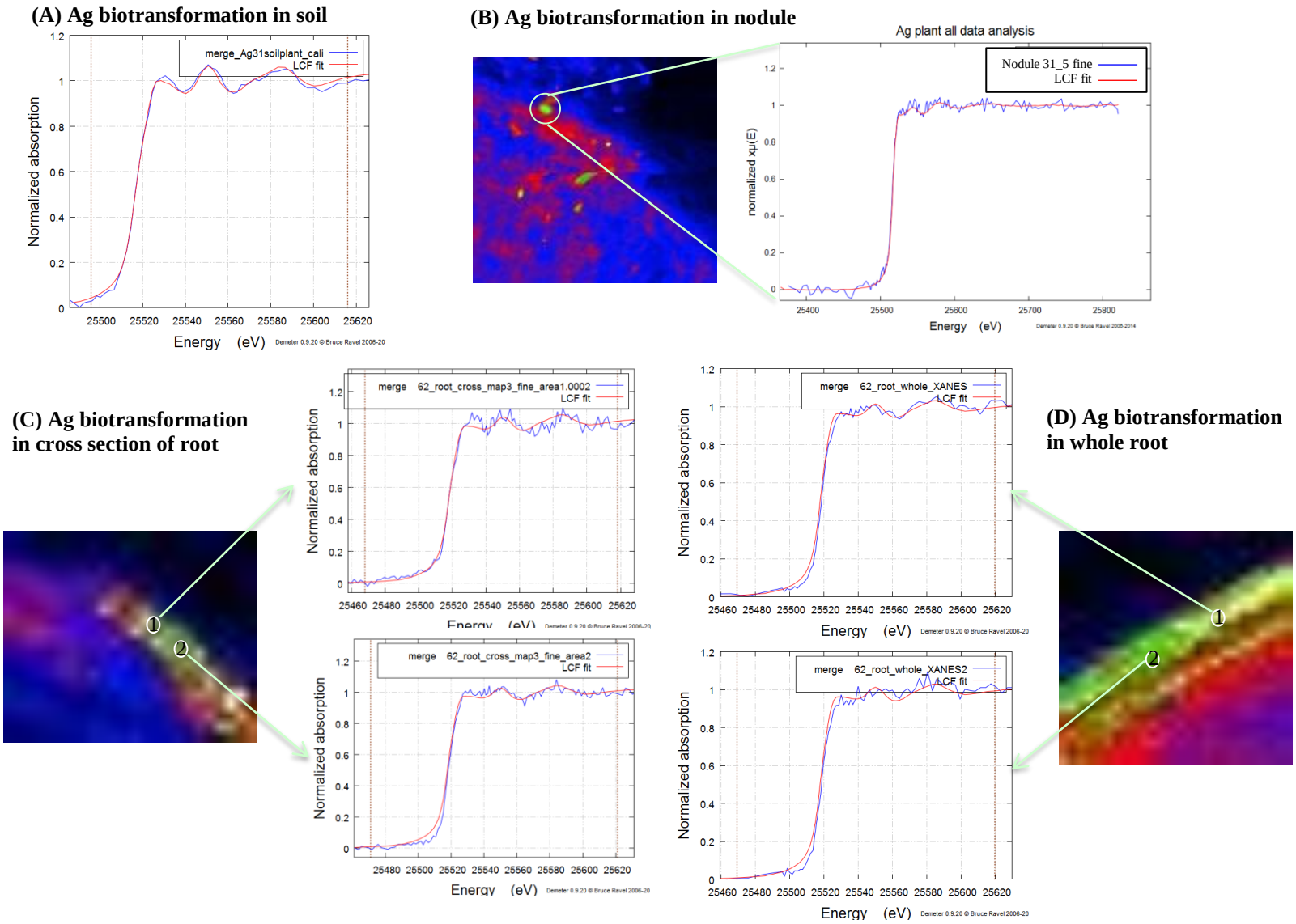

Figure 4. 7 Ag transformation in plant-soil system. (**A**) Ag biotransformation in soil; (**B**) Ag biotransformation in nodule; (**C**) Ag biotransformation in cross section of root; (**D**) Ag biotransformation in whole root.

Table 4. 1 Analysis of Ag speciation in soil and soybean tissues

XANES	Sample Name	Reference compounds					
		Ag_3PO_4	Ag-GSH	Ag NP	Ag_2S	Ag-citrate	Note
Bulk	31.25 mg/kg Ag NPs amended soil		0.048	0.778	0.183		
Micro	31.25 mg/kg Ag NPs treated nodule		0.16	0.836			
Micro	62.5 mg/kg Ag NPs treated root (cross section)		0.515	0.488			Position 1
Micro	62.5 mg/kg Ag NPs treated root (cross section)		0.6	0.396			Position 2
Micro	62.5 mg/kg Ag NPs treated whole root		0.589	0.396			Position 1
Micro	62.5 mg/kg Ag NPs treated whole root		0.586	0.397			Position 2

Table 4. 2 Macronutrient content in nodule, root and shoot of Ag NPs treated soybean

Element	Plant tissue	Ag NPs treatments (mg/kg)					
		Control	**3.9**	**7.8**	**15.6**	**31.2**	**62.5**
K	Nodule	182527±34124	236594±5961	256173±8779	261814±27623	317991±15448	
	Root	215179±45057	210201±45540	321566±52482	223535±43465	355221±11888	196968±16307
	Shoot	251043±6695	263149±8926	256101±3103	252251±7489	225472±1994	181573±11115
P	Nodule	42322±8889	57304±2608	63638±2162	62210±6112	76712±5137	
	Root	19117±2511	20198±769	22747±2140	24074±1515	28010±1222	20604±759
	Shoot	21530±1910	23393±720	26546±830	26359±1210	30637±802	16883±707
S	Nodule	20425±3642	27206±674	28084±928	26794±1734	29471±1025	
	Root	19962±3519	18622±2201	22243±2863	17372±2156	21635±858	18784±900
	Shoot	18056±625	18112±669	19573±429	17853±908	19559±1103	15329±937
Mg	Nodule	25144±4106	33708±578	32999±773	34032±1488	30200±1604	
	Root	43387±6912	39718±6827	34958±4369	34559±6728	63427±5444	32577±2555
	Shoot	42658±1514	41424±1389	41105±1360	39351±1235	42138±2582	42370±2063
Ca	Nodule	19801±4263	27488±1058	27309±599	28859±4533	31142±1983	
	Root	40586±1710	47128±2913	39442±3478	45337±2595	40387±881	40784±1843
	Shoot	122688±6076	123983±3178	130561±4160	122653±2972	114359±5389	75785±3414
Na	Nodule	2749±566	3664±290	4170±390	4783±497	4539±1043	
	Root	11027±782	9741±964	11358±979	11958±320	12368±825	26790±1800
	Shoot	1165±328	864±181	452±72	977±206	328±37	280±32

Table 4. 3 Micronutrient content in nodule, root and shoot of Ag NPs treated soybean

Element	Plant tissue	Ag NPs treatments (mg/kg)					
		Control	**3.9**	**7.8**	**15.6**	**31.2**	**62.5**
Fe	Nodule	3530±699	4843±252	4769±534	5165±400	6830±700	
	Root	16881±3639	16505±3705	6502±969	13962±1904	9805±1268	6431±684
	Shoot	631±14	627±112	449±30	472±28	451±28	505±18
Cu	Nodule	136±51	95±4	87±5	90±20	98±25	
	Root	567±41	453±26	383±32	492±46	346±9.5	492±19
	Shoot	67±4	59±2	51±5	47±5	45±12	27±2
B	Nodule	105±50	67±2	75±10	50±9	45±60	
	Root	79±2.4	114±18	81±6.7	106±14	85±3	118±14
	Shoot	194±8	190±8	212±19	173±8	227±25	220±10
Mn	Nodule	109±50	94±4	98±12	95±6	131±38	
	Root	422±62	507±109	595±121	493±109	629±19	764±55
	Shoot	693±35	679±51	762±63	681±60	618±32	827±32
Zn	Nodule	259±71	272±18	346±22	340±101	527±78	
	Root	276±9	277±10	261±16	307±39	255±6	294±8
	Shoot	365±24	320±120	349±18	324±16	361±21	278±10
Mo	Nodule	178±60	133±7	209±19	113±9	70±80	
	Root	0	0	0	1.6±8	0	0
	Shoot	0	0	0	0	24±12	11±6

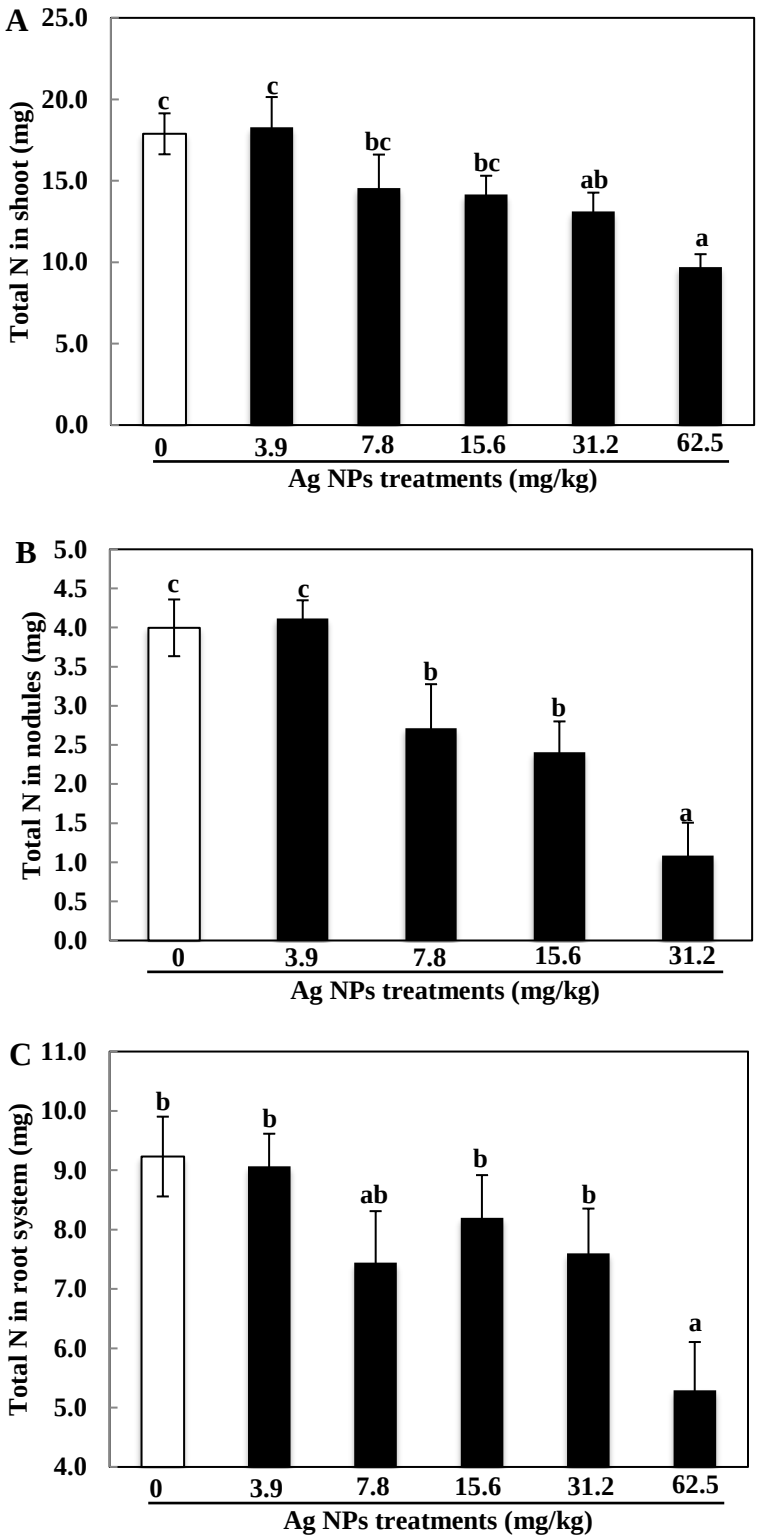

Figure 4. 8 Analysis of total N in soybean treated with different concentrations of Ag NPs. **Figure A-C** represent total N content in shoot, nodule, and root system of soybean, respectively.

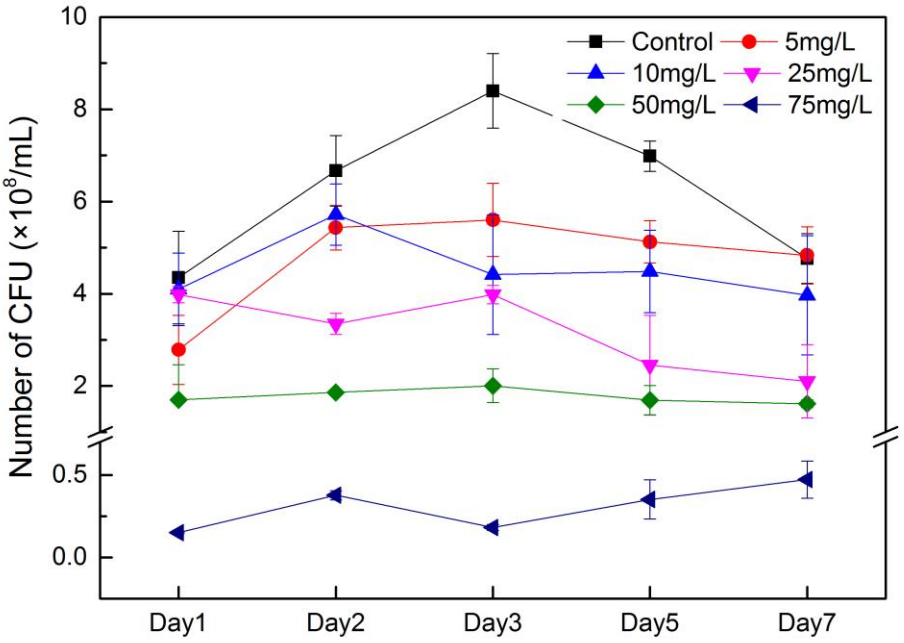

Figure 4. 9 Growth curve of Bradyrhizobium grown in HM medium treated with different concentrations of Ag NPs for 7 days.

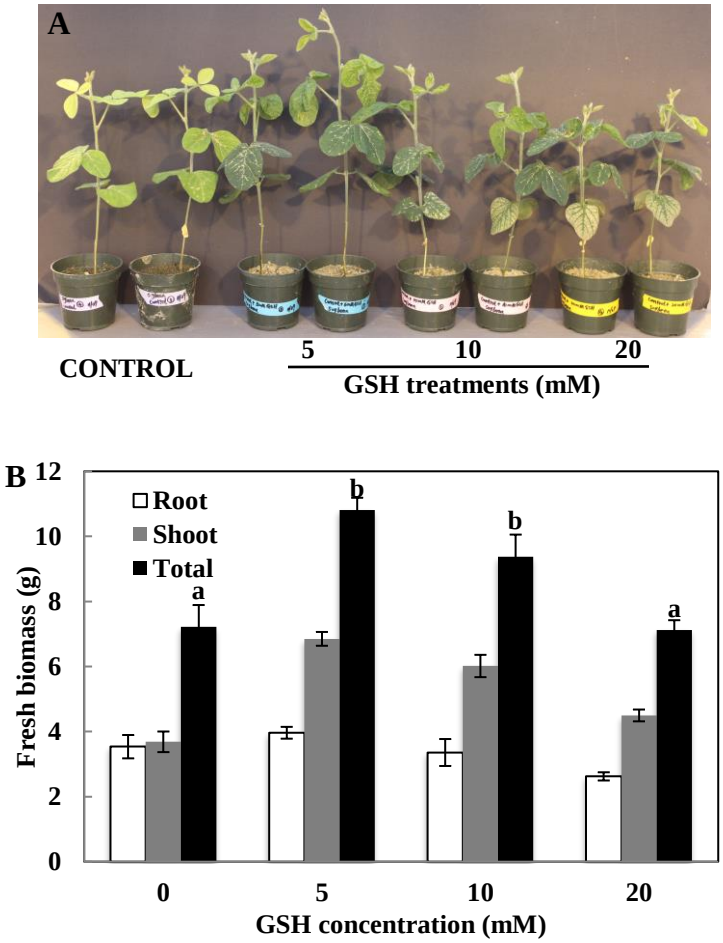

Figure 4. 10 Effects of different concentrations of GSH on soybean growth. (**A**) phenotypic image of soybean grown in the presences of different concentrations of GSH; (**B**) Fresh biomass of soybean.

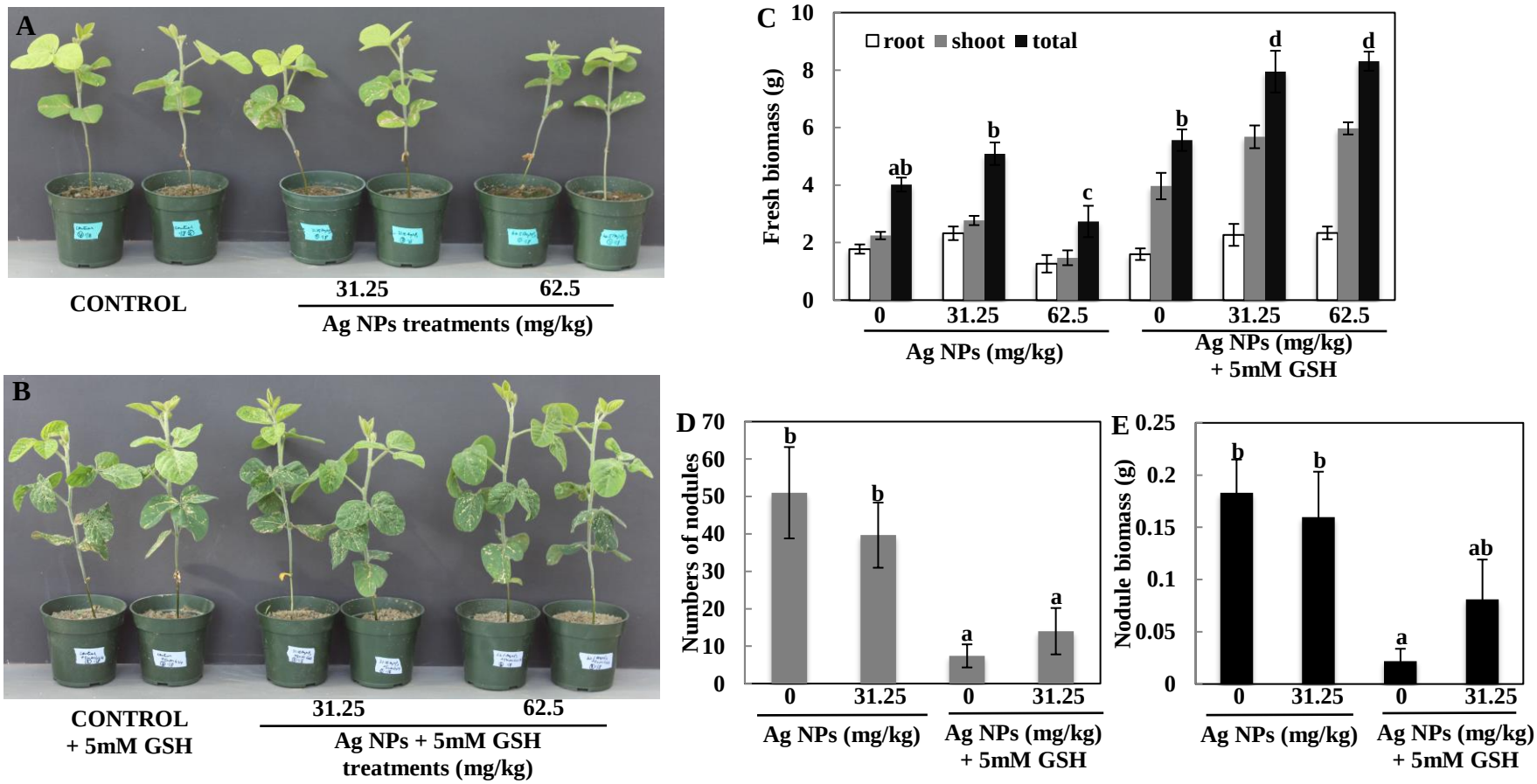

Figure 4. 11 Physiological effects of GSH on Ag NPs treated soybean growth. **Figure A** and **B** represent phenotypic images of soybean treated with Ag NPs alone and (Ag NPs + 5 mM GSH), respectively; **Figure C-E** represent fresh biomass, numbers of nodules, and nodule biomass, respectively.

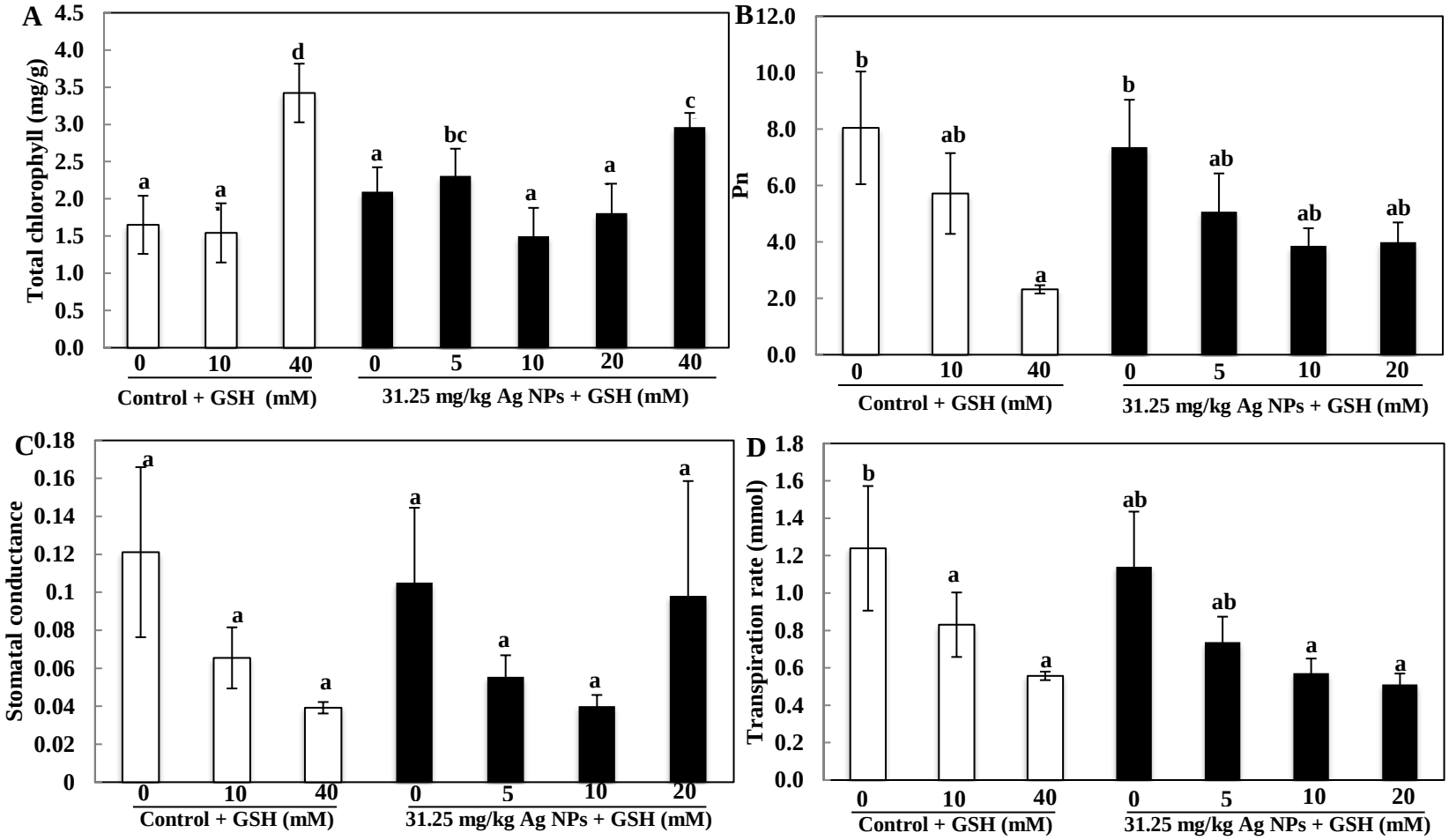

Figure 4. 12 The presences of GSH impact on photosynthesis system in Ag NPs treated soybean. **Figure A-D** represent total chlorophyll content, net photosynthetic rate, stomatal conductance and transpiration rate, respectively.

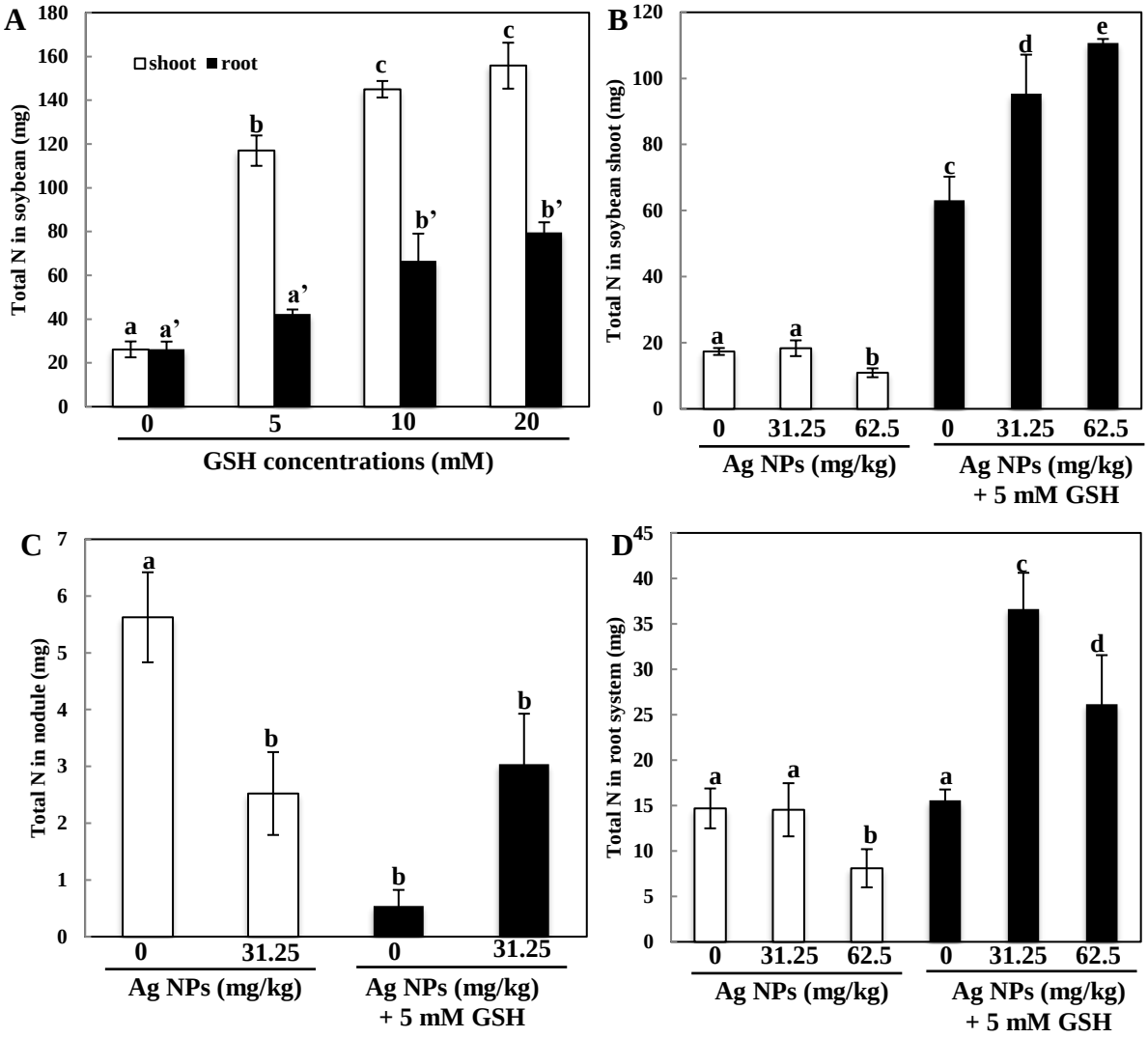

Figure 4. 13 Analysis of total N in Ag NPs treated soybean with or without the presences of GSH. (**A**) effects of different concentrations of GSH on total N; (**B**) total N in shoot; (**C**) total N in nodule; (**D**) total N in root system.

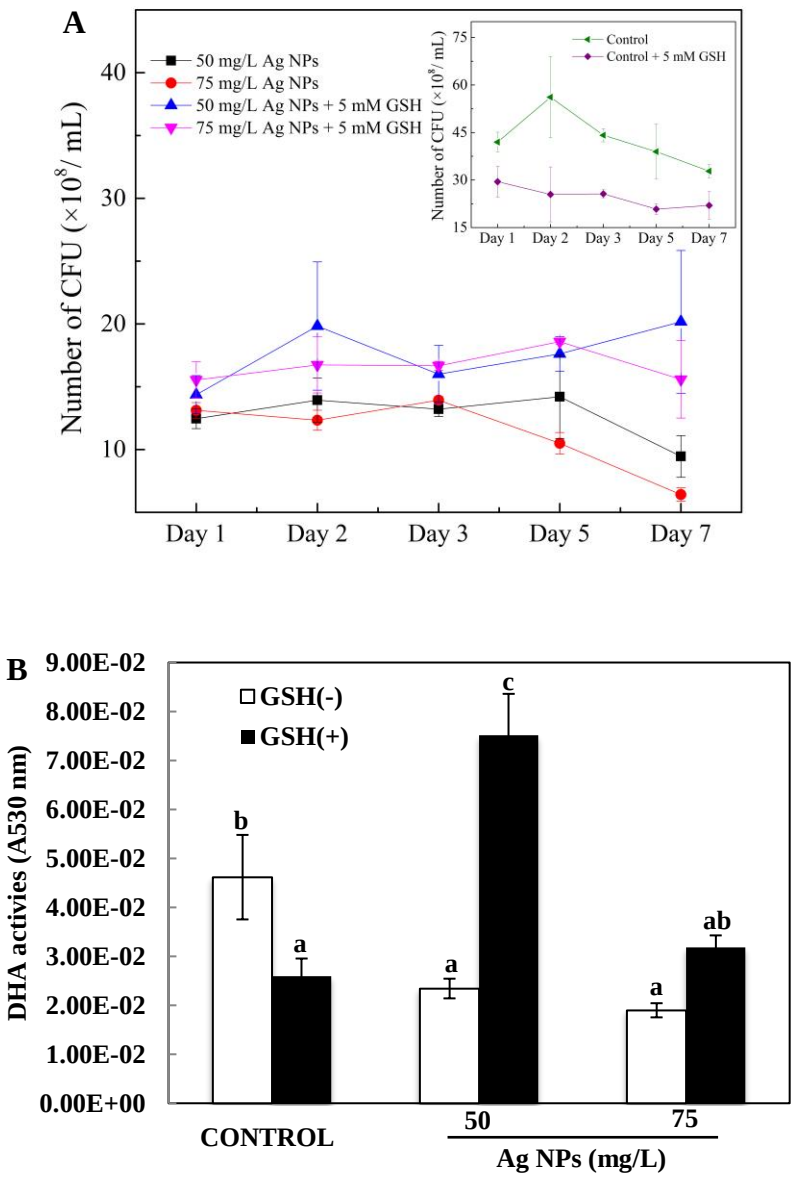

Figure 4. 14 Growth curve of Ag NPs treated Bradyrhizobium with or without the presences of GSH. (**A**) growth curve; (**B**) dehydrogenase activities in the Ag NPs treatment w/ or w/o the additions of GSH.

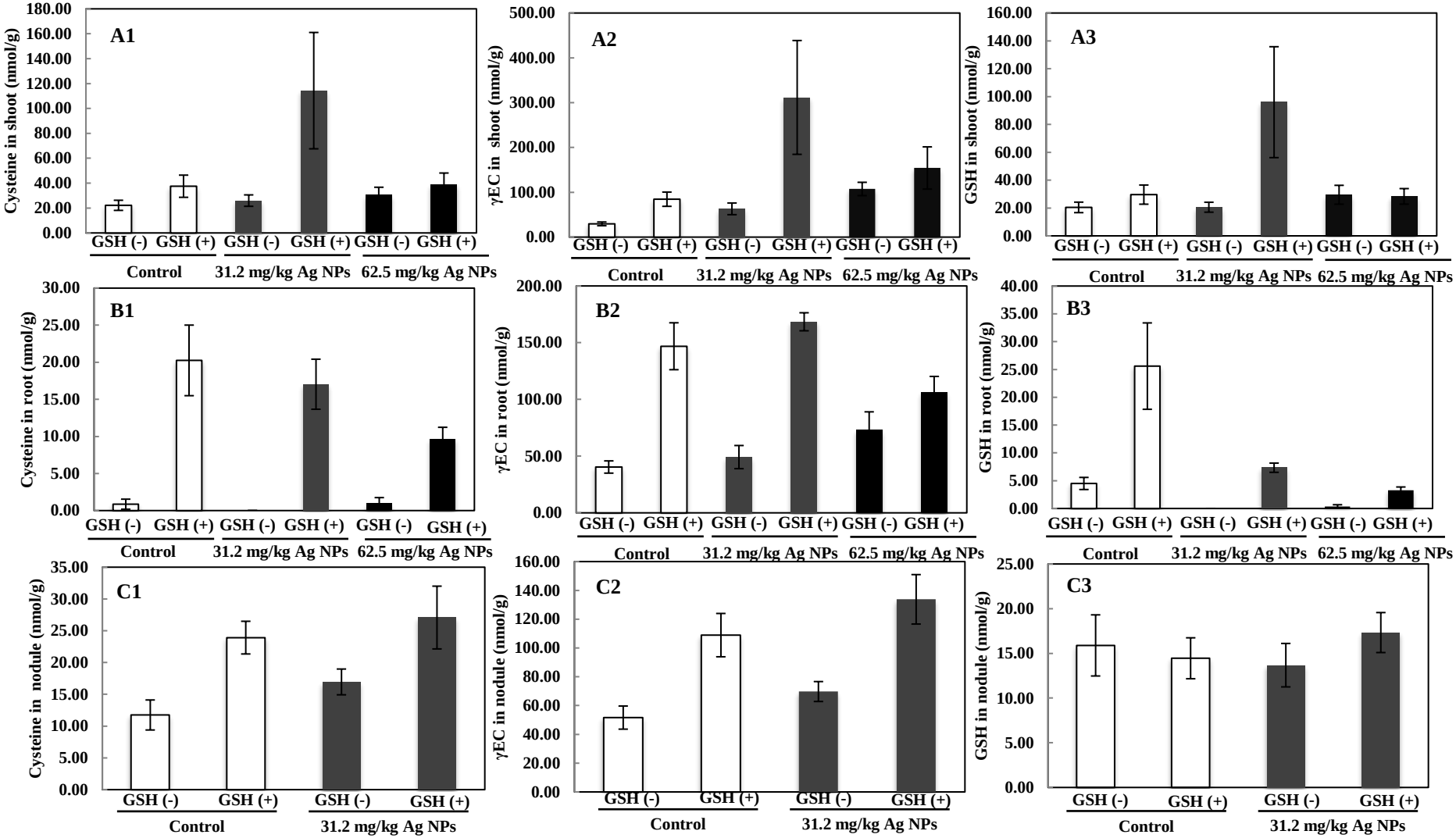

Figure 4. 15 The contents of thiol compounds in Ag NPs treated soybean tissues with or without 5 mM GSH addition. Figure **A1**, **B1**, and **C1** represent the cysteine contents in soybean shoots, roots, and nodules, respectively; Figure **A2**, **B2**, and **C2** represent the gamma-EC contents in soybean shoots, roots, and nodules, respectively; Figure **A3**, **B3**, and **C3** represent the GSH content in soybean shoots, roots, and nodules, respectively.

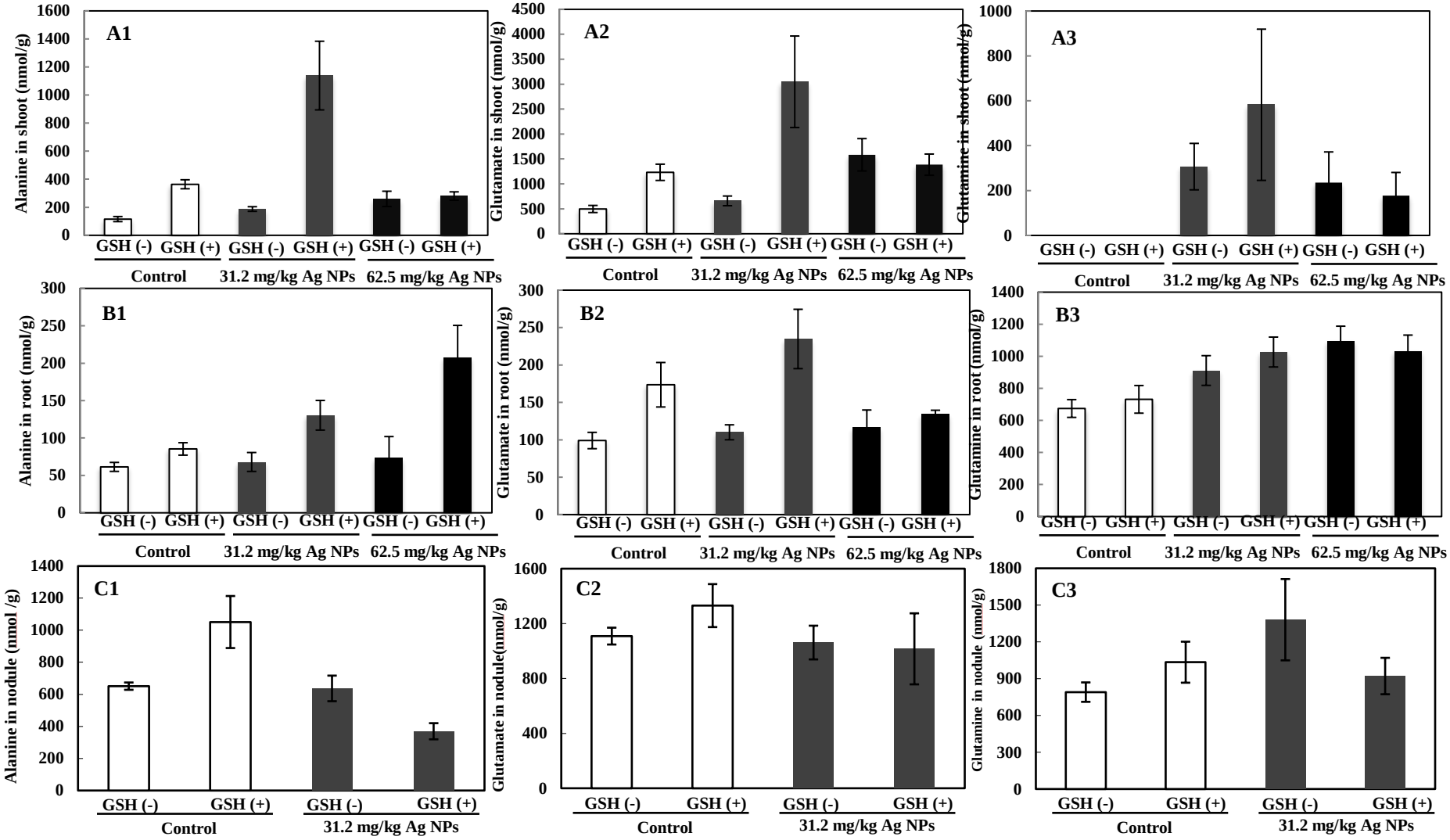

Figure 4. 16 The contents of amino acids in Ag NPs treated soybean tissues with or without 5 mM GSH addition. Figure **A1**, **B1**, and **C1** represent the alanine contents in soybean shoots, roots, and nodules, respectively; Figure **A2**, **B2**, and **C2** represent the glutamate contents in soybean shoots, roots, and nodules, respectively; Figure **A3**, **B3**, and **C3** represent the glutamine content in soybean shoots, roots, and nodules, respectively.

CHAPTER 5

CONCLUSIONS AND PERSPECTIVE

5.1 Conclusions

The potential risks from metal-based nanoparticles (NPs) in the environment have increased with the rapidly rising demand for and use of nano-enabled consumer products. Plant's central roles in ecosystem function and food chain integrity ensure intimate contact with water and soil systems, both of which are considered sinks for NPs accumulation. Thus, this study has mainly focused on three objectives: (1) analysis of *A. thaliana* for physiological and molecular response to CeO_2 and In_2O_3 NPs exposure; (2) investigation of the enhanced level of GSH on alleviation Ag NPs toxicity to *Crambe abyssinica*; (3) characterization of the role of glutathione in detoxification of silver nanoparticles and enhancement of nitrogen assimilation in soybean (*Glycine max*).

The effects of CeO_2 and In_2O_3 NPs exposure on *A. thaliana* were investigated. Exposure at 250 ppm CeO_2 NPs significantly increased plant biomass but at 500-2000 ppm, plant growth was decreased by up to 85% in a dose dependent fashion. At 1000 and 2000 ppm CeO_2 NPs, chlorophyll production was reduced by nearly 60% and 85%, respectively, and anthocyanin production was increased 3-5 fold. MDA production, a measure of lipid peroxidation, was unaffected by exposure to 250-500 ppm CeO_2 NPs, but at 1000 ppm, MDA formation was increased by 2.5-fold. Exposure to 25-2000 ppm In_2O_3 NPs had no effect on *Arabidopsis thaliana* biomass and only minor effects (15%) on root elongation. Total chlorophyll and MDA production were unaffected by In_2O_3 NPs

exposure. High level of MDA indicated that oxidative stress occurred in NPs treated *A. thaliana*. Thus, we further investigated the defense mechanisms of *A. thaliana* in response to CeO_2 and In_2O_3 NPs exposure. Excessive amounts of total ROS were measured upon exposure to both NPs, demonstrating clear oxidative stress in *Arabidopsis*. Analysis of ROS scavenger activity indicated that activities of SOD, CAT, APX, and POD were significantly elevated upon exposure to CeO_2 NPs, while these elevations were only evident for SOD and POD activities in the In_2O_3 NP treatments. In addition, the activities of GST and GR were increased approximately 15% and 51% by 1000 mg/L CeO_2 and In_2O_3 treatment, respectively. Molecular response to NPs exposures as measured by qPCR showed that both types of elements altered the expression of genes central to the stress response such as the sulfur assimilation and GSH biosynthesis pathway; a series of genes known to be significant in the detoxification of metal toxicity in plants. Interestingly, In_2O_3 NPs exposure resulted in a 3.8-4.6 fold increase in GS transcript production whereas CeO_2 NPs yielded only a 2-fold increase.

Ag NPs are widely used in consumer products and their release has raised serious concerns about risk of their exposure to the environment and to human health. We have previously engineered *Crambe abyssinica* plants expressing the *bacterial* γ-glutamylecysteine synthase (γ-ECS) for enhancing GSH levels. In this study, we investigated if enhanced levels of GSH and its derivatives can protect plants from Ag NPs and Ag^+ ions. Our results showed that transgenic lines, when exposed to Ag NPs and $AgNO_3$ (Ag^+ ions), were significantly more tolerant, attaining 28%-46% higher biomass and 34-49% more chlorophyll contents, as well as maintaining 35-46% higher transpiration rates as compared to wild type (WT) plants. Transgenic γ-ECS lines showed

2-6 folds of Ag accumulation in shoot and slightly lower or no difference in roots relative to WT plant. The levels of MDA in γ-ECS lines was also 27.3-32.5% lower than in WT Crambe. These results indicate that GSH and related peptides protect plants from Ag nanotoxicity.

The aim of the third objective was to investigate the physiological effects of Ag NPs on soybean and to characterize the role of GSH in detoxification of Ag NPs and enhancement of nitrogen assimilation. Our results indicated that the presences of Ag NPs could result in significantly low biomass and completely inhibit nodule formation at the exposure dose as low as 62.5 mg/kg. In addition, Ag NPs could alter the photosynthesis system in soybean in terms of net photosynthetic rate, stomatal conductance, transpiration rate, as well as total chlorophyll content. The total N in Ag NPs treated soybean nodule suggested that 31.2 mg/kg Ag NPs could severely reduce the total N level as compared to the control. Elemental analysis demonstrated that Ag uptake in soybean root and nodule was in dose-response manor, however, no Ag accumulation was found in soybean shoot. Synchrotron based micro X-ray fluorescent microscopy was applied to analyze Ag speciation in plant tissue. We found that more than 50% Ag in the root was converted to Ag-GSH, the rest part of Ag still remained in Ag NPs. The second part of this objective was to characterize the role of GSH. The additions of GSH could notably enhance the fresh biomass of Ag NPs treated soybean. However, the total number of nodules was significantly lowered as compared to the non-GSH control group. The total N level indicated that the presences of GSH could significantly increase the N level in both shoot and root of Ag NPs treated soybean. Thus, plant might utilize GSH as a nitrogen source and might need very less help from the symbiotic relationship with rhizobium to

assimilate the N. In order to further understand the underlying mechanism that GSH can counteract Ag nanotoxicity and enhance total N level in soybean, the related works, including amino acid analysis, GSH content, the important genes involved in GSH biodegradation pathway, are currently underway.

5.2 Perspective

Significant gaps remain in our understanding on the mechanisms of molecular responses of plants to oxidative stress induced by NPs. In order to reveal plant responses at protein and DNA levels to NPs exposure, global assays such as proteomics, RNA-seq or DNA microarrays and metabolomics must be developed and applied. At the current time, there are few reports of using DNA-microarray to reveal molecular responses of plants such as *A. thaliana* to NPs such as TiO_2, ZnO, Ag NPs, and CdS QD, respectively.[26, 86, 224] Furthermore, specific and highly responsive genes with regard to metal-based NPs exposure need to be explored through biotechnology. Clearly, when a plant initiates defense to resist the effects of metal-based NPs stresses, more than one detoxification pathway may be activated. The question is whether all of these pathways contribute equally to detoxify/resist metals or oxidative stresses. If not, we should to examine which detoxification pathway(s) is (are) dominant in the entire system and how detoxification pathways vary with plant species and/or particle type.

Assessing the overall environmental implications of metal-based NPs is another critical knowledge gap. To date, the literature is replete with studies investigating nanotoxicity to a range of biota (microorganism, plants and animals) under conditions and concentrations that are likely quite far from being environmentally realistic. Using

environmentally relevant concentrations are necessary to understand rate and disposition within terrestrial ecosystems, including potential for trophic transfer and food chain contamination. As such, applying mathematic models is a useful approach to predict the concentrations of different metal-based NPs in the environment.[225, 226] In addition, it is necessary to emphasize the importance of nanotoxicity studies on plants under the field or field-like conditions. The presence of metal-based NPs in the vegetative tissues of edible crops has been reported but quantification in actual edible tissue is far less common. In the meantime, the questions such as which types of NPs can effectively translocate to the fruits and whether molecular and biochemical mechanisms exist in plants to minimize or prevent NPs translocation should be addressed. Regarding to trophic transfer of metal-based NPs along food chain, increased system complexity (such as numbers of NPs, species of living organisms, trophic levels, temperature and exposure time) will be required to better represent the environmentally realistic conditions so as to accurately describe the fate and behavior of NPs in the food chain.

Due to increasing demands for nanotechnology and nanomaterials, the potential risks of metal-based NPs on crops and other terrestrial plants is an area of research where much more focus is warranted. Nanomaterials may not only affect crop yield and quality, but also the diversity of microorganisms in the rhizosphere and endosphere. Given the critical role of plants and plant-based symbiotic microbes in critical carbon and nitrogen cycles, caution is clearly warranted. Filling the critical knowledge gaps of nanomaterial fate and effects in terrestrial environments is the only way to enable accurate and meaningful exposure and risk assessment, both for human health and the environment.

APPENDIX I

List of primers used in qPCR

Gene name	Primer sequence (5'-3')
Actin-F	CGTGACCTTACTGATTAC
Actin-R	TTCTCCTTGATGTCTCTT
ATPS1 - F	ACAGTGGTTTCGATATTCCCG
ATPS1 - R	CACGTTTCTCTACTGGATGACC
APR1 - F	AAGGCTTGGATTACTGGTCAG
APR1 - R	ATTCCCTTCAACATTCGCAAC
SiR - F	CGACCCATTAAACCAAACTGC
SiR - R	CGTAGTCCAGACCAACCTTTT
CYSC1 - F	CTTATTGGGAAAACGCCTCTTG
CYSC1 - R	GCTACAAGTTGGCTGGAAATG
GSH1 - F	CCAAACGGATTTCTCAGCATG
GSH1 - R	GGCAAAGTACATAGGGACATCG
APSK – F	TGTTGTTGTTCGTGCTTGT
APSK – R	CGTGTGACCGTTAATGGATT
FRO-F	GCTTCCGCCGATTTCTTAAGGC
FRO-R	AACGGAGTTATCCCGCTTCCTC
IRT-F	ACTTCAAACTGCGCCGGAAGAATG
IRT-R	AGCTTTGTTGACGCACGGTTC
FER-F	CAACGTTGCTATGAAGGGACTAGC
FER-R	ACTCTTCCTCCTCTTTGGTTCTGG

qRT-PCR amplification program:

For genes encoding sulfur assimilation and GSH biosynthesis pathway: 95 °C for 15 min; 95 °C for 15 s, 55 °C for 30 s, 72 °C for 1 min, repeating 40 cycles; 95 °C for 15 s, 55 °C for 15 s, melting curve for 20 min; 95 °C for 15s.

For genes encoding iron transporters: 95 °C for 15 min; 95 °C for 15s, 59 °C for 30s, 72 °C for 10 s, repeating 40 cycles; 72 °C for 10 min; 95 °C for 15 s, 59 °C for 15 s, melting curve for 20 min; 95 °C for 15 s.

APPENDIX II

Hydroponic set up

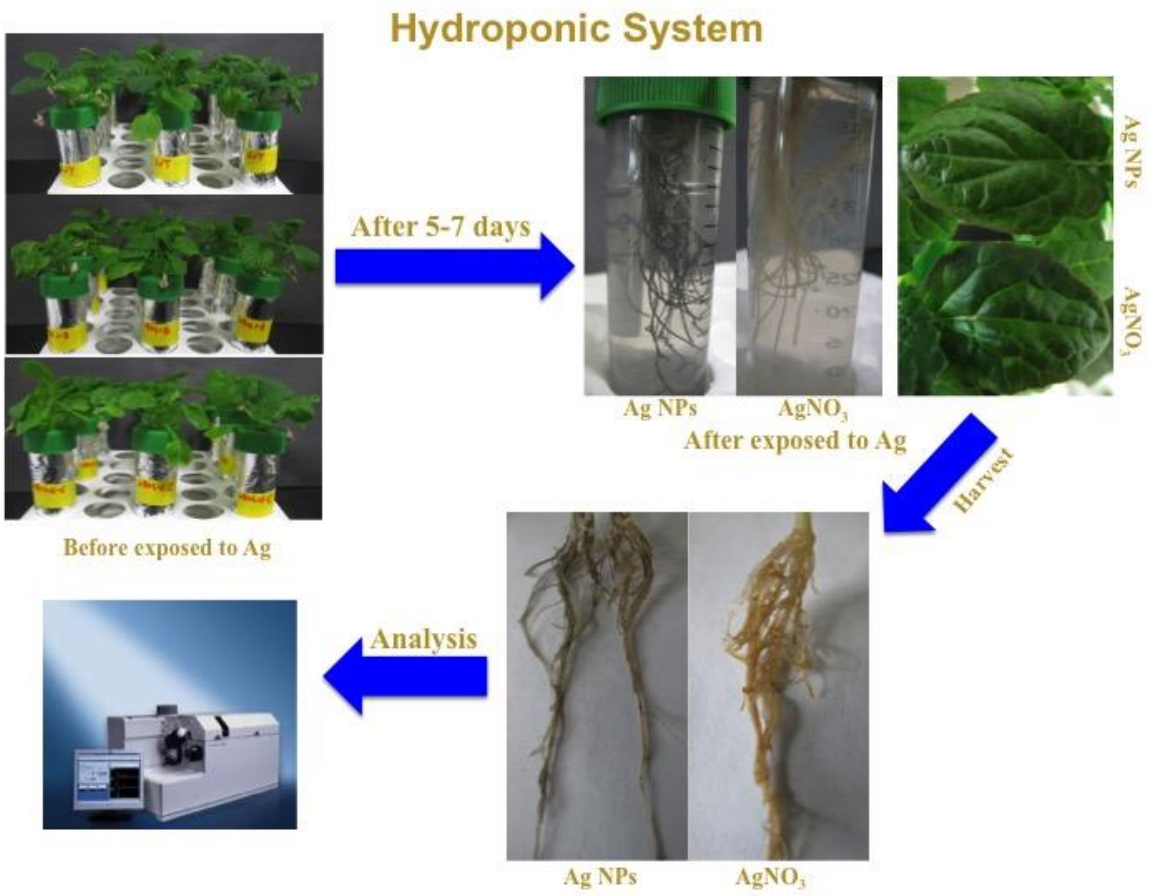

APPENDIX III

HM medium for Bradyrhizobium

HM Media (in 1 L):

Na_2HPO4: 0.125 g;

Na_2SO4: 0.25 g;

NH_4Cl: 0.32 g;

$MgSO_4 \bullet 7H_2O$: 0.18 g;

Yeast extract: 0.25 g;

D-Arabinose: 1 g;

Na-Gluconate: 1 g;

$FeCl_3$ (1 mM): 0.004 g;

$CaCl_2 \bullet 2H_2O$: 0.013 g;

HEPES: 1.3 g;

MES: 1.1 g

Adjust pH 6.6 with NaOH.

Take to 1 liter and autoclave for 30 minutes.

Media can be stored at room temperature.

BIBLIOGRAPHY

1. Nel, A.; Xia, T.; Mädler, L.; Li, N., Toxic potential of materials at the nanolevel. *Science* **2006,** *311* (5761), 622-627.
2. Keller, A. A.; Lazareva, A., Predicted Releases of Engineered Nanomaterials: From Global to Regional to Local. *Environmental Science & Technology Letters* **2013,** *1* (1), 65-70.
3. Weir, A.; Westerhoff, P.; Fabricius, L.; Hristovski, K.; von Goetz, N., Titanium dioxide nanoparticles in food and personal care products. *Environmental science & technology* **2012,** *46* (4), 2242-2250.
4. Osmond, M. J.; Mccall, M. J., Zinc oxide nanoparticles in modern sunscreens: an analysis of potential exposure and hazard. *Nanotoxicology* **2010,** *4* (1), 15-41.
5. Corma, A.; Atienzar, P.; Garcia, H.; Chane-Ching, J.-Y., Hierarchically mesostructured doped CeO2 with potential for solar-cell use. *Nature materials* **2004,** *3* (6), 394-397.
6. Salata, O. V., Applications of nanoparticles in biology and medicine. *Journal of nanobiotechnology* **2004,** *2* (1), 3.
7. Giljohann, D. A.; Seferos, D. S.; Daniel, W. L.; Massich, M. D.; Patel, P. C.; Mirkin, C. A., Gold Nanoparticles for Biology and Medicine. *Angewandte Chemie International Edition* **2010,** *49* (19), 3280-3294.
8. Elechiguerra, J. L.; Burt, J. L.; Morones, J. R.; Camacho-Bragado, A.; Gao, X.; Lara, H. H.; Yacaman, M. J., Interaction of silver nanoparticles with HIV-1. *J nanobiotechnol* **2005,** *3* (6), 1-10.
9. Rasmussen, J. W.; Martinez, E.; Louka, P.; Wingett, D. G., Zinc oxide nanoparticles for selective destruction of tumor cells and potential for drug delivery applications. *Expert opinion on drug delivery* **2010,** *7* (9), 1063-1077.
10. Somasundaran, P.; Fang, X.; Ponnurangam, S.; Li, B., Nanoparticles: characteristics, mechanisms and modulation of biotoxicity. *KONA powder and particle journal* **2010,** *28* (0), 38-49.
11. Deng, Y.-q.; White, J. C.; Xing, B.-s., Interactions between engineered nanomaterials and agricultural crops: implications for food safety. *Journal of Zhejiang University SCIENCE A* **2014,** *15* (8), 552-572.
12. Zhao, J.; Wang, Z.; Dai, Y.; Xing, B., Mitigation of CuO nanoparticle-induced bacterial membrane damage by dissolved organic matter. *Water research* **2013,** *47* (12), 4169-4178.
13. Ramsden, C.; Henry, T.; Handy, R., Sub-lethal effects of titanium dioxide nanoparticles on the physiology and reproduction of zebrafish. *Aquatic Toxicology* **2013,** *126*, 404-413.
14. Yang, S. P.; Bar-Ilan, O.; Peterson, R. E.; Heideman, W.; Hamers, R. J.; Pedersen, J. A., Influence of humic acid on titanium dioxide nanoparticle toxicity to developing zebrafish. *Environmental science & technology* **2013,** *47* (9), 4718-4725.

15. Wan, R.; Mo, Y.; Feng, L.; Chien, S.; Tollerud, D. J.; Zhang, Q., DNA Damage Caused by Metal Nanoparticles: Involvement of Oxidative Stress and Activation of ATM†. *Chemical research in toxicology* **2012,** *25* (7), 1402-1411.
16. Wang, Z.; Li, N.; Zhao, J.; White, J. C.; Qu, P.; Xing, B., CuO nanoparticle interaction with human epithelial cells: cellular uptake, location, export, and genotoxicity. *Chemical research in toxicology* **2012,** *25* (7), 1512-1521.
17. Asli, S.; Neumann, P. M., Colloidal suspensions of clay or titanium dioxide nanoparticles can inhibit leaf growth and transpiration via physical effects on root water transport. *Plant, cell & environment* **2009,** *32* (5), 577-584.
18. Dimkpa, C.; McLean, J.; Latta, D.; Manangón, E.; Britt, D.; Johnson, W.; Boyanov, M.; Anderson, A., CuO and ZnO nanoparticles: phytotoxicity, metal speciation, and induction of oxidative stress in sand-grown wheat. *J Nanopart Res* **2012,** *14* (9), 1-15.
19. Pokhrel, L. R.; Dubey, B., Evaluation of developmental responses of two crop plants exposed to silver and zinc oxide nanoparticles. *Science of The Total Environment* **2013,** *452–453* (0), 321-332.
20. Ma, C.; Chhikara, S.; Xing, B.; Musante, C.; White, J. C.; Dhankher, O. P., Physiological and molecular response of Arabidopsis thaliana (L.) to nanoparticle cerium and indium oxide exposure. *ACS Sustainable Chemistry & Engineering* **2013,** *1* (7), 768-778.
21. Panda, K. K.; Achary, V. M. M.; Krishnaveni, R.; Padhi, B. K.; Sarangi, S. N.; Sahu, S. N.; Panda, B. B., In vitro biosynthesis and genotoxicity bioassay of silver nanoparticles using plants. *Toxicology in Vitro* **2011,** *25* (5), 1097-1105.
22. Mirzajani, F.; Askari, H.; Hamzelou, S.; Farzaneh, M.; Ghassempour, A., Effect of silver nanoparticles on Oryza sativa L. and its rhizosphere bacteria. *Ecotoxicology and environmental safety* **2013,** *88*, 48-54.
23. Zhao, L.; Peng, B.; Hernandez-Viezcas, J. A.; Rico, C.; Sun, Y.; Peralta-Videa, J. R.; Tang, X.; Niu, G.; Jin, L.; Varela-Ramirez, A., Stress response and tolerance of Zea mays to CeO2 nanoparticles: Cross talk among H2O2, heat shock protein, and lipid peroxidation. *ACS nano* **2012,** *6* (11), 9615-9622.
24. Gill, S. S.; Tuteja, N., Reactive oxygen species and antioxidant machinery in abiotic stress tolerance in crop plants. *Plant Physiology and Biochemistry* **2010,** *48* (12), 909-930.
25. Kumari, M.; Khan, S. S.; Pakrashi, S.; Mukherjee, A.; Chandrasekaran, N., Cytogenetic and genotoxic effects of zinc oxide nanoparticles on root cells of Allium cepa. *Journal of Hazardous Materials* **2011,** *190* (1–3), 613-621.
26. Landa, P.; Vankova, R.; Andrlova, J.; Hodek, J.; Marsik, P.; Storchova, H.; White, J. C.; Vanek, T., Nanoparticle-specific changes in Arabidopsis thaliana gene expression after exposure to ZnO, TiO2, and fullerene soot. *Journal of Hazardous Materials* **2012,** *241–242* (0), 55-62.
27. Zhang, Z.; He, X.; Zhang, H.; Ma, Y.; Zhang, P.; Ding, Y.; Zhao, Y., Uptake and distribution of ceria nanoparticles in cucumber plants. *Metallomics* **2011,** *3* (8), 816-822.
28. Yin, L.; Cheng, Y.; Espinasse, B.; Colman, B. P.; Auffan, M.; Wiesner, M.; Rose, J.; Liu, J.; Bernhardt, E. S., More than the ions: the effects of silver nanoparticles on Lolium multiflorum. *Environmental science & technology* **2011,** *45* (6), 2360-2367.

29. Lin, D.; Xing, B., Root Uptake and Phytotoxicity of ZnO Nanoparticles. *Environmental Science & Technology* **2008,** *42* (15), 5580-5585.
30. Hernandez-Viezcas, J.; Castillo-Michel, H.; Servin, A.; Peralta-Videa, J.; Gardea-Torresdey, J., Spectroscopic verification of zinc absorption and distribution in the desert plant< i> Prosopis juliflora-velutina</i>(velvet mesquite) treated with ZnO nanoparticles. *Chemical Engineering Journal* **2011,** *170* (2), 346-352.
31. Du, W.; Sun, Y.; Ji, R.; Zhu, J.; Wu, J.; Guo, H., TiO2 and ZnO nanoparticles negatively affect wheat growth and soil enzyme activities in agricultural soil. *Journal of Environmental Monitoring* **2011,** *13* (4), 822-828.
32. Priester, J. H.; Ge, Y.; Mielke, R. E.; Horst, A. M.; Moritz, S. C.; Espinosa, K.; Gelb, J.; Walker, S. L.; Nisbet, R. M.; An, Y.-J.; Schimel, J. P.; Palmer, R. G.; Hernandez-Viezcas, J. A.; Zhao, L.; Gardea-Torresdey, J. L.; Holden, P. A., Soybean susceptibility to manufactured nanomaterials with evidence for food quality and soil fertility interruption. *Proceedings of the National Academy of Sciences* **2012,** *109* (37), E2451–E2456.
33. Zhao, L.; Peralta-Videa, J. R.; Ren, M.; Varela-Ramirez, A.; Li, C.; Hernandez-Viezcas, J. A.; Aguilera, R. J.; Gardea-Torresdey, J. L., Transport of Zn in a sandy loam soil treated with ZnO NPs and uptake by corn plants: Electron microprobe and confocal microscopy studies. *Chemical Engineering Journal* **2012,** *184* (0), 1-8.
34. Mukherjee, A.; Peralta-Videa, J. R.; Bandyopadhyay, S.; Rico, C. M.; Zhao, L.; Gardea-Torresdey, J. L., Physiological effects of nanoparticulate ZnO in green peas (Pisum sativum L.) cultivated in soil. *Metallomics* **2014,** *6* (1), 132-138.
35. De La Torre-Roche, R.; Hawthorne, J.; Musante, C.; Xing, B.; Newman, L. A.; Ma, X.; White, J. C., Impact of Ag Nanoparticle Exposure on p,p′ -DDE Bioaccumulation by Cucurbita pepo (Zucchini) and Glycine max (Soybean). *Environmental Science & Technology* **2012,** *47* (2), 718-725.
36. Zhao, L.; Peralta-Videa, J. R.; Varela-Ramirez, A.; Castillo-Michel, H.; Li, C.; Zhang, J.; Aguilera, R. J.; Keller, A. A.; Gardea-Torresdey, J. L., Effect of surface coating and organic matter on the uptake of CeO2 NPs by corn plants grown in soil: Insight into the uptake mechanism. *Journal of Hazardous Materials* **2012,** *225–226* (0), 131-138.
37. Ma, Y.; He, X.; Zhang, P.; Zhang, Z.; Guo, Z.; Tai, R.; Xu, Z.; Zhang, L.; Ding, Y.; Zhao, Y.; Chai, Z., Phytotoxicity and biotransformation of La2O3 nanoparticles in a terrestrial plant cucumber (Cucumis sativus). *Nanotoxicology* **2011,** *5* (4), 743-753.
38. Sun, D.; Hussain, H. I.; Yi, Z.; Siegele, R.; Cresswell, T.; Kong, L.; Cahill, D. M., Uptake and cellular distribution, in four plant species, of fluorescently labeled mesoporous silica nanoparticles. *Plant cell reports* **2014**, 1-14.
39. Ghafariyan, M. H.; Malakouti, M. J.; Dadpour, M. R.; Stroeve, P.; Mahmoudi, M., Effects of magnetite nanoparticles on soybean chlorophyll. *Environmental science & technology* **2013,** *47* (18), 10645-10652.
40. Zhai, G.; Walters, K. S.; Peate, D. W.; Alvarez, P. J.; Schnoor, J. L., Transport of gold nanoparticles through plasmodesmata and precipitation of gold ions in woody poplar. *Environmental Science & Technology Letters* **2014,** *1* (2), 146-151.

41. Kim, J. S.; Kuk, E.; Yu, K. N.; Kim, J.-H.; Park, S. J.; Lee, H. J.; Kim, S. H.; Park, Y. K.; Park, Y. H.; Hwang, C.-Y.; Kim, Y.-K.; Lee, Y.-S.; Jeong, D. H.; Cho, M.-H., Antimicrobial effects of silver nanoparticles. *Nanomedicine: Nanotechnology, Biology and Medicine* **2007,** *3* (1), 95-101.
42. Pal, S.; Tak, Y. K.; Song, J. M., Does the Antibacterial Activity of Silver Nanoparticles Depend on the Shape of the Nanoparticle? A Study of the Gram-Negative Bacterium Escherichia coli. *Applied and Environmental Microbiology* **2007,** *73* (6), 1712-1720.
43. Deepa, M.; Sudhakar, P.; Nagamadhuri, K. V.; Reddy, K. B.; Krishna, T. G.; Prasad, T. N. V. K. V., First evidence on phloem transport of nanoscale calcium oxide in groundnut using solution culture technique. *Applied Nanoscience* **2014**, 1-7.
44. Hong, J.; Peralta-Videa, J. R.; Rico, C. M.; Sahi, S. V.; Viveros, M. N.; Bartonjo, J.; Zhao, L.; Gardea-Torresdey, J. L., Evidence of Translocation and Physiological Impacts of Foliar Applied CeO2 Nanoparticles on Cucumber (Cucumis sativus) Plants. *Environmental science & technology* **2014**.
45. Shi, J.; Peng, C.; Yang, Y.; Yang, J.; Zhang, H.; Yuan, X.; Chen, Y.; Hu, T., Phytotoxicity and accumulation of copper oxide nanoparticles to the Cu-tolerant plant Elsholtzia splendens. *Nanotoxicology* **2014,** *8* (2), 179-188.
46. Larue, C.; Laurette, J.; Herlin-Boime, N.; Khodja, H.; Fayard, B.; Flank, A.-M.; Brisset, F.; Carriere, M., Accumulation, translocation and impact of TiO2 nanoparticles in wheat (Triticum aestivum spp.): Influence of diameter and crystal phase. *Science of The Total Environment* **2012,** *431* (0), 197-208.
47. Wang, Z.; Xie, X.; Zhao, J.; Liu, X.; Feng, W.; White, J. C.; Xing, B., Xylem- and Phloem-Based Transport of CuO Nanoparticles in Maize (Zea mays L.). *Environmental Science & Technology* **2012,** *46* (8), 4434-4441.
48. Faisal, M.; Saquib, Q.; Alatar, A. A.; Al-Khedhairy, A. A.; Hegazy, A. K.; Musarrat, J., Phytotoxic hazards of NiO-nanoparticles in tomato: A study on mechanism of cell death. *Journal of Hazardous Materials* **2013,** *250–251* (0), 318-332.
49. Ma, Y.; Kuang, L.; He, X.; Bai, W.; Ding, Y.; Zhang, Z.; Zhao, Y.; Chai, Z., Effects of rare earth oxide nanoparticles on root elongation of plants. *Chemosphere* **2010,** *78* (3), 273-279.
50. Zhang, P.; Ma, Y.; Zhang, Z.; He, X.; Zhang, J.; Guo, Z.; Tai, R.; Zhao, Y.; Chai, Z., Biotransformation of Ceria Nanoparticles in Cucumber Plants. *ACS Nano* **2012,** *6* (11), 9943-9950.
51. Rico, C. M.; Morales, M. I.; McCreary, R.; Castillo-Michel, H.; Barrios, A. C.; Hong, J.; Tafoya, A.; Lee, W.-Y.; Varela-Ramirez, A.; Peralta-Videa, J. R.; Gardea-Torresdey, J. L., Cerium Oxide Nanoparticles Modify the Antioxidative Stress Enzyme Activities and Macromolecule Composition in Rice Seedlings. *Environmental Science & Technology* **2013,** *47* (24), 14110-14118.
52. Larue, C.; Veronesi, G.; Flank, A.-M.; Surble, S.; Herlin-Boime, N.; Carrière, M., Comparative Uptake and Impact of TiO2 Nanoparticles in Wheat and Rapeseed. *Journal of Toxicology and Environmental Health, Part A* **2012,** *75* (13-15), 722-734.

53. Servin, A. D.; Castillo-Michel, H.; Hernandez-Viezcas, J. A.; Diaz, B. C.; Peralta-Videa, J. R.; Gardea-Torresdey, J. L., Synchrotron Micro-XRF and Micro-XANES Confirmation of the Uptake and Translocation of TiO2 Nanoparticles in Cucumber (Cucumis sativus) Plants. *Environmental Science & Technology* **2012,** *46* (14), 7637-7643.
54. Judy, J. D.; Unrine, J. M.; Rao, W.; Wirick, S.; Bertsch, P. M., Bioavailability of Gold Nanomaterials to Plants: Importance of Particle Size and Surface Coating. *Environmental Science & Technology* **2012,** *46* (15), 8467-8474.
55. Hernandez-Viezcas, J. A.; Castillo-Michel, H.; Andrews, J. C.; Cotte, M.; Rico, C.; Peralta-Videa, J. R.; Ge, Y.; Priester, J. H.; Holden, P. A.; Gardea-Torresdey, J. L., In Situ Synchrotron X-ray Fluorescence Mapping and Speciation of CeO2 and ZnO Nanoparticles in Soil Cultivated Soybean (Glycine max). *ACS Nano* **2013,** *7* (2), 1415-1423.
56. Servin, A. D.; Morales, M. I.; Castillo-Michel, H.; Hernandez-Viezcas, J. A.; Munoz, B.; Zhao, L.; Nunez, J. E.; Peralta-Videa, J. R.; Gardea-Torresdey, J. L., Synchrotron Verification of TiO2 Accumulation in Cucumber Fruit: A Possible Pathway of TiO2 Nanoparticle Transfer from Soil into the Food Chain. *Environmental Science & Technology* **2013,** *47* (20), 11592-11598.
57. Adani, F.; Papa, G.; Schievano, A.; Cardinale, G.; D'Imporzano, G.; Tambone, F., Nanoscale Structure of the Cell Wall Protecting Cellulose from Enzyme Attack. *Environmental Science & Technology* **2010,** *45* (3), 1107-1113.
58. CARPITA, N.; SABULARSE, D.; MONTEZINOS, D.; DELMER, D. P., Determination of the Pore Size of Cell Walls of Living Plant Cells. *Science* **1979,** *205* (4411), 1144-1147.
59. Davison, B. H.; Parks, J.; Davis, M. F.; Donohoe, B. S., Plant Cell Walls: Basics of Structure, Chemistry, Accessibility and the Influence on Conversion. In *Aqueous Pretreatment of Plant Biomass for Biological and Chemical Conversion to Fuels and Chemicals*, John Wiley & Sons, Ltd: 2013; pp 23-38.
60. Gapper, C.; Dolan, L., Control of Plant Development by Reactive Oxygen Species. *Plant Physiology* **2006,** *141* (2), 341-345.
61. Kim, J.-H.; Lee, Y.; Kim, E.-J.; Gu, S.; Sohn, E. J.; Seo, Y. S.; An, H. J.; Chang, Y.-S., Exposure of Iron Nanoparticles to Arabidopsis thaliana Enhances Root Elongation by Triggering Cell Wall Loosening. *Environmental science & technology* **2014,** *48* (6), 3477-3485.
62. Dimkpa, C. O.; McLean, J. E.; Martineau, N.; Britt, D. W.; Haverkamp, R.; Anderson, A. J., Silver Nanoparticles Disrupt Wheat (Triticum aestivum L.) Growth in a Sand Matrix. *Environmental Science & Technology* **2012,** *47* (2), 1082-1090.
63. Gardea-Torresdey, J. L.; Parsons, J. G.; Gomez, E.; Peralta-Videa, J.; Troiani, H. E.; Santiago, P.; Yacaman, M. J., Formation and Growth of Au Nanoparticles inside Live Alfalfa Plants. *Nano Letters* **2002,** *2* (4), 397-401.
64. López-Moreno, M. L.; de la Rosa, G.; Hernández-Viezcas, J. Á.; Castillo-Michel, H.; Botez, C. E.; Peralta-Videa, J. R.; Gardea-Torresdey, J. L., Evidence of the differential biotransformation and genotoxicity of ZnO and CeO2 nanoparticles on soybean (Glycine max) plants. *Environmental science & technology* **2010,** *44* (19), 7315-7320.

65. Franklin, N. M.; Rogers, N. J.; Apte, S. C.; Batley, G. E.; Gadd, G. E.; Casey, P. S., Comparative Toxicity of Nanoparticulate ZnO, Bulk ZnO, and ZnCl2 to a Freshwater Microalga (Pseudokirchneriella subcapitata): The Importance of Particle Solubility. *Environmental Science & Technology* **2007,** *41* (24), 8484-8490.
66. López-Moreno, M. L.; de la Rosa, G.; Hernández-Viezcas, J. A.; Peralta-Videa, J. R.; Gardea-Torresdey, J. L., XAS corroboration of the uptake and storage of CeO2 nanoparticles and assessment of their differential toxicity in four edible plant species. *Journal of agricultural and food chemistry* **2010,** *58* (6), 3689.
67. Majumdar, S.; Peralta-Videa, J. R.; Bandyopadhyay, S.; Castillo-Michel, H.; Hernandez-Viezcas, J.-A.; Sahi, S.; Gardea-Torresdey, J. L., Exposure of cerium oxide nanoparticles to kidney bean shows disturbance in the plant defense mechanisms. *Journal of hazardous materials* **2014,** *278*, 279-287.
68. Zhang, P.; Ma, Y.; Zhang, Z.; He, X.; Guo, Z.; Tai, R.; Ding, Y.; Zhao, Y.; Chai, Z., Comparative toxicity of nanoparticulate/bulk Yb2O3 and YbCl3 to cucumber (Cucumis sativus). *Environmental Science & Technology* **2011,** *46* (3), 1834-1841.
69. Wang, P.; Menzies, N. W.; Lombi, E.; McKenna, B. A.; Johannessen, B.; Glover, C. J.; Kappen, P.; Kopittke, P. M., Fate of ZnO nanoparticles in soils and cowpea (Vigna unguiculata). *Environmental science & technology* **2013,** *47* (23), 13822-13830.
70. Dimkpa, C. O.; Latta, D. E.; McLean, J. E.; Britt, D. W.; Boyanov, M. I.; Anderson, A. J., Fate of CuO and ZnO Nano- and Microparticles in the Plant Environment. *Environmental Science & Technology* **2013,** *47* (9), 4734-4742.
71. Kim, S.; Lee, S.; Lee, I., Alteration of Phytotoxicity and Oxidant Stress Potential by Metal Oxide Nanoparticles in Cucumis sativus. *Water Air Soil Pollut* **2012,** *223* (5), 2799-2806.
72. Lee, W.-M.; Kwak, J. I.; An, Y.-J., Effect of silver nanoparticles in crop plants Phaseolus radiatus and Sorghum bicolor: Media effect on phytotoxicity. *Chemosphere* **2012,** *86* (5), 491-499.
73. Feng, Y.; Cui, X.; He, S.; Dong, G.; Chen, M.; Wang, J.; Lin, X., The role of metal nanoparticles in influencing arbuscular mycorrhizal fungi effects on plant growth. *Environmental science & technology* **2013,** *47* (16), 9496-9504.
74. Yoon, S.-J.; Kwak, J. I.; Lee, W.-M.; Holden, P. A.; An, Y.-J., Zinc oxide nanoparticles delay soybean development: A standard soil microcosm study. *Ecotoxicology and Environmental Safety* **2014,** *100* (0), 131-137.
75. Song, U.; Jun, H.; Waldman, B.; Roh, J.; Kim, Y.; Yi, J.; Lee, E. J., Functional analyses of nanoparticle toxicity: A comparative study of the effects of TiO2 and Ag on tomatoes (Lycopersicon esculentum). *Ecotoxicology and Environmental Safety* **2013,** *93* (0), 60-67.
76. Zhao, L.; Sun, Y.; Hernandez-Viezcas, J. A.; Servin, A. D.; Hong, J.; Niu, G.; Peralta-Videa, J. R.; Duarte-Gardea, M.; Gardea-Torresdey, J. L., Influence of CeO2 and ZnO nanoparticles on cucumber physiological markers and bioaccumulation of Ce and Zn: A life cycle study. *Journal of agricultural and food chemistry* **2013,** *61* (49), 11945-11951.
77. Arora, S.; Sharma, P.; Kumar, S.; Nayan, R.; Khanna, P.; Zaidi, M., Gold-nanoparticle induced enhancement in growth and seed yield of Brassica juncea. *Plant Growth Regulation* **2012,** *66* (3), 303-310.

78. Raliya, R.; Tarafdar, J. C., ZnO Nanoparticle Biosynthesis and Its Effect on Phosphorous-Mobilizing Enzyme Secretion and Gum Contents in Clusterbean (Cyamopsis tetragonoloba L.). *Agric Res* **2013,** *2* (1), 48-57.
79. Rico, C. M.; Hong, J.; Morales, M. I.; Zhao, L.; Barrios, A. C.; Zhang, J.-Y.; Peralta-Videa, J. R.; Gardea-Torresdey, J. L., Effect of Cerium Oxide Nanoparticles on Rice: A Study Involving the Antioxidant Defense System and In Vivo Fluorescence Imaging. *Environmental Science & Technology* **2013,** *47* (11), 5635-5642.
80. Schwabe, F.; Schulin, R.; Limbach, L. K.; Stark, W.; Bürge, D.; Nowack, B., Influence of two types of organic matter on interaction of CeO< sub> 2</sub> nanoparticles with plants in hydroponic culture. *Chemosphere* **2013,** *91* (4), 512-520.
81. Taylor, A. F.; Rylott, E. L.; Anderson, C. W.; Bruce, N. C., Investigating the Toxicity, Uptake, Nanoparticle Formation and Genetic Response of Plants to Gold. *PloS one* **2014,** *9* (4), e93793.
82. Atha, D. H.; Wang, H.; Petersen, E. J.; Cleveland, D.; Holbrook, R. D.; Jaruga, P.; Dizdaroglu, M.; Xing, B.; Nelson, B. C., Copper oxide nanoparticle mediated DNA damage in terrestrial plant models. *Environmental science & technology* **2012,** *46* (3), 1819-1827.
83. Ghosh, M.; Bandyopadhyay, M.; Mukherjee, A., Genotoxicity of titanium dioxide (TiO2) nanoparticles at two trophic levels: Plant and human lymphocytes. *Chemosphere* **2010,** *81* (10), 1253-1262.
84. Patlolla, A. K.; Berry, A.; May, L.; Tchounwou, P. B., Genotoxicity of silver nanoparticles in Vicia faba: a pilot study on the environmental monitoring of nanoparticles. *International journal of environmental research and public health* **2012,** *9* (5), 1649-1662.
85. Ruffini Castiglione, M.; Giorgetti, L.; Geri, C.; Cremonini, R., The effects of nano-TiO2 on seed germination, development and mitosis of root tip cells of Vicia narbonensis L. and Zea mays L. *J Nanopart Res* **2011,** *13* (6), 2443-2449.
86. Kaveh, R.; Li, Y.-S.; Ranjbar, S.; Tehrani, R.; Brueck, C. L.; Van Aken, B., Changes in Arabidopsis thaliana Gene Expression in Response to Silver Nanoparticles and Silver Ions. *Environmental Science & Technology* **2013,** *47* (18), 10637-10644.
87. Møller, I. M.; Jensen, P. E.; Hansson, A., Oxidative modifications to cellular components in plants. *Annu. Rev. Plant Biol.* **2007,** *58*, 459-481.
88. Apel, K.; Hirt, H., Reactive oxygen species: metabolism, oxidative stress, and signal transduction. *Annu. Rev. Plant Biol.* **2004,** *55*, 373-399.
89. Carocho, M.; Ferreira, I. C. F. R., A review on antioxidants, prooxidants and related controversy: Natural and synthetic compounds, screening and analysis methodologies and future perspectives. *Food and Chemical Toxicology* **2013,** *51* (0), 15-25.
90. Mourato, M.; Reis, R.; Martins, M. L. L., Characterization of plant antioxidative system in response to abiotic stresses: a focus on heavy metal toxicity. **2012**.
91. Freinbichler, W.; Colivicchi, M. A.; Stefanini, C.; Bianchi, L.; Ballini, C.; Misini, B.; Weinberger, P.; Linert, W.; Varešlija, D.; Tipton, K. F., Highly reactive oxygen species: detection, formation, and possible functions. *Cellular and Molecular Life Sciences* **2011,** *68* (12), 2067-2079.

92. Lee, S. S.; Song, W.; Cho, M.; Puppala, H. L.; Nguyen, P.; Zhu, H.; Segatori, L.; Colvin, V. L., Antioxidant properties of cerium oxide nanocrystals as a function of nanocrystal diameter and surface coating. *ACS nano* **2013,** *7* (11), 9693-9703.
93. Speranza, A.; Crinelli, R.; Scoccianti, V.; Taddei, A. R.; Iacobucci, M.; Bhattacharya, P.; Ke, P. C., In vitro toxicity of silver nanoparticles to kiwifruit pollen exhibits peculiar traits beyond the cause of silver ion release. *Environmental Pollution* **2013,** *179* (0), 258-267.
94. Hopkins, F. G.; Harris, W. a. s. i. t. t. b. L. J., ON GLUTATHIONE: A REINVESTIGATION. *Journal of Biological Chemistry* **1929,** *84* (1), 269-320.
95. Cobbett, C. S.; May, M. J.; Howden, R.; Rolls, B., The glutathione-deficient, cadmium-sensitive mutant,cad2–1, ofArabidopsis thalianais deficient in γ-glutamylcysteine synthetase. *The Plant Journal* **1998,** *16* (1), 73-78.
96. Dhankher, O. P.; Li, Y.; Rosen, B. P.; Shi, J.; Salt, D.; Senecoff, J. F.; Sashti, N. A.; Meagher, R. B., Engineering tolerance and hyperaccumulation of arsenic in plants by combining arsenate reductase and γ-glutamylcysteine synthetase expression. *Nature biotechnology* **2002,** *20* (11), 1140-1145.
97. Mugford, S. G.; Lee, B. R.; Koprivova, A.; Matthewman, C.; Kopriva, S., Control of sulfur partitioning between primary and secondary metabolism. *The Plant Journal* **2011,** *65* (1), 96-105.
98. Na, G.; Salt, D. E., The role of sulfur assimilation and sulfur-containing compounds in trace element homeostasis in plants. *Environmental and Experimental Botany* **2011,** *72* (1), 18-25.
99. Noctor, G.; Mhamdi, A.; Chaouch, S.; Han, Y.; Neukermans, J.; MARQUEZ‐GARCIA, B.; Queval, G.; Foyer, C. H., Glutathione in plants: an integrated overview. *Plant, cell & environment* **2012,** *35* (2), 454-484.
100. Grill, E.; Löffler, S.; Winnacker, E.-L.; Zenk, M. H., Phytochelatins, the heavy-metal-binding peptides of plants, are synthesized from glutathione by a specific γ-glutamylcysteine dipeptidyl transpeptidase (phytochelatin synthase). *Proceedings of the National Academy of Sciences* **1989,** *86* (18), 6838-6842.
101. Cobbett, C. S., Phytochelatin biosynthesis and function in heavy-metal detoxification. *Current Opinion in Plant Biology* **2000,** *3* (3), 211-216.
102. Mishra, S.; Srivastava, S.; Tripathi, R. D.; Govindarajan, R.; Kuriakose, S. V.; Prasad, M. N. V., Phytochelatin synthesis and response of antioxidants during cadmium stress in Bacopa monnieri L◊. *Plant Physiology and Biochemistry* **2006,** *44* (1), 25-37.
103. Li, Y.; Dankher, O. P.; Carreira, L.; Smith, A. P.; Meagher, R. B., The shoot-specific expression of γ-glutamylcysteine synthetase directs the long-distance transport of thiol-peptides to roots conferring tolerance to mercury and arsenic. *Plant physiology* **2006,** *141* (1), 288-298.
104. Paulose, B.; Kandasamy, S.; Dhankher, O. P., Expression profiling of Crambe abyssinica under arsenate stress identifies genes and gene networks involved in arsenic metabolism and detoxification. *BMC plant biology* **2010,** *10* (1), 108.
105. Zulfiqar, A.; Paulose, B.; Chhikara, S.; Dhankher, O. P., Identifying genes and gene networks involved in chromium metabolism and detoxification in Crambe abyssinica. *Environmental Pollution* **2011,** *159* (10), 3123-3128.

106. Hund-Rinke, K.; Simon, M., Ecotoxic effect of photocatalytic active nanoparticles (TiO2) on algae and daphnids. *Environmental science and pollution research international* **2006,** *13* (4), 225-32.
107. Matei, A.; Cernica, I.; Cadar, O.; Roman, C.; Schiopu, V., Synthesis and characterization of ZnO ,Äì polymer nanocomposites. *Int J Mater Form* **2008,** *1* (1), 767-770.
108. Garner, K. L.; Keller, A. A., Emerging patterns for engineered nanomaterials in the environment: a review of fate and toxicity studies. *J Nanopart Res* **2014,** *16* (8), 1-28.
109. Chang, Y.-N.; Zhang, M.; Xia, L.; Zhang, J.; Xing, G., The toxic effects and mechanisms of CuO and ZnO nanoparticles. *Materials* **2012,** *5* (12), 2850-2871.
110. Bour, A.; Mouchet, F.; Silvestre, J.; Gauthier, L.; Pinelli, E., Environmentally relevant approaches to assess nanoparticles ecotoxicity: A review. *Journal of hazardous materials* **2015,** *283*, 764-777.
111. Colman, B. P.; Arnaout, C. L.; Anciaux, S.; Gunsch, C. K.; Hochella Jr, M. F.; Kim, B.; Lowry, G. V.; McGill, B. M.; Reinsch, B. C.; Richardson, C. J., Low concentrations of silver nanoparticles in biosolids cause adverse ecosystem responses under realistic field scenario. *PLoS One* **2013,** *8* (2), e57189.
112. Colman, B. P.; Espinasse, B.; Richardson, C. J.; Matson, C. W.; Lowry, G. V.; Hunt, D. E.; Wiesner, M. R.; Bernhardt, E. S., Emerging contaminant or an old toxin in disguise? Silver nanoparticle impacts on ecosystems. *Environmental science & technology* **2014,** *48* (9), 5229-5236.
113. Birbaum, K.; Brogioli, R.; Schellenberg, M.; Martinoia, E.; Stark, W. J.; G√°nther, D.; Limbach, L. K., No Evidence for Cerium Dioxide Nanoparticle Translocation in Maize Plants. *Environmental Science & Technology* **2010,** *44* (22), 8718-8723.
114. L√≥pez-Moreno, M. L.; de la Rosa, G.; Hern√°ndez-Viezcas, J. Å.; Castillo-Michel, H.; Botez, C. E.; Peralta-Videa, J. R.; Gardea-Torresdey, J. L., Evidence of the Differential Biotransformation and Genotoxicity of ZnO and CeO2 Nanoparticles on Soybean (Glycine max) Plants. *Environmental Science & Technology* **2010,** *44* (19), 7315-7320.
115. Priester, J. H.; Ge, Y.; Mielke, R. E.; Horst, A. M.; Moritz, S. C.; Espinosa, K.; Gelb, J.; Walker, S. L.; Nisbet, R. M.; An, Y.-J.; Schimel, J. P.; Palmer, R. G.; Hernandez-Viezcas, J. A.; Zhao, L.; Gardea-Torresdey, J. L.; Holden, P. A., Soybean susceptibility to manufactured nanomaterials with evidence for food quality and soil fertility interruption. *Proceedings of the National Academy of Sciences* **2012,** *109* (37), E2451,ÄìE2456.
116. LoÃÅpez-Moreno, M. L.; de la Rosa, G.; HernaÃÅndez-Viezcas, J. A.; Peralta-Videa, J. R.; Gardea-Torresdey, J. L., X-ray Absorption Spectroscopy (XAS) Corroboration of the Uptake and Storage of CeO2 Nanoparticles and Assessment of Their Differential Toxicity in Four Edible Plant Species. *Journal of Agricultural and Food Chemistry* **2010,** *58* (6), 3689-3693.

117. Zhao, L.; Peng, B.; Hernandez-Viezcas, J. A.; Rico, C.; Sun, Y.; Peralta-Videa, J. R.; Tang, X.; Niu, G.; Jin, L.; Varela-Ramirez, A.; Zhang, J.-y.; Gardea-Torresdey, J. L., Stress Response and Tolerance of Zea mays to CeO2 Nanoparticles: Cross Talk among H2O2, Heat Shock Protein, and Lipid Peroxidation. *ACS Nano* **2012,** *6* (11), 9615-9622.
118. Lin, S.; Reppert, J.; Hu, Q.; Hudson, J. S.; Reid, M. L.; Ratnikova, T. A.; Rao, A. M.; Luo, H.; Ke, P. C., Uptake, Translocation, and Transmission of Carbon Nanomaterials in Rice Plants. *Small* **2009,** *5* (10), 1128-1132.
119. Dixit, A. R.; Dhankher, O. P., A novel stress-associated protein 'AtSAP10'from Arabidopsis thaliana confers tolerance to nickel, manganese, zinc, and high temperature stress. **2011**.
120. Lichtenthaler, H. K., [34] Chlorophylls and carotenoids: Pigments of photosynthetic biomembranes. In *Methods in Enzymology*, Academic Press: 1987; Vol. Volume 148, pp 350-382.
121. Gould, K. S.; McKelvie, J.; Markham, K. R., Do anthocyanins function as antioxidants in leaves? Imaging of H2O2 in red and green leaves after mechanical injury. *Plant, Cell & Environment* **2002,** *25* (10), 1261-1269.
122. Jeong, S.-W.; Das, P. K.; Jeoung, S. C.; Song, J.-Y.; Lee, H. K.; Kim, Y.-K.; Kim, W. J.; Park, Y. I.; Yoo, S.-D.; Choi, S.-B.; Choi, G.; Park, Y.-I., Ethylene Suppression of Sugar-Induced Anthocyanin Pigmentation in Arabidopsis. *Plant Physiology* **2010,** *154* (3), 1514-1531.
123. Jambunathan, N., Determination and Detection of Reactive Oxygen Species (ROS), Lipid Peroxidation, and Electrolyte Leakage in Plants. In *Plant Stress Tolerance*, Sunkar, R., Ed. Humana Press: 2010; Vol. 639, pp 291-297.
124. Dixit, V.; Pandey, V.; Shyam, R., Differential antioxidative responses to cadmium in roots and leaves of pea (Pisum sativum L. cv. Azad). *Journal of Experimental Botany* **2001,** *52* (358), 1101-1109.
125. Jing, G.; Huang, H.; Yang, B.; Li, J.; Zheng, X.; Jiang, Y., Effect of pyrogallol on the physiology and biochemistry of litchi fruit during storage. *Chemistry Central Journal* **2013,** *7* (1), 19.
126. Su, M.; Chen, K.; Ye, Z.; Zhang, B.; Guo, J.; Xu, C.; Sun, C.; Zhang, J.; Li, X.; Wu, A., Physical changes and physiological characteristics of red and green peel during nectarine (cv. Hu018) maturation. *Journal of the Science of Food and Agriculture* **2012,** *92* (7), 1448-1454.
127. Schaedle, M.; Bassham, J. A., Chloroplast glutathione reductase. *Plant Physiology* **1977,** *59* (5), 1011-1012.
128. Livak, K. J.; Schmittgen, T. D., Analysis of Relative Gene Expression Data Using Real-Time Quantitative PCR and the 2,àíŒîŒîCT Method. *Methods* **2001,** *25* (4), 402-408.
129. Garc√≠a, A.; Espinosa, R.; Delgado, L. a.; Casals, E.; Gonz√°lez, E.; Puntes, V. c.; Barata, C.; Font, X.; S√°nchez, A., Acute toxicity of cerium oxide, titanium oxide and iron oxide nanoparticles using standardized tests. *Desalination* **2011,** *269* (1, Äì3), 136-141.

130. Jiang, H.-S.; Li, M.; Chang, F.-Y.; Li, W.; Yin, L.-Y., Physiological analysis of silver nanoparticles and AgNO3 toxicity to Spirodela polyrhiza. *Environmental Toxicology and Chemistry* **2012,** *31* (8), 1880-1886.
131. Shi, J.; Abid, A. D.; Kennedy, I. M.; Hristova, K. R.; Silk, W. K., To duckweeds (Landoltia punctata), nanoparticulate copper oxide is more inhibitory than the soluble copper in the bulk solution. *Environmental Pollution* **2011,** *159* (5), 1277-1282.
132. Oukarroum, A.; Polchtchikov, S.; Perreault, F. ß.; Popovic, R., Temperature influence on silver nanoparticles inhibitory effect on photosystem II photochemistry in two green algae, Chlorella vulgaris and Dunaliella tertiolecta. *Environ Sci Pollut Res* **2012,** *19* (5), 1755-1762.
133. De La Torre-Roche, R.; Hawthorne, J.; Musante, C.; Xing, B.; Newman, L. A.; Ma, X.; White, J. C., Impact of Ag Nanoparticle Exposure on p,p,Ä≤-DDE Bioaccumulation by Cucurbita pepo (Zucchini) and Glycine max (Soybean). *Environmental Science & Technology* **2012,** *47* (2), 718-725.
134. Nair, P. M. G.; Chung, I. M., Physiological and molecular level effects of silver nanoparticles exposure in rice (Oryza sativa L.) seedlings. *Chemosphere* **2014,** *112*, 105-113.
135. Chen, J.; Liu, X.; Wang, C.; Yin, S.-S.; Li, X.-L.; Hu, W.-J.; Simon, M.; Shen, Z.-J.; Xiao, Q.; Chu, C.-C., Nitric oxide ameliorates zinc oxide nanoparticles-induced phytotoxicity in rice seedlings. *Journal of hazardous materials* **2015,** *297*, 173-182.
136. Rajeshwari, A.; Kavitha, S.; Alex, S. A.; Kumar, D.; Mukherjee, A.; Chandrasekaran, N.; Mukherjee, A., Cytotoxicity of aluminum oxide nanoparticles on Allium cepa root tip—effects of oxidative stress generation and biouptake. *Environmental Science and Pollution Research* **2015**, 1-10.
137. Mittler, R.; Vanderauwera, S.; Gollery, M.; Van Breusegem, F., Reactive oxygen gene network of plants. *Trends in Plant Science* **2004,** *9* (10), 490-498.
138. Mittler, R., Oxidative stress, antioxidants and stress tolerance. *Trends in plant science* **2002,** *7* (9), 405-410.
139. Dalton, D. A.; Boniface, C.; Turner, Z.; Lindahl, A.; Kim, H. J.; Jelinek, L.; Govindarajulu, M.; Finger, R. E.; Taylor, C. G., Physiological roles of glutathione S-transferases in soybean root nodules. *Plant physiology* **2009,** *150* (1), 521-530.
140. Pauly, N.; Pucciariello, C.; Mandon, K.; Innocenti, G.; Jamet, A.; Baudouin, E.; Hérouart, D.; Frendo, P.; Puppo, A., Reactive oxygen and nitrogen species and glutathione: key players in the legume–Rhizobium symbiosis. *Journal of Experimental Botany* **2006,** *57* (8), 1769-1776.
141. Kitamura, Y.; Ohta, M.; Ikenaga, T.; Watanabe, M., Responses of anthocyanin-producing and non-producing cells of Glehnia littoralis to radical generators. *Phytochemistry* **2002,** *59* (1), 63-68.
142. Wang, H.; Arakawa, O.; Motomura, Y., Influence of maturity and bagging on the relationship between anthocyanin accumulation and phenylalanine ammonia-lyase (PAL) activity in 'Jonathan'apples. *Postharvest Biology and Technology* **2000,** *19* (2), 123-128.

143. Kováčik, J.; Klejdus, B.; Hedbavny, J.; Štork, F.; Bačkor, M., Comparison of cadmium and copper effect on phenolic metabolism, mineral nutrients and stress-related parameters in Matricaria chamomilla plants. *Plant and soil* **2009,** *320* (1-2), 231-242.
144. Pourcel, L.; Routaboul, J.-M.; Cheynier, V.; Lepiniec, L.; Debeaujon, I., Flavonoid oxidation in plants: from biochemical properties to physiological functions. *Trends in plant science* **2007,** *12* (1), 29-36.
145. Zhao, L.; Sun, Y.; Hernandez-Viezcas, J. A.; Hong, J.; Majumdar, S.; Niu, G.; Duarte-Gardea, M.; Peralta-Videa, J. R.; Gardea-Torresdey, J. L., Monitoring the Environmental Effects of CeO2 and ZnO Nanoparticles Through the Life Cycle of Corn (Zea mays) Plants and in Situ μ-XRF Mapping of Nutrients in Kernels. *Environmental Science & Technology* **2015,** *49* (5), 2921-2928.
146. Nath, M.; Tuteja, N., NPKS uptake, sensing, and signaling and miRNAs in plant nutrient stress. *Protoplasma* **2015**, 1-20.
147. Vert, G.; Grotz, N.; Dédaldéchamp, F.; Gaymard, F.; Guerinot, M. L.; Briat, J.-F.; Curie, C., IRT1, an Arabidopsis transporter essential for iron uptake from the soil and for plant growth. *The Plant Cell* **2002,** *14* (6), 1223-1233.
148. Ma, C.; Chhikara, S.; Minocha, R.; Long, S.; Musante, C.; White, J. C.; Xing, B.; Dhankher, O. P., Reduced Silver Nanoparticle Phytotoxicity in Crambe abyssinica with Enhanced Glutathione Production by Overexpressing Bacterial γ-Glutamylcysteine Synthase. *Environmental Science & Technology* **2015**.
149. Hashimoto, K.; Kudla, J., Calcium decoding mechanisms in plants. *Biochimie* **2011,** *93* (12), 2054-2059.
150. Batistič, O.; Kudla, J., Analysis of calcium signaling pathways in plants. *Biochimica et Biophysica Acta (BBA)-General Subjects* **2012,** *1820* (8), 1283-1293.
151. Fujita, M.; Fujita, Y.; Noutoshi, Y.; Takahashi, F.; Narusaka, Y.; Yamaguchi-Shinozaki, K.; Shinozaki, K., Crosstalk between abiotic and biotic stress responses: a current view from the points of convergence in the stress signaling networks. *Current opinion in plant biology* **2006,** *9* (4), 436-442.
152. Torres, M. A.; Dangl, J. L., Functions of the respiratory burst oxidase in biotic interactions, abiotic stress and development. *Current opinion in plant biology* **2005,** *8* (4), 397-403.
153. Waters, B. M.; Blevins, D. G.; Eide, D. J., Characterization of FRO1, a pea ferric-chelate reductase involved in root iron acquisition. *Plant Physiology* **2002,** *129* (1), 85-94.
154. Bereczky, Z.; Wang, H.-Y.; Schubert, V.; Ganal, M.; Bauer, P., Differential regulation of nramp and irt metal transporter genes in wild type and iron uptake mutants of tomato. *Journal of Biological Chemistry* **2003,** *278* (27), 24697-24704.
155. Ravet, K.; Touraine, B.; Boucherez, J.; Briat, J. F.; Gaymard, F.; Cellier, F., Ferritins control interaction between iron homeostasis and oxidative stress in Arabidopsis. *The Plant Journal* **2009,** *57* (3), 400-412.
156. Rogers, E. E.; Eide, D. J.; Guerinot, M. L., Altered selectivity in an Arabidopsis metal transporter. *Proceedings of the National Academy of Sciences* **2000,** *97* (22), 12356-12360.

157. Korshunova, Y. O.; Eide, D.; Clark, W. G.; Guerinot, M. L.; Pakrasi, H. B., The IRT1 protein from Arabidopsis thaliana is a metal transporter with a broad substrate range. *Plant molecular biology* **1999,** *40* (1), 37-44.
158. Mugford, S. G.; Lee, B.-R.; Koprivova, A.; Matthewman, C.; Kopriva, S., Control of sulfur partitioning between primary and secondary metabolism. *The Plant Journal* **2011,** *65* (1), 96-105.
159. Cobbett, C. S., Phytochelatins and Their Roles in Heavy Metal Detoxification. *Plant Physiology* **2000,** *123* (3), 825-832.
160. Dhankher, O. P.; Li, Y.; Rosen, B. P.; Shi, J.; Salt, D.; Senecoff, J. F.; Sashti, N. A.; Meagher, R. B., Engineering tolerance and hyperaccumulation of arsenic in plants by combining arsenate reductase and [gamma]-glutamylcysteine synthetase expression. *Nat Biotech* **2002,** *20* (11), 1140-1145.
161. Li, Y.; Dankher, O. P.; Carreira, L.; Smith, A. P.; Meagher, R. B., The Shoot-Specific Expression of g-Glutamylcysteine Synthetase Directs the Long-Distance Transport of Thiol-Peptides to Roots Conferring Tolerance to Mercury and Arsenic. *Plant physiology.* **2006,** *141* (1), 288.
162. Dimkpa, C.; McLean, J. E.; Martineu, N.; Britt, D.; Haverkamp, R. G.; Anderson, A., Silver Nanoparticles Disrupt Wheat (Triticum aestivum L.) Growth in a Sand Matrix. *Environmental Science & Technology* **2012**.
163. Leustek, T.; Saito, K., Sulfate transport and assimilation in plants. *Plant physiology* **1999,** *120* (3), 637-644.
164. Takahashi, H.; Kopriva, S.; Giordano, M.; Saito, K.; Hell, R. d., Sulfur assimilation in photosynthetic organisms: molecular functions and regulations of transporters and assimilatory enzymes. *Annual review of plant biology* **2011,** *62*, 157-184.
165. Zulfiqar, A.; Paulose, B.; Chhikara, S.; Dhankher, O. P., Identifying genes and gene networks involved in chromium metabolism and detoxification in< i> Crambe abyssinica</i>. *Environmental Pollution* **2011,** *159* (10), 3123-3128.
166. Hoecke, K. V.; Quik, J. T.; Mankiewicz-Boczek, J.; Schamphelaere, K. A. D.; Elsaesser, A.; Meeren, P. V. d.; Barnes, C.; McKerr, G.; Howard, C. V.; Meent, D. V. D., Fate and effects of CeO2 nanoparticles in aquatic ecotoxicity tests. *Environmental science & technology* **2009,** *43* (12), 4537-4546.
167. Matei, A.; Cernica, I.; Cadar, O.; Roman, C.; Schiopu, V., Synthesis and characterization of ZnO–polymer nanocomposites. *International Journal of Material Forming* **2008,** *1* (1), 767-770.
168. Castiglione, M. R.; Giorgetti, L.; Geri, C.; Cremonini, R., The effects of nano-TiO2 on seed germination, development and mitosis of root tip cells of Vicia narbonensis L. and Zea mays L. *Journal of Nanoparticle Research* **2011,** *13* (6), 2443-2449.
169. Bystrzejewska-Piotrowska, G.; Golimowski, J.; Urban, P. L., Nanoparticles: their potential toxicity, waste and environmental management. *Waste Management* **2009,** *29* (9), 2587-2595.
170. Somasundaran, P.; Fang, X.; Ponnurangam, S.; Li, B., Nanoparticles: characteristics, mechanisms and modulation of biotoxicity. *KONA powder and particle journal* **2010,** *28* (1), 38-49.

171. Klaine, S. J.; Alvarez, P. J.; Batley, G. E.; Fernandes, T. F.; Handy, R. D.; Lyon, D. Y.; Mahendra, S.; McLaughlin, M. J.; Lead, J. R., Nanomaterials in the environment: behavior, fate, bioavailability, and effects. *Environmental Toxicology and Chemistry* **2008,** *27* (9), 1825-1851.
172. Lowry, G. V.; Gregory, K. B.; Apte, S. C.; Lead, J. R., Transformations of nanomaterials in the environment. *Environmental science & technology* **2012,** *46* (13), 6893-6899.
173. Hawthorne, J.; Musante, C.; Sinha, S. K.; White, J. C., Accumulation and phytotoxicity of engineered nanoparticles to Cucurbita pepo. *International journal of phytoremediation* **2012,** *14* (4), 429-442.
174. López-Moreno, M. L.; de la Rosa, G.; Hernández-Viezcas, J. A.; Peralta-Videa, J. R.; Gardea-Torresdey, J. L., X-ray absorption spectroscopy (XAS) corroboration of the uptake and storage of CeO2 nanoparticles and assessment of their differential toxicity in four edible plant species. *Journal of agricultural and food chemistry* **2010,** *58* (6), 3689-3693.
175. Petrochenko, P. E.; Zhang, Q.; Wang, H.; Sun, T.; Wildt, B.; Betz, M. W.; Goering, P. L.; Narayan, R. J., In vitro cytotoxicity of rare earth oxide nanoparticles for imaging applications. *International Journal of Applied Ceramic Technology* **2012,** *9* (5), 881-892.
176. Geranio, L.; Heuberger, M.; Nowack, B., The behavior of silver nanotextiles during washing. *Environmental Science & Technology* **2009,** *43* (21), 8113-8118.
177. Zheng, L. P.; Zhang, Z.; Zhang, B.; Wang, J. W. In *Antifungal properties of Ag-SiO2 core-shell nanoparticles against phytopathogenic fungi*, Advanced Materials Research, Trans Tech Publ: 2012; pp 814-818.
178. Savithramma, N.; Lingarao, M.; Ankanna, S.; Venkateswarlu, P., Screening of medicinal plants for effective Biogenesis of silver nanoparticles and efficient antimicrobial activity. *Int J Phar Sci Res* **2012,** *3*, 1141-8.
179. Reinsch, B.; Levard, C.; Li, Z.; Ma, R.; Wise, A.; Gregory, K.; Brown Jr, G.; Lowry, G., Sulfidation of silver nanoparticles decreases Escherichia coli growth inhibition. *Environmental science & technology* **2012,** *46* (13), 6992-7000.
180. Wang, J.; Koo, Y.; Alexander, A.; Yang, Y.; Westerhof, S.; Zhang, Q.; Schnoor, J. L.; Colvin, V. L.; Braam, J.; Alvarez, P. J., Phytostimulation of poplars and Arabidopsis exposed to silver nanoparticles and Ag+ at sublethal concentrations. *Environmental science & technology* **2013,** *47* (10), 5442-5449.
181. Ravindran, A.; Prathna, T.; Verma, V. K.; Chandrasekaran, N.; Mukherjee, A., Bovine serum albumin mediated decrease in silver nanoparticle phytotoxicity: root elongation and seed germination assay. *Toxicological & Environmental Chemistry* **2012,** *94* (1), 91-98.
182. Stampoulis, D.; Sinha, S. K.; White, J. C., Assay-dependent phytotoxicity of nanoparticles to plants. *Environmental science & technology* **2009,** *43* (24), 9473-9479.
183. Gubbins, E. J.; Batty, L. C.; Lead, J. R., Phytotoxicity of silver nanoparticles to Lemna minor L. *Environmental Pollution* **2011,** *159* (6), 1551-1559.

184. Chhikara, S.; Dutta, I.; Paulose, B.; Jaiwal, P. K.; Dhankher, O. P., Development of an Agrobacterium-mediated stable transformation method for industrial oilseed crop Crambe abyssinica 'BelAnn'. *Industrial Crops and Products* **2012,** *37* (1), 457-465.
185. Murashige, T.; Skoog, F., A revised medium for rapid growth and bio assays with tobacco tissue cultures. *Physiologia plantarum* **1962,** *15* (3), 473-497.
186. Minocha, R.; Shortle, W. C.; Long, S. L.; Minocha, S. C., A rapid and reliable procedure for extraction of cellular polyamines and inorganic ions from plant tissues. *Journal of Plant Growth Regulation* **1994,** *13* (4), 187-193.
187. Jambunathan, N., Determination and detection of reactive oxygen species (ROS), lipid peroxidation, and electrolyte leakage in plants. *Plant stress tolerance: methods and protocols* **2010**, 291-297.
188. Minocha, R.; Thangavel, P.; Dhankher, O. P.; Long, S., Separation and quantification of monothiols and phytochelatins from a wide variety of cell cultures and tissues of trees and other plants using high performance liquid chromatography. *Journal of Chromatography A* **2008,** *1207* (1), 72-83.
189. Dimkpa, C. O.; McLean, J. E.; Martineau, N.; Britt, D. W.; Haverkamp, R.; Anderson, A. J., Silver nanoparticles disrupt wheat (Triticum aestivum L.) growth in a sand matrix. *Environmental science & technology* **2013,** *47* (2), 1082-1090.
190. Wang, Z.; Xie, X.; Zhao, J.; Liu, X.; Feng, W.; White, J. C.; Xing, B., Xylem-and phloem-based transport of CuO nanoparticles in maize (Zea mays L.). *Environmental science & technology* **2012,** *46* (8), 4434-4441.
191. Burklew, C. E.; Ashlock, J.; Winfrey, W. B.; Zhang, B., Effects of aluminum oxide nanoparticles on the growth, development, and microRNA expression of tobacco (Nicotiana tabacum). *PloS one* **2012,** *7* (5), e34783.
192. Jiang, H. S.; Li, M.; Chang, F. Y.; Li, W.; Yin, L. Y., Physiological analysis of silver nanoparticles and AgNO3 toxicity to Spirodela polyrhiza. *Environmental Toxicology and Chemistry* **2012,** *31* (8), 1880-1886.
193. Oukarroum, A.; Polchtchikov, S.; Perreault, F.; Popovic, R., Temperature influence on silver nanoparticles inhibitory effect on photosystem II photochemistry in two green algae, Chlorella vulgaris and Dunaliella tertiolecta. *Environmental Science and Pollution Research* **2012,** *19* (5), 1755-1762.
194. Larue, C.; Laurette, J.; Herlin-Boime, N.; Khodja, H.; Fayard, B.; Flank, A.-M.; Brisset, F.; Carriere, M., Accumulation, translocation and impact of TiO 2 nanoparticles in wheat (Triticum aestivum spp.): influence of diameter and crystal phase. *Science of the total environment* **2012,** *431*, 197-208.
195. Corral-Diaz, B.; Peralta-Videa, J. R.; Alvarez-Parrilla, E.; Rodrigo-García, J.; Morales, M. I.; Osuna-Avila, P.; Niu, G.; Hernandez-Viezcas, J. A.; Gardea-Torresdey, J. L., Cerium oxide nanoparticles alter the antioxidant capacity but do not impact tuber ionome in Raphanus sativus (L). *Plant Physiology and Biochemistry* **2014,** *84* (0), 277-285.
196. Gao, J.; Xu, G.; Qian, H.; Liu, P.; Zhao, P.; Hu, Y., Effects of nano-TiO2 on photosynthetic characteristics of Ulmus elongata seedlings. *Environmental Pollution* **2013,** *176* (0), 63-70.

197. Nair, P. M. G.; Kim, S.-H.; Chung, I. M., Copper oxide nanoparticle toxicity in mung bean (Vigna radiata L.) seedlings: physiological and molecular level responses of in vitro grown plants. *Acta Physiologiae Plantarum* **2014,** *36* (11), 2947-2958.
198. Majumdar, S.; Peralta-Videa, J. R.; Bandyopadhyay, S.; Castillo-Michel, H.; Hernandez-Viezcas, J.-A.; Sahi, S.; Gardea-Torresdey, J. L., Exposure of cerium oxide nanoparticles to kidney bean shows disturbance in the plant defense mechanisms. *Journal of Hazardous Materials* **2014,** *278* (0), 279-287.
199. Townsend, D. M.; Tew, K. D.; Tapiero, H., The importance of glutathione in human disease. *Biomedicine & Pharmacotherapy* **2003,** *57* (3), 145-155.
200. Khan, H.; Khan, M. F.; Jan, S.; Ullah, N., The protective role of glutathione in silver induced toxicity in blood components. *Pakistan journal of pharmaceutical sciences* **2011,** *24* (2), 123-128.
201. Li, Y.; Dhankher, O. P.; Carreira, L.; Balish, R. S.; Meagher, R. B., Arsenic and mercury tolerance and cadmium sensitivity in Arabidopsis plants expressing bacterial γ - glutamylcysteine synthetase. *Environmental toxicology and chemistry* **2005,** *24* (6), 1376-1386.
202. Clemens, S., Toxic metal accumulation, responses to exposure and mechanisms of tolerance in plants. *Biochimie* **2006,** *88* (11), 1707-1719.
203. Li, Y.; Dhankher, O. P.; Carreira, L.; Lee, D.; Chen, A.; Schroeder, J. I.; Balish, R. S.; Meagher, R. B., Overexpression of phytochelatin synthase in Arabidopsis leads to enhanced arsenic tolerance and cadmium hypersensitivity. *Plant and Cell Physiology* **2004,** *45* (12), 1787-1797.
204. De La Torre-Roche, R.; Hawthorne, J.; Musante, C.; Xing, B.; Newman, L. A.; Ma, X.; White, J. C., Impact of Ag nanoparticle exposure on p, p′ -DDE bioaccumulation by Cucurbita pepo (Zucchini) and Glycine max (Soybean). *Environmental science & technology* **2013,** *47* (2), 718-725.
205. Piccapietra, F.; Allué, C. G.; Sigg, L.; Behra, R., Intracellular silver accumulation in Chlamydomonas reinhardtii upon exposure to carbonate coated silver nanoparticles and silver nitrate. *Environmental science & technology* **2012,** *46* (13), 7390-7397.
206. Zhao, L.; Peralta-Videa, J. R.; Ren, M.; Varela-Ramirez, A.; Li, C.; Hernandez-Viezcas, J. A.; Aguilera, R. J.; Gardea-Torresdey, J. L., Transport of Zn in a sandy loam soil treated with ZnO NPs and uptake by corn plants: Electron microprobe and confocal microscopy studies. *Chemical Engineering Journal* **2012,** *184*, 1-8.
207. Alidoust, D.; Isoda, A., Phytotoxicity assessment of γ-Fe2O3 nanoparticles on root elongation and growth of rice plant. *Environmental earth sciences* **2014,** *71* (12), 5173-5182.
208. Parisi, C.; Vigani, M.; Cerezo, E. R. *Proceedings of a Workshop on" Nanotechnology for the agricultural sector: from research to the field"*; Institute for Prospective and Technological Studies, Joint Research Centre: 2014.
209. Bourguignon, F.; Bénassy-Quéré, A.; Dercon, S.; Estache, A.; Gunning, J.; Kanbur, R.; Klasen, S.; Maxwell, S.; Platteau, J.; Spadaro, A., Millennium Development Goals at Midpoint: Where Do We Stand and Where Do We Need to Go? European Report on Development. 2008.

210. Masson-Boivin, C.; Giraud, E.; Perret, X.; Batut, J., Establishing nitrogen-fixing symbiosis with legumes: how many rhizobium recipes? *Trends in microbiology* **2009,** *17* (10), 458-466.
211. Herridge, D. F.; Peoples, M. B.; Boddey, R. M., Global inputs of biological nitrogen fixation in agricultural systems. *Plant and Soil* **2008,** *311* (1-2), 1-18.
212. Ge, Y.; Priester, J. H.; Van De Werfhorst, L. C.; Walker, S. L.; Nisbet, R. M.; An, Y.-J.; Schimel, J. P.; Gardea-Torresdey, J. L.; Holden, P. A., Soybean Plants Modify Metal Oxide Nanoparticle Effects on Soil Bacterial Communities. *Environmental Science & Technology* **2014,** *48* (22), 13489-13496.
213. Stacey, G.; Libault, M.; Brechenmacher, L.; Wan, J.; May, G. D., Genetics and functional genomics of legume nodulation. *Current opinion in plant biology* **2006,** *9* (2), 110-121.
214. Frendo, P.; Harrison, J.; Norman, C.; Jiménez, M. J. H.; Van de Sype, G.; Gilabert, A.; Puppo, A., Glutathione and homoglutathione play a critical role in the nodulation process of Medicago truncatula. *Molecular plant-microbe interactions* **2005,** *18* (3), 254-259.
215. Groten, K.; Vanacker, H.; Dutilleul, C.; Bastian, F.; Bernard, S.; Carzaniga, R.; Foyer, C. H., The roles of redox processes in pea nodule development and senescence. *Plant, Cell & Environment* **2005,** *28* (10), 1293-1304.
216. Diamond, D., QuikChem Method 13-107-06-2-D. In *Lachat Instruments Inc.*, Lachat Instruments Inc.: 1992.
217. COLE, E. J. ASSESSING KILN-PRODUCED HARDWOOD BIOCHAR FOR IMPROVING SOIL HEALTH IN A TEMPERATE CLIMATE AGRICULTURAL SOIL. Dissertation, 2015.
218. Burdock, T.; Brooks, M.; Ghaly, A., A dehydrogenase activity test for monitoring the growth of Streptomyces venezuelae in a nutrient rich medium. *Journal of Bioprocessing & Biotechniques* **2012,** *2011*.
219. Minocha, R.; Long, S., Simultaneous separation and quantitation of amino acids and polyamines of forest tree tissues and cell cultures within a single high-performance liquid chromatography run using dansyl derivatization. *Journal of Chromatography A* **2004,** *1035* (1), 63-73.
220. Ma, C.; Chhikara, S.; Minocha, R.; Long, S.; Musante, C.; White, J. C.; Xing, B.; Dhankher, O. P., Reduced Silver Nanoparticle Phytotoxicity in Crambe abyssinica with Enhanced Glutathione Production by Overexpressing Bacterial γ-Glutamylcysteine Synthase. *Environmental science & technology* **2015,** *49* (16), 10117-10126.
221. Larue, C.; Castillo-Michel, H.; Sobanska, S.; Cécillon, L.; Bureau, S.; Barthès, V.; Ouerdane, L.; Carrière, M.; Sarret, G., Foliar exposure of the crop Lactuca sativa to silver nanoparticles: evidence for internalization and changes in Ag speciation. *Journal of hazardous materials* **2014,** *264*, 98-106.
222. Unrine, J. M.; Colman, B. P.; Bone, A. J.; Gondikas, A. P.; Matson, C. W., Biotic and abiotic interactions in aquatic microcosms determine fate and toxicity of Ag nanoparticles. Part 1. Aggregation and dissolution. *Environmental science & technology* **2012,** *46* (13), 6915-6924.

223. Godde, D.; Dannehl, H., Stress-induced chlorosis and increase in D1-protein turnover precede photoinhibition in spinach suffering under magnesium/sulphur deficiency. *Planta* **1994,** *195* (2), 291-300.
224. Marmiroli, M.; Pagano, L.; Savo Sardaro, M. L.; Villani, M.; Marmiroli, N., Genome-Wide Approach in Arabidopsis thaliana to Assess the Toxicity of Cadmium Sulfide Quantum Dots. *Environmental Science & Technology* **2014,** *48* (10), 5902-5909.
225. Sun, T. Y.; Gottschalk, F.; Hungerbühler, K.; Nowack, B., Comprehensive probabilistic modelling of environmental emissions of engineered nanomaterials. *Environmental Pollution* **2014,** *185* (0), 69-76.
226. Gottschalk, F.; Sun, T.; Nowack, B., Environmental concentrations of engineered nanomaterials: review of modeling and analytical studies. *Environmental pollution* **2013,** *181*, 287-300.